Impaired vasopressin neuromodulation promotes social behavior deficits in a mouse model of Autism Spectrum Disorder

Doctoral Thesis presented by

Maria Helena Bortolozzo Gleich

Thesis Director:

Dr. Félix Leroy

PhD Program in Neuroscience

Instituto de Neurociencias

Universidad Miguel Hernández de Elche

- 2025 -

Sant Joan d'Alacant, 2025

The doctoral thesis entitled: “Impaired vasopressin neuromodulation promotes social behavior deficits in a mouse model of Autism Spectrum Disorder” is submitted under the format of thesis by compendium of the following publications:

- Bortolozzo-Gleich, M. H., Bouisset, G., Geng, L., Ruiz-Pino, A., Nomura, Y., Han, S., Li, Y., Léroy, F. Impaired vasopressin neuromodulation of the lateral septum leads to social behavior deficits in *Shank3B*$^{+/-}$ male mice. *Nat Commun* **16**, 6783 (2025).

  PMID: 40702006

  DOI: https://doi.org/10.1038/s41467-025-61994-6

Sant Joan d'Alacant, 2025

Dr. Félix Leroy, Director of the doctoral thesis entitled “Impaired vasopressin neuromodulation promotes social behavior deficits in a mouse model of Autism Spectrum Disorder”,

INFORMS:

That Ms. *Maria Helena Bortolozzo Gleich* has carried out under our supervision the work entitled “Impaired vasopressin neuromodulation promotes social behavior deficits in a mouse model of Autism Spectrum Disorder” in accordance with the terms and conditions defined in his Research Plan and in accordance with the Code of Good Practice of the University Miguel Hernández of Elche, satisfactorily fulfilling the objectives foreseen for its public defence as a doctoral thesis.

I sign for appropriate purposes,

in Sant Joan d’Alacant, 11 of September of 2025

Thesis director

Dr. Félix Leroy

Sant Joan d'Alacant, 2025

Dr. Maria Cruz Morenilla Palao, Coordinator of the Neuroscience PhD program at the Institute of Neuroscience in Alicante, a joint centre of the Miguel Hernández University (UMH) and the Spanish National Research Council (CSIC),

INFORMS:

That Ms. *Maria Helena Bortolozzo Gleich* has carried out under our supervision the work entitled “Impaired vasopressin neuromodulation promotes social behavior deficits in a mouse model of Autism Spectrum Disorder” in accordance with the terms and conditions defined in his Research Plan and in accordance with the Code of Good Practice of the University Miguel Hernández de Elche, fulfilling the objectives satisfactorily for its public defence as a doctoral thesis.

Which I sign for the appropriate purposes, in Sant Joan d’Alacant, 11 of September, 2025

Dra. Maria Cruz Morenilla Palao

The project that gave rise to these results received the support of a fellowship from “la Caixa” Foundation (ID 100010434). The fellowship code is LCF/BQ/DI20/11780018.

In loving memory of my mom, Marilene Bortolozzo,
who taught me that the hardest part of loving a dreamer
is watching them go.

Table of Contents

List of abbreviations

AVP - Arginine Vasopressin

ASD - Autism Spectrum Disorder

LS - Lateral Septum

BNST - Bed Nucleus of the Stria Terminalis

WT - Wild Type

AVPR1a - Vasopressin Receptor 1a

AVPR1b - Vasopressin Receptor 1b

AVPR2 - Vasopressin Receptor 2

OXT - Oxytocin

PVN - Paraventricular Nucleus

SON - Supraoptic Nucleus

SCN - Suprachiasmatic Nucleus

CNS - Central Nervous System

GABA - Gamma-Aminobutyric Acid

VGLUT1 - Vesicular Glutamate Transporter 1

AAV - Adeno-Associated Virus

CNO - Clozapine-N-oxide

DAPI - 4′,6-diamidino-2-phenylindole

RNA - Ribonucleic Acid

PCR - Polymerase Chain Reaction

SNP - Single Nucleotide Polymorphism

OTR - Oxytocin Receptor

SSRI - Selective Serotonin Reuptake Inhibitor

ADHD - Attention-Deficit/Hyperactivity Disorder

MIA - Maternal Immune Activation

VPA - Valproic Acid

CA2 - Cornu Ammonis area 2 (of hippocampus)

i.p. - Intraperitoneal

AUC - Area Under the Curve

ROC - Receiver Operating Characteristic

SVM - Support Vector Machine

fMRI - Functional Magnetic Resonance Imaging

CSF - Cerebrospinal Fluid

Acknowledgments

This thesis includes the work I conducted during my PhD at the Laboratory of Cognition and Social Interactions. I am immensely grateful to everyone who accompanied and assisted me throughout this journey.

Firstly, I express my gratitude to my mentor, Félix Leroy, who generously provided me with a place in his laboratory when I was transitioning from a closing lab. This work was conducted under his direct supervision and he taught me invaluable skills in the field of circuits and system neuroscience. I extend my thanks to every individual in the lab, beginning with Antonia, who patiently introduced me to techniques such as immunohistochemistry and *in situ* hybridization. A special thanks to Noelia, with whom I collaborated, learning essential skills ranging from surgeries to the conceptualization and interpretation of experimental data. To Guillaume, who helped me to conclude this history and improved the quality of it. To Lucía, Paula, and Yuki, who became dear friends of mine and made the day-to-day work lighter. Javi, who assisted with the bureaucratic aspects of the work, allowing us to have more time to focus on the scientific aspects of research. And a heartfelt appreciation to Bibian, an indispensable figure crucial to the internalization efforts at the Institute.

I also want to express my gratitude to all the friends I made in Alicante, who made me feel at home despite being continents apart from my hometown. A special thanks to Diana, Mike, Joan and Kevin, who warmly received me when I first arrived in Spain and introduced me to lab research. I learned so much from you guys.

To all my family and friends back in Brasil. Specially Caro, Camila, Tati and Sebbah, who always felt close despite the physical distance and were consistently there for me. To my brother, Juliano, who was the first person to show me that I could indeed dream big. None of this would have been achievable without his support. Thanks to my mom, dad and grandma for supporting my journey to university and abroad. Finally, to my life partner, Roberto, who consistently supported me during this journey and taught me uncountable lessons in scientific thinking. As he once told me, “there is not easy path from Earth to the stars”.

Abstract

The arginine vasopressin neuropeptide (AVP) has been repetitively implicated in autism spectrum disorders (ASD), but yet the mechanisms linking AVP to ASD remain poorly understood. We characterized social behaviors associated with the pathology in male mice of the *Shank3B*$^{+/-}$ mouse model of ASD and found a decrease not just in sociability (preference for a conspecific over an object), but also in social aggression. We then investigated the lateral septum (LS), a key region for the regulation of these two behaviors and found evidence for a decrease in vasopressinergic neuromodulation from the bed nucleus of the stria terminalis (BNST) to LS. Manipulating AVP^{+} neurons from the posterior BNST of wild type mice, we show that release of AVP from the BNST to LS promotes sociability and social aggression. Altogether, our results demonstrate that a decrease in septal vasopressinergic neuromodulation leads to the social behavioral defects exhibited by *Shank3B*$^{+/-}$ male mice. In addition, we show that blocking the vasopressin receptor 1a (AVPR1a) in the lateral septum of WT mice impairs sociability but not social aggression, while blocking of the vasopressin receptor 1b (AVPR1b) prevents social aggression with no effect on sociability. This segregation of action allowed us to selectively rescue sociability or social aggression in *Shank3B*$^{+/-}$ male mice through activation of AVPR1a or AVPR1b respectively. Overall, our findings unravel a mechanism by which a single peptide release within the same region facilitates two separate behaviors through distinct receptors and offer key insights for AVP based translational applications in ASD patients.

Resumen

El neuropéptido arginina vasopresina (AVP) ha sido repetidamente implicado en los trastornos del espectro autista (TEA), pero aún se entienden poco los mecanismos que vinculan la AVP con el TEA. Caracterizamos los comportamientos sociales asociados con la patología en ratones machos del modelo *Shank3B*$^{+/-}$ de TEA y encontramos una disminución no solo en la sociabilidad (preferencia por un congénere en lugar de un objeto), sino también en la agresión social. Luego investigamos el septo lateral (LS), una región clave en la regulación de estos dos comportamientos y encontramos evidencia de una disminución en la neuromodulación vasopresinérgica desde el núcleo de la estría terminal (BNST) hacia el LS. Al manipular las neuronas AVP^{+} del BNST posterior en ratones silvestres, demostramos que la liberación de AVP desde el BNST hacia el LS promueve la sociabilidad y la agresión social. En conjunto, nuestros resultados demuestran que una disminución en la neuromodulación vasopresinérgica septal conduce a los defectos de comportamiento social observados en ratones macho *Shank3B*$^{+/-}$. Además, mostramos que el bloqueo del receptor de vasopresina 1a (AVPR1a) en el septo lateral de ratones silvestres deteriora la sociabilidad pero no la agresión social, mientras que el bloqueo del receptor de vasopresina 1b (AVPR1b) disminuye la agresión social sin afectar la sociabilidad. Esta segregación funcional nos permitió rescatar selectivamente la sociabilidad o la agresión social en ratones machos *Shank3B*$^{+/-}$ mediante la activación de AVPR1a o AVPR1b respectivamente. En general, nuestros hallazgos revelan un mecanismo por el cual la liberación de un solo péptido en una misma región facilita dos comportamientos distintos a través de receptores diferentes y ofrecen claves importantes para aplicaciones traslacionales basadas en AVP en pacientes con TEA.

1 | Introduction

Chapter 1 | Introduction

1.1 An overview of vasopressin and its synthesis in the brain

Vasopressin (AVP) is a hormone and neuropeptide that has been evolutionarily conserved across species. In mammals, AVP functions both peripherally and centrally. As a hormone released into the bloodstream from the posterior pituitary, it plays a key role in maintaining water balance, regulating blood pressure and supporting circadian homeostasis. In the brain, where it acts as a neuropeptide, AVP modulates a variety of behaviors, including stress responsiveness, social bonding, aggression and parental care[1].

1.1.1 Structure, synthesis and secretion of AVP

In rodents, the mature AVP -comprising nine amino acid residues- is synthesized in the cell bodies of magnocellular neurons, primarily located in the paraventricular and supraoptic nuclei of the hypothalamus, as well as in extra-hypothalamic regions such as the bed nucleus of the stria terminalis and amygdala. Upon synthesis, it is encapsulated within membrane-bound neurosecretory granules, alongside the glycopeptide vasopressin and its carrier protein, neurophysin, as depicted below[2]:

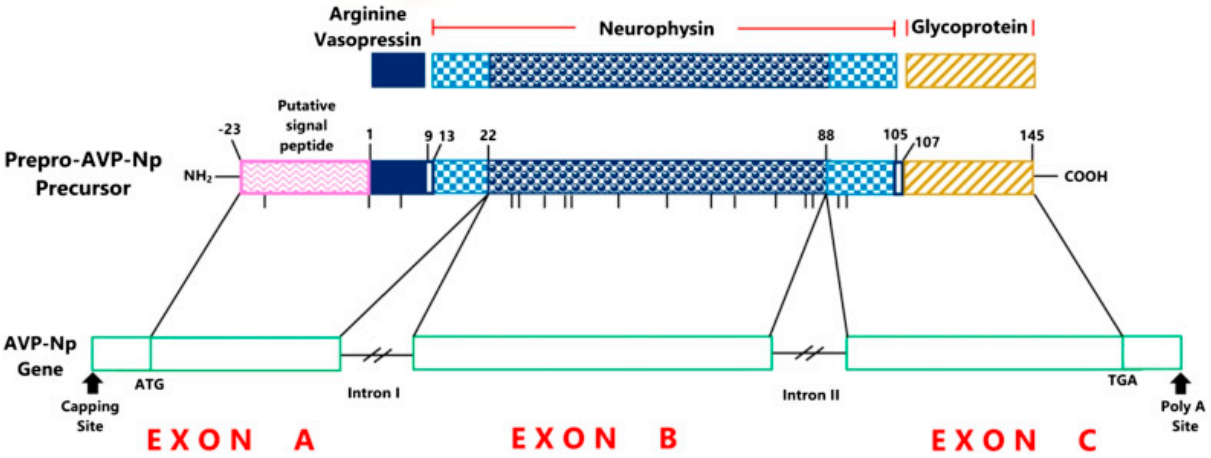

Figure 1. Schematic representation of the structural organization of the AVP gene and ancillary proteins. (Figure adapted from Schmale H, Heinsohn S, Richter D. Structural organization of the rat gene for the arginine vasopressin-neurophysin precursor. EMBO J 1983;2(5):763–7).

The cleavage occurs during the axonal transport in the pituitary stalk into the posterior pituitary, in a classical neurosecretory pathway. Upon the stimulation for the secretion, the peptide is released in the blood. In addition to this classical axonal release that goes into the circulation, AVP can also be released in extracellular compartments of the brain[3]. The concentration of AVP in this case is estimated to be 100 times higher than the plasma concentration. The dendrites originating from the magnocellular cells consist of the predominant source of AVP release in the brain[4].

It's worth noting that the structure of AVP closely resembles another peptide, oxytocin (OX), differing by only two amino acids. In addition to this structural similarity, the *Avp* and *Ox* genes are located on the same chromosome, separated by 1500 genes[5].

1.1.2 AVP synthesis in the brain

In the central nervous system (CNS), the primary sources of AVP synthesis are three hypothalamic nuclei: the paraventricular nucleus (PVN), the supraoptic nucleus (SON), and the suprachiasmatic nucleus (SCN). Within the PVN and SON, two distinct populations of neurons, magnocellular and parvocellular, produce AVP and oxytocin (OXT). Magnocellular neurons project to the posterior pituitary, releasing these neuropeptides into the bloodstream to regulate peripheral functions such as water balance and blood pressure. In contrast, parvocellular neurons project within the brain, modulating neural circuits involved in stress response and social behaviors. Notably, recent studies have revealed that some magnocellular neurons, particularly those producing OXT, also send collateral projections to extrahypothalamic brain regions, indicating a more complex role in central nervous system functions beyond their traditional endocrine activities[6–8].

Additionally, AVP synthesis occurs in other brain regions, including the nucleus circularis, preoptic area, olfactory bulb, anterior hypothalamus, retina, medial amygdala and bed nucleus of the stria terminalis[9].

Bed nucleus of the stria terminalis

The bed nucleus of the stria terminalis (BNST) was first described as a gray matter structure that surrounds the stria terminalis and that expands in its caudal and rostral ends. The caudal portion is now recognized as part of the amygdala, while the rostral

section, positioned ventrally to the lateral septum and dorsally to the hypothalamic area, is delineated as the BNST[10] (Fig. 2).

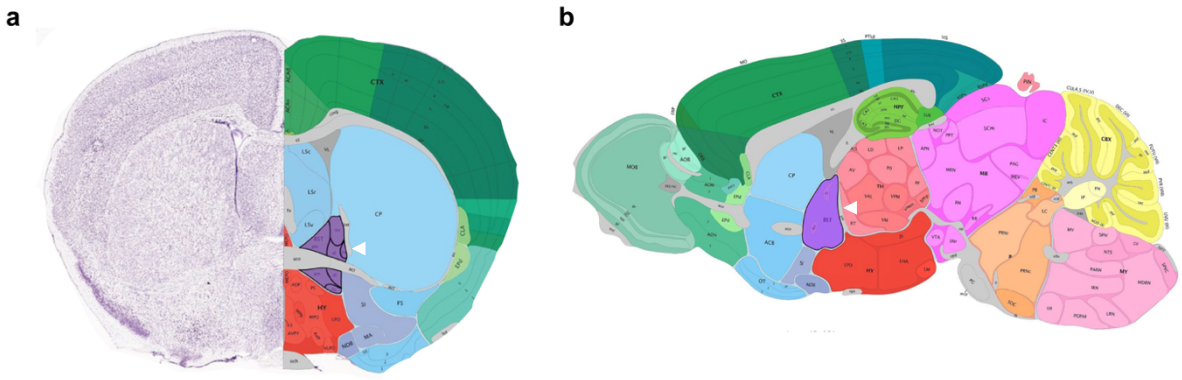

Figure 2. Anatomical view of the BNST. a. Coronal section of the mouse brain with BNST highlighted in purple and arrow indicating it in white. **b.** Sagittal section of the mouse brain with BNST highlighted in purple and arrow indicating it in white. (Figure adapted from Allen Brain Atlas).

This region connects to other limbic structures and is thought to play an important role in the control of autonomic, neuroendocrine and behavioral responses. Some hypothesize that the BNST acts as a relay center between these limbic cognitive centers and the nuclei involved in the processing of reward, anxiety and stress. For these reasons, the BNST seems to have a central role in the integration of physiological and behavioral responses and connecting it to other structures of the brain[11,12].

AVP expression in the BNST is sexually dimorphic manner, with males exhibiting a greater number of AVP^{+} cells and a higher quantity of peptide expression per cell compared to females[13,14]. These cells are also regulated by steroids as they express the AVP peptide mainly in the presence of gonadal hormones[15]. The posterior part of BNST stands out as the most sexually distinct sub-region of the mouse brain[16,17]. It receives rich inputs from the olfactory bulb, accessory olfactory bulb and medial amygdala, while projecting outputs to the ventral tegmental area, hypothalamus and lateral septum[18–20].

Evidence points in the direction that the vasopressinergic cells in the BNST can be involved in a variety of social behaviors, such as: social investigation, affiliative

behaviors, competition, aggression, anxiety and social memory[21]. Studies have demonstrated that the number of AVP cells in the BNST positively correlates with aggression in some species of rodents (California mice)[22]. Moreover, knockdown of AVP^+ cells in the BNST seems to decrease male to male social investigation[23], while lesioning of its posterior aspect markedly reduces male ano-genital sniffing of female social targets and induces deficits in sexual behavior[24–26].

Given these intricate connections, it's reasonable to infer that the posterior BNST plays a crucial role in modulating instinctual sex-specific social behaviors, such as social interaction, aggression, mating and parental care. However, the precise mechanisms and neural circuits by which vasopressinergic BNST cells modulate social behaviors are still unclear and should be investigated taking into consideration the sex of the animals.

1.1.3 The target regions of vasopressinergic neuron projections

The outputs of BNST vasopressinergic cells were primarily investigated through indirect studies that measured the loss of AVP innervation following gonadectomy or BNST lesions. Axonal degeneration was found in the lateral septum, ventral pallidum, horizontal diagonal band, lateral preoptic area, medial preoptic area, lateral habenula, extended amygdala, medial amygdala, ventral tegmental area, dorsal raphe, lateral hypothalamus and periaqueductal gray[27,28].

Lateral septum

The lateral septum (LS) is a broad region centralized in the brain surrounded by the lateral ventricles. It can be subdivided in medial, lateral and triangular areas and is mainly composed by GABAergic spiny neurons. Due to its location, the LS can be considered an ideal center for integrating cortical signals and to regulate the activity of other brain regions as the hypothalamic and midbrain nuclei that control motivated behaviors[29].

The LS is richly innervated by vasopressinergic fibers and AVP receptors[30]. Indirect evidence indicates that the lateral septum receives steroid-dependent AVP signal, likely from the BNST. In rats, castrated animals have less AVP fibers in LS[13] (Fig. 3).

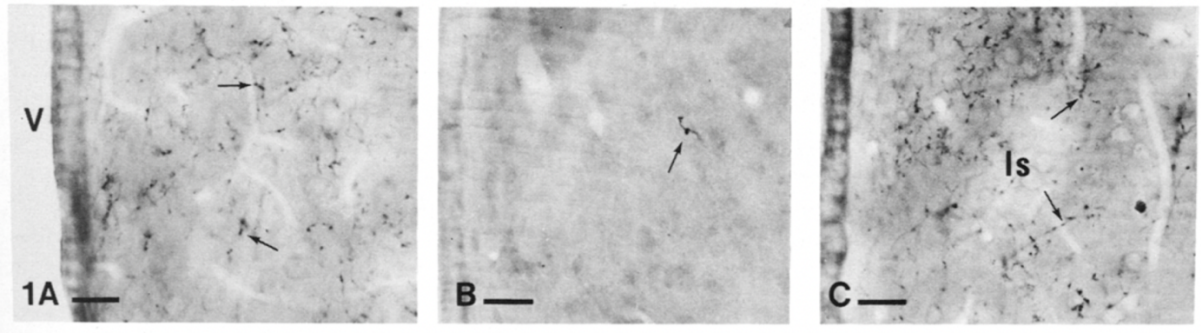

Figure 3. Transverse sections of the lateral septum of 26-day-old male rats, stained specifically for the presence of vasopressin. a. Sham-operated rat. **b.** Neonatally castrated rat. **c.** Neonatally castrated rat which received twice 1 mg testosterone propionate in the first week of life. Arrows point at individual vasopressin fibers. (Figure adapted from De Vries et al., 1983)

Similarly, to the BNST, the LS AVP innervation exhibits sexual dimorphism, with a higher density of fibers in the LS of male rats compared to female rats[31] (Fig. 4). This dimorphism may be attributed to the steroid-dependent nature of the fibers innervation.

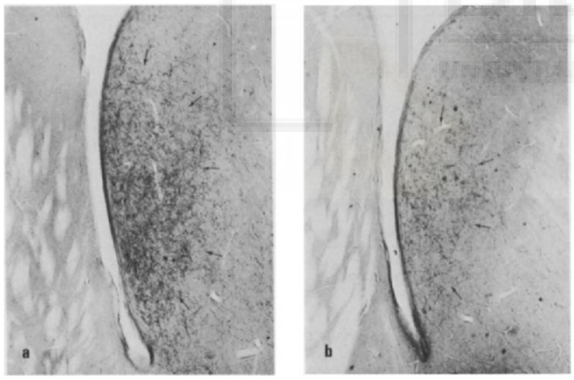

Figure 4. Transverse sections of the lateral septum of the rat stained immunocytochemically for the presence of vasopressin. Note that the density of the vasopressin fiber network (arrows) is higher in the male (a) than in the female rat (b). (Figure adapted from De Vries et al., 1981)

Lesions in the BNST, combined with tract tracing and AVP immunofluorescence, have shown that the posterior BNST is responsible for the sexually dimorphic innervation of the LS[32]. However, direct evidence pinpointing the exact origin of vasopressinergic projections to the LS in mice remained elusive. Recent studies employing *Avp*-Cre mice and anterograde viral tracing have now confirmed that these projections originate from the BNST and exhibit sexual dimorphism[21] (Fig. 5).

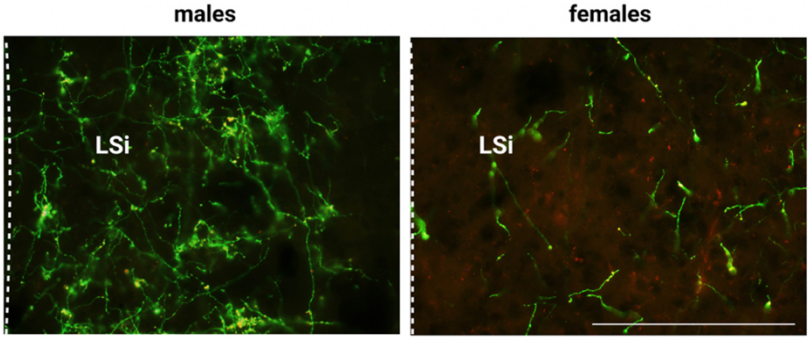

Figure 5. BNST AVP cell outputs in males and female mice. Example of merged images of the LS that received BNST AVP cell output fibers (green) and presynaptic puncta (red) labeled with GFP-2A-Synaptophysin-mRuby virus. (Figure adapted from Rigney et al., 2023)

These findings underscore the critical importance of considering sexual dimorphism in research on social behavior. Moreover, given the LS role in promoting motivated behaviors and its rich innervation with AVP, a peptide known to be involved in social behaviors, it stands out as an ideal center for investigating the influences of peptide release on social behavior.

1.2 AVP receptors

The AVP receptors are vasopressin receptor 1a (AVPR1a), vasopressin receptor 1b (AVPR1b) and vasopressin receptor 2 (AVPR2). These receptors are G protein-coupled that work by the interaction with trimeric G proteins. Each of the receptors have a different tissue expression. In the human and rodent brain, AVP can bind to three receptors: AVPR1a, AVPR1b and oxytocin receptor[33].

The expression of the AVPR1a is pronounced within the murine LS. Global knockout experiments of this receptor have demonstrated a reduction in social interaction[34], while AVPR1a antagonistic infusion directly into the LS impaired social recognition[35], indicating a crucial role for AVPR1a in mediating social behaviors through its action in the LS.

Likewise, AVPR1b contributes to the activation of the hypothalamo-pituitary-adrenal axis and is found in the CA2 region of the hippocampus and the anterior region of the amygdala, areas implicated in social behavior[36]. The CA2 region expresses AVPR1b in its terminals projecting into the dLS[37]. Knockout of this receptor reduces aggressive behavior[38], while AVPR1b antagonist infusion directly into the LS impairs aggression[39]. Together, these findings underscore the significant roles of AVPR1a and

AVPR1b in regulating various social behaviors through their respective actions in the LS.

1.3 AVP function in the brain and behavior

Vasopressin serves as a neuropeptide intricately involved in diverse social behavioral responses. Compelling evidence suggests that AVP has a significant role in regulating sociability and antagonistic social behaviors, such as social aggression[21].

1.3.1 AVP and social interaction

The ability to interact socially and distinguish between familiar and unfamiliar individuals is a fundamental skill essential for navigating social environments across species. In studies involving rodents, the administration of arginine vasopressin (AVP) via subcutaneous injections in male rats has been shown to prolong the duration of social memory, enabling the retention of information from past social interactions[40]. Further investigations revealed that injecting AVP directly into the brain's ventricles immediately after initial encounters with other animals enhanced social memory, mirroring the effects observed with peripheral AVP administration[41]. Conversely, administering peripheral AVP antagonists impaired social recognition in intact male rats, although no such effect was observed in castrated individuals, suggesting a role for sex hormones in regulating social recognition[42].

Additionally, central administration of anti-AVP serum resulted in impaired social recognition in male rats[43]. These experiments collectively demonstrate that targeted delivery of AVP, both by peripheral and central administration routes, influences aspects of social interactions. However, an intriguing question remains: what is the specific contribution of individual brain regions in promoting social interactions?

Recent studies have begun to unravel this question by exploring the involvement of AVP-innervated regions on social behavior. In this scenario, AVP in the LS plays a prominent role in regulating social recognition and social memory. Studies involving AVPR1a knock-out mice reveal that re-expressing AVPR1a in the LS, and its overexpression in WT, can normalize and enhance social memory[44,45]. In rats, social recognition impairment stemming from early life stress, correlates with a diminished AVP release response in the LS[46]. Furthermore, male Brattleboro rats lacking AVP

showed impaired social recognition, which was restored by micro dialysis of AVP into the septum[47]. In other species like the prairie vole (*Microtus ochrogaster*), variations in the density of AVP fibers in the septal region correspond to different types of parental behavior and the use of AVPR1a antagonists promotes a reduction in parental responsiveness[48].

Other aspects of social behavior also appear to be mediated by the AVP peptide in the LS. Monogamy, the practice of forming a long-term pair bond with a single mate, holds social significance in various contexts and it can predict stability, parental care, allocation of resources and social cohesion. Septal AVP has also been correlated with monogamy in some species of animals. Monogamous mice (*Peromyscus californicus*) have more AVP receptors in the LS when compared to polygamous mice (*Peromyscus maniculatus*)[49].

In studies involving healthy adult human volunteers, AVP in the LS seems to play a role in social recognition. The intranasal administration of AVP has been shown to enhance the activity of this brain region during the observation photography of faces in fMRI studies[50]. These findings underscore the significance of AVP in the LS concerning social recognition processes in humans.

In addition to the LS, other brain regions seem to be involved in the modulation of social behaviors through AVP action. In humans, fMRI studies suggest that AVP can influence a circuitry involving the pre-frontal cortex (PFC) and amygdala during the processing of emotions, particularly in facial recognition[51]. Additionally, among children diagnosed with Autism Spectrum Disorder (ASD), a condition known for impairing social function, a negative functional connectivity between the amygdala and supramarginal gyrus was observed alongside lower AVP plasma levels, specifically in boys[52]. This points to a sexual dimorphism in both vasopressin expression in the human brain and the associated behaviors, mirroring observations made in rodents.

Cortical regions such as the PFC serve as centers for motivation, affiliation, empathy, and social hierarchy, which are all crucial components in social interactions. Studies have shown that prairie voles treated to exhibit social deficits exhibit reduced expression of *Avpr1a* mRNA in the PFC, leading to decreased sociability[53,54]. Regarding subcortical regions, the BNST is linked to fear response and social anxiety

in humans, particularly in reaction to unpredictability[55]. In juvenile rats, $BNST^{AVP}$ neurons are implicated in the facilitation of social play[56]. Additionally, a reduction in AVP expression in the BNST, achieved through knock-down, is associated with decreased exploration time toward a social stimulus in male subjects[57].

Given the compelling evidence for the role of AVP in modulating social behaviors, it becomes essential to focus research efforts on specific brain regions where AVP exerts its influence. The LS and the BNST emerge as two particularly relevant structures. Both are richly innervated by AVP and are deeply involved in distinct but complementary aspects of social interaction, such as social recognition, pair bonding, stress reactivity, and social play. Investigating AVP signaling within these regions offers a promising avenue for understanding the neural mechanisms underlying complex social behaviors and their dysregulation in conditions such as social anxiety or ASD.

1.3.2 AVP and social aggression

The modulation of aggressive behavior by AVP is conserved in different species. In Zebrafish (*Danio rerio*), the levels of AVP in the brain is higher in animals winning after an aggressive encounter[58]. While sexually naive prairie voles typically exhibit minimal territorial aggression, the exposure to AVP during early postnatal stages can elevate aggression levels to a degree comparable to that observed in post-mated animals[59]. However, in ecological experiments performed in free-living ground squirrels (*Urocitellus richardsonii*), AVP administration via osmotic minipump increased social vocalization but decreased social aggression[60].

Results from laboratory studies in rodents also present conflicting findings. For instance, injections of AVP in the hypothalamus have been found to promote aggression in hamsters[61]. While research conducted on rats has shown that the release of AVP in the lateral septum LS facilitates intermale aggression, whereas AVP release in the BNST diminishes such behavior[62].

Contrary to these findings, a study observed a denser AVP-immunoreactive (AVP-ir) innervation in the LS and higher AVP-ir neural density in the BNST in male mice with long attack latency compared to those with short latency[63]. Similarly, a study in rats found a negative correlation between LS AVP levels and intermale aggression[64]. It is

important to notice that in both studies, aggressive and non-aggressive mice were defined based on latency to attack rather than the display of aggressive behavior.

In contrast, Peromyscus californicus (California mouse) exhibits higher aggression levels compared to Peromyscus leucopus (white-footed mouse), with a positive correlation observed between aggression and AVP-ir in the BNST and LS[65]. In addition, California mice newborns that receive more retrieval care from their fathers tend to exhibit higher aggression levels in adulthood compared to those receiving less care and these animals display increased AVP-ir fibers in the dorsal fiber tracts of the BNST[66].

In mice, AVPR1b expression in the CA2 have been demonstrated to regulate social aggression. Findings suggest that the hippocampal CA2 region plays a crucial role in responding to male intruders with aggression. Furthermore, the AVPR1b receptor, likely by regulating synaptic plasticity in the CA2 region, serves as an essential mediator in this process[67]. Moreover, AVPR1b is expressed at the pre-synaptic terminals of CA2 pyramidal neurons where its activation facilitates the flow of information from CA2 to LS to promote social aggression[39].

Conversely, studies in mice have shown decreased aggression in animals treated with AVP and OT, whereas the combination of OT and an intraperitoneal AVPR1a antagonist increased aggression[68], suggesting that AVPR1a may not play a significant role in promoting aggressive behavior. Supporting this, experiments with AVPR1a knockout (KO) mice revealed that the absence of this receptor does not impair aggression[69]. In contrast, AVPR1b appears to be crucial for the proper expression of aggressive behavior. Mice lacking AVPR1b (*Avpr1b*$^{-/-}$) display significant impairments in aggression, including increased latency to attack and reduced attack frequency[70–72]. Furthermore, oral administration of an AVPR1b antagonist has been shown to reduce aggressive behavior in hamsters[73].

As described previously, the vasopressinergic system within the LS and BNST is sexually dysmorphic, with females presenting less BNST AVP^{+} cells and less LS^{AVP} fiber innervation. For these reasons, the regulation of social behaviors modulated by AVP might differ between sex. Studies focusing on investigating aggression in female rats have demonstrated that enhanced OT release within the vLS, combined with a

reduction in the release of AVP within the dLS may be promoting aggression in female rats[74]. This suggests a negative correlation between LS^{AVP} release and aggression in females.

In humans, a positive correlation of cerebrospinal fluid (CSF) AVP concentration with history of non-directed general aggression (e.g., property assaults and emotional outbursts) and aggression towards individuals can be found[75]. Moreover, in men intranasal administration of AVP is reported to heighten the emotional response to neutral stimuli, leading to an increased perception of threat[76,77]. Like findings in rodent models, this observation suggests that AVP may enhance aggression, although it's important to acknowledge that consensus is lacking among studies. For instance, another study reported no differences in CSF AVP levels between violent offenders and controls[78].

Taken together, these results highlight the conflicting findings regarding the modulation of aggressive behavior by the AVP peptide. These discrepancies may be attributed to the experimental specificity, such as whether AVP administration is central or peripheral, as well as the species and the specific interactions with various AVP receptors involved. Studies unraveling the contributions of specific vasopressinergic brain circuits and their interaction with particular receptors are necessary to elucidate these discrepancies in results. Despite these variations, a consistent theme across studies is the prominent role of the LS and BNST as key hubs in the regulation of AVP-mediated social behaviors, including aggression.

1.4 The role of AVP in pathologies that impair social functioning

Neuropeptides have recently gained attention as potential involvements in a variety of conditions such as anxiety, depression, attentional hyperactive deficit disorders (ADHD), substance abuse disorder, schizophrenia and autism spectrum disorder (ASD). As social interactions are tightly regulated by several neuropeptides, including arginine-vasopressin, several studies have linked AVP-mediated neuromodulation to ASD[79–81].

1.4.1 Autism spectrum disorder (ASD)

ASD is described as a pervasive neurodevelopmental disorder, where the core symptoms include deficits in social communication accompanied by anomalous socioemotional responses in diverse contexts. Other relevant symptoms include restrictive and repetitive patterns of behaviors[82].

Despite the deficits in social interaction, increased aggression is also often associated with ASD. Studies have shown that children under the age of 6 with autism display markedly higher levels of aggression than their non-autistic peers. However, as these children mature, their aggression levels tend to normalize and become comparable to those of their non-autistic counterparts[83]. Additionally, other studies support the idea that factors such as younger age, lower family income, and communication challenges can contribute to aggression in male autistic individuals, with a noted sex difference[84]. In adults, a study found that aggression may diminish in severity over time[85]. Taken together, these findings indicate that while aggression is often associated with ASD, there is a consensus that these behaviors tend to be more pronounced in younger children.

The prevalence of ASD, with a ratio of 4.3:1 for boys to girls, is on the rise and varies between countries[86,87]. Discrepancies in sex and geographic prevalence may arise from differences in diagnostic criteria and potential misdiagnosis in women due to variations in symptom presentation. The etiology of ASD remains elusive, with the potential involvement of multiple causative factors, such as genetical, environmental and stress vulnerability[88].

Recently, research exploring the role of AVP in ASD has garnered significant interest. In human studies, certain single-nucleotide polymorphisms (SNPs) of AVPR1b, such as rs35369693 and rs28632197, have been linked to ASD[89]. While SNPs including rs11174815, rs7294536, rs3759292, and rs10877969 of AVPR1a have also shown associations with ASD[90,91].

Low levels of AVP in cerebrospinal fluid (CSF) have been proposed as an early biomarker of ASD in humans[92]. Additionally, the blood level of AVP has been found to correlate with the severity of certain symptoms[93,94]. In peripheral blood mononuclear cells, the expression of AVPR1a has shown a positive correlation with improvements

in social and behavioral function in children with autism[95]. Moreover, maternal levels of AVP have been associated with the symptoms of offspring, with lower levels observed in mothers of children diagnosed with ASD[96].

Despite what is known from human studies, research conducted in animal models is essential for thoroughly investigating the mechanisms underlying ASD and identifying potential treatments.

Animal models for studying ASD

The animal models employed to investigate ASD can be classified into two distinct categories: genetic and environmental. The first englobe mutation in the OTR, NLGN, SRC homology 3 and multiple ankyrin repeat domains protein (SHANK), Contactin Associated Protein 2 (CNTNAP2), Melanoma Antigen Gene Family Member L2 (MAGEL2) and a zinc-finger transcription factor TSHZ3[97–99]. The second category involves drug-induced models, typically utilizing valproic acid (VPA), where administration of VPA to pregnant mice can result in offspring exhibiting neurodevelopmental and behavioral characteristics similar to ASD symptoms. In addition, immunological models, which involve inducing maternal immune activation (MIA) through the administration of polyribocytidylic acid (poly I:C) during embryonic ages E 11.5–13.5[100].

Researchers utilize various behavioral tasks to identify symptoms associated with ASD including deficits in sociability (preference for interacting with an object over a conspecific), repetitive behaviors and restricted interests[101]. A variety of species are used for this aim, including *Drosophila melanogaster* and zebrafish, but the frequent most used are rodents[102,103].

In rodents, AVP treatment has been shown to ameliorate social deficits in certain mouse models. In the OTR-deficient mouse model, AVP acts on AVPR1a to improve social deficits[97]. Similarly, in the CNTAP2-deficient mouse model, where the CNTAP2 gene is implicated in ASD-like symptoms, AVP treatment mediated by OT receptors has been found to improve social deficits[104]. Furthermore, in the MAGEL2 mouse model, characterized by a deficiency in the MAGEL2 gene associated with ASD-like symptoms and Prader-Willi Syndrome, deficits in the expression of AVP^{+} fibers in the LS are correlated with impairments in social discrimination[105].

The *Shank3B* knockout mice are a validated model for studying ASD-related behaviors and are widely utilized in autism research. These mice exhibit characteristics such as atypical reciprocal social interactions and repetitive grooming[106]. This mouse model is created using gene targeting to delete the SHANK3 gene, which encodes essential proteins for the formation of core signalling complexes and plays a role in assembling synaptic scaffolding proteins located in the post-synaptic density of excitatory glutamatergic synapses[107].

In humans, mutations in the SHANK3 gene have been linked to ASD[108]. In *Shank3* rats, impairments in long-term social recognition memory were mitigated by OX administration, despite nearly normal endogenous levels of both OX and AVP[109,110]. However, the AVP system in the *Shank3* mouse line remains relatively unexplored. These findings suggest that Shank3B mice offer a valuable avenue for investigating the role of AVP modulation in ASD.

Treatments for ASD

Currently there is no cure or medication to directly treat ASD. Some medications are used to treat associated symptoms such as anxiety and depression. Commonly prescribed drugs include selective serotonin reuptake inhibitors (SSRIs), dopamine and noradrenaline stimulant methylphenidate and antipsychotics. However, recent strategies to the treat the core symptoms of the pathology envision to target neuroinflammation, synaptic dysfunctions and central AVP, OT and serotonin release[111].

From the current used medications, SSRIs show promise in enhancing both eye contact and mood, thereby decreasing the occurrence and severity of repetitive behaviors[112]. Conversely, Ritalin, a dopamine reuptake inhibitor, is utilized to treat hyperactivity and lack of attention. This drug has been demonstrated to influence the vasopressinergic system and to act via the AVPR1a[113,114].

Direct administration of AVP has been employed to alleviate symptoms associated with ASD. In rat studies, maternal VPA injections, which induce social deficits, were associated with decreased vasopressinergic serum levels. Intranasal AVP treatment subsequently led to symptom improvement[115]. In humans, a phase 2 randomized clinical trial demonstrated that 4 weeks AVP intranasal administration in children aged

6 to 13 years improved social abilities and responsiveness, with a decrease in repetitive behaviors and anxiety. The most robust response was observed in patients with high-plasma AVP levels, and this response was contingent upon the expression pattern of the AVPR1a and OT receptors[116].

Given the potential for AVP to bind to oxytocin receptors, as previously mentioned, it's noteworthy that various animal trials investigating OT treatment have indicated favourable outcomes. In children, even a single intranasal administration of OT led to enhanced nonverbal information-based judgments[117]. While findings have been inconsistent, a recent meta-analysis revealed moderate evidence suggesting that a six-week OT treatment regimen could ameliorate reduced interest and repetitive behaviors in children with ASD, with effects persisting for at least six months[118].

Recently, there has been a surge in interest in AVP receptor antagonists, particularly AVPR1a selective molecules. In a double-blinded crossover study conducted in 2017, the intravenous infusion of a highly selective AVPR1a antagonist, RG7713, was shown to improve social sensitivity and communication in adult men with high-functioning ASD[119]. Additionally, a double-blinded, placebo-controlled clinical trial involving 223 adult men with high-functioning ASD, utilizing another AVPR1a antagonist, the RG7714 commercially known as Balovaptan, demonstrated improvements in socialization and communication after three months of treatment. However, no enhancements in social responsiveness were noted[120]. Subsequent phase 3 trials involving high-functioning children and adults receiving six months of drug treatment failed to show effectiveness in improving social communication[121,122].

In conclusion, there are conflicting findings regarding the efficacy of AVP treatments for ASD, particularly concerning AVP antagonist drugs. These discrepancies underscore the need for a more comprehensive understanding of the AVP brain circuits implicated in ASD, as well as the receptor mechanisms through which this neuropeptide influences behavior.

To address this, the main objective of this research is to investigate the role of AVP release from the BNST to the LS in social behavior regulation, using the *Shank3B*$^{+/-}$ male mouse model of ASD. Specifically, this study aims to:

1. Determine whether impairments in AVP signaling from the BNST to LS contribute to the social behavior deficits exhibited by the *Shank3b*$^{+/-}$ mouse model of ASD.
2. Elucidate the receptor-specific mechanisms of AVP action within this circuit, with the goal of identifying potential targets for novel therapeutic interventions.

2 | Methods

Chapter 2 | Methods

2.1 Ethical approval

All the experimental procedures were in conformity with the directive 2010/63/EU of the European Parliament and of the Council, and the RD 53/2013 Spanish regulation on the protection of animals use for scientific purposes, approved by the government of the Autonomous Community of Valencia, under the supervision of the Consejo Superior de Investigaciones Científicas and the Miguel Hernandez University Committee for Animal use in Laboratory.

2.2 Animals

8- to 16-week-old male C57BL6/J (Jackson Laboratories, #000664), *Avp-Cre*$^{+/-}$ mice (Jackson Laboratories, #023530) and *Shank3B*$^{+/-}$ mice (Jackson Laboratories, #017688) were used as experimental subjects. For experiments with mutant mice, wild type (WT) littermates were used as control group. Same age Balb/cByJ (Jackson Laboratories, #001026) male mice were used as intruders during the resident intruder test and C57BL6/J male mice (Jackson Laboratories, #000664) as stimulus mice during the social interaction tests.

2.3 Stereotaxic surgeries

Surgical procedure

Animals were anesthetized with isoflurane and placed in the stereotaxic apparatus. An intramuscular injection of Carpofren was used as anti-inflammatory drug. Eyes were covered with ophthalmic gel (Viscotears 2mg/g) to prevent corneal desiccation. The hair of the head was removed, and the tissue was sterilized. Following the opening of the head´s tissue, a small craniotomy was performed above the target region and a thin glass pipette was placed on the desired depth to deliver the viral content. Injections were performed using the nano-inject II (Drummond Scientific) with a rate of 23 nl every 11 seconds with a 10 second delay between each. With the heterozygous animals, both Cre and WT littermates were injected with the Cre-

dependent viruses. The skin was then closed with surgical glue and animals rested in a recovery chamber until restoration of normal locomotor activity.

Viral vectors

· For anterograde tracing, 100 nL of AAV2/1 syn.FLEX.GCaMP6f.WPRE.SV40 (Addgene, #100833-AAV1) was injected unilaterally in the posterior BNST of *Avp-Cre* mice (injections coordinates accordingly to the Allen Brain Atlas: AP: +0.02 mm, ML: ±0.75, DV: -4.75 from the cranium). These coordinates were used for all subsequent BNST injections.

· For retrograde tracing, 100 nl of the herpes simplex virus hEF1a.LSIL.GFP (Rachael Neve, Massachusetts General Hospital, #RN406) was injected into the LS of *Avp-Cre* mice (coordinates: AP: +0.24 mm, ML: ±0.50, DV: -3.30 from the cranium). These coordinates were used for all subsequent LS injections.

· For AVP^{+} cell labelling in VGLUT1 experiments, AAV2/9EF1a.DIO.hChR2 (E123T/T159C).eYFP8 (Addgene, #35509) was injected in the posterior BNST of *Avp-Cre* x *Shank3B*$^{+/-}$ and WT controls mice.

· For chemogenetic experiment, 200 nl of AAV2/8 hSyn.DIO.hM4D(Gi)-mCherry (Addgene, #44362-AAV8) was bilaterally injected in the posterior BNST of *Avp-Cre* mice and WT littermates.

· For fiber-photometry calcium recording, 100nl of AAV2/1 syn.FLEX.GCaMP6f.WPRE.SV40 (Addgene, #100833-AAV1) was bilaterally injected in the posterior BNST of *Avp-Cre* mice.

· For AVP biosensor recordings, 200nl of AAV9-hSyn-AVP0.3 was unilaterally injected in LS of C57BL6/J.

· For optogenetic silencing experiments, 200 nl of AAV2/1 hSyn1-DIO-eOPN3-mScarlet-WPRE (Addgene, #125713-AAV1) was injected bilaterally in the posterior BNST of *Avp-Cre* and WT littermates.

· For the *Avp* knock-down experiment, 200 nl of AAV2/9 GFP.U6.anti-*Avp*-shRNA or AAV2/9 GFP.U6.scramble-shRNA (Vector Biolabs, #253437-shAAV) were injected bilaterally in the BNST of C57BL6/J mice as experimental or control condition

respectively. All viruses expressed for a minimum of 2 weeks before the beginning of experiments except for the shRNA-expressing AAVs that expressed for 1 week only.

Fiber optic implants

Animals were anesthetized with isoflurane and placed in the stereotaxic apparatus. An intramuscular injection of Carpofren was used as anti-inflammatory drug. The above-scalp tissue was sterilized and completely removed. VetbondTM (3M™ #7000002814) was applied on the peripheries of the cut to hold the tissue. Two screws were placed on the back of the cranium to provide a sturdy foundation for the implant. A craniotomy was performed above the target region and an optical ferrule (200 µm core, black ceramic ferrule, Neurophotometrics) was lowered until the desired depth. Superglue was applied to hold the lens in position and dental cement (GC FujiCEM 2) was applied to cover the exposed skull and to maintain the optical ferrule in place. For fiber-photometry calcium and vasopressin recordings, the optical ferrule implant was placed in LS at the following coordinates AP: +0.24, ML: 0.5, DV: -2.80 (from the cranium). For optogenetics silencing of BNST terminals, the optical ferrule implant was placed in LS at the following coordinates AP: +0.24, ML: 0, DV: -2.80 (from the cranium). Animals remained undisturbed for a week after the procedure.

Guide cannula implants

The mouse scalp was removed and scored before a hole was drilled (AP: +0.24, ML: ±0.00). A cannula guide extending 2.4 mm below the pedestal (Plastics One, #C315G 2-G11-SPC) was lowered slowly and kept in place using superglue. The skull was then covered with dental cement (GC FujiCEM 2) and dummy cannulas (Plastics One, #C315DC-SPC) were inserted into the guides. The mice were returned to their home cages and left to recover for at least 3 days. Mice were immobilized by the experimenter and the dummy cannula was removed. A cannula (Plastics One, #C315I-SPC) projecting 1.7 mm from the tip of the cannula guide was mounted.

2.4 Histology and immunohistochemistry

Animals were anesthetized with isoflurane and intracardially perfused with 10 mL saline. The brains were quickly extracted and incubated in 4% PFA overnight. The

brains were washed for 1 hour in PBS and 50µm slices of the regions of interested were sliced using a Leica VT1000S vibratome (Leica Biosystems).

Immunohistochemistry

The slices were permeabilized for 2 hours in PBS with 0.5% Triton-X100 (T9284, Sigma-Aldrich) before being incubated overnight at 4°C with primary antibodies diluted in PBS with 0.5% Triton-X in PBS. The slices were washed in PBS for 1 hour then incubated for 2 hours or overnight at 4°C with secondary antibodies from Thermo-Fisher Scientific at a concentration of 1:500 diluted in PBS with 0.1% Triton-X. Hoechst counterstain was applied (Hoechst 33342 at 1:1000 for 30 minutes in PBS at RT) prior to mounting the slice using fluoromount (Sigma-Aldrich).

c-Fos labelling

For c-Fos labelling, primary incubation was performed overnight at 4°C with anti-c-Fos antibody (1:1000, Abcam, #ab190289). Secondary incubation was performed with an anti-rabbit antibody conjugated to Alexa 488 (#A11039) at a concentration of 1:500 for 2 hours at room temperature.

Anti-vasopressin labelling

For vasopressin labelling primary incubation was performed overnight at 4°C with anti-vasopressin antibody (1:1000, Merck, #PC234L). Secondary incubation was performed with an anti-rabbit antibody conjugated to Alexa 488 (#A11039) (1:500) overnight.

Anti-VGLUT1 labelling

For anti-VLGUT1 labelling primary incubation was performed overnight at 4°C with anti-VGLUT1 antibody (1:2000, Millipore, #ab5905). Secondary incubation was performed with an anti-guinea pig antibody conjugated to Alexa 594 (#A11076) (1:500) for 2 hours at room temperature.

RFP labelling

For RFP labelling intensification of the signal, primary incubation was performed overnight at 4°C with rabbit anti-RFP (1:500, Rockland Antibody, #600-401-379) and

secondary incubation was performed with anti-rabbit antibody conjugated to Alexa 568 (#A11011) (1:500) for 2 hours at room temperature.

GFP labelling

For intensification of the GFP labelling, primary incubation was performed overnight at 4°C with and chicken anti-GFP (1:1000, Aves, #GFP-1020) antibodies. Secondary incubation was performed with anti-chicken antibody conjugated to 488 (#A11039) (1:500) overnight.

2.5 In situ hybridization

Animals were anesthetized using isoflurane and decapitated. The brains were quickly extracted and immersed in dry-ice cooled 2-methylbutane for 6 seconds before being stored at 80°C. 20µm slices of the region of interest were prepared using a Leica cryostat (CM3050 S, Leica Biosystems) and mounted on Superfrost Plus microscope slides (12-550-15, FisherBrand). The slices were then processed following the RNAscope® Multiplex Fluorescent Detection Reagents v2 (CN:232110, ACD Bio) with the probes for *Avp* in C1 (#401391) and *Avpr1a* in C3 (#418061-C3). Protease IV was applied for 2 minutes and the TSA Vivid Dyes 520 for AVP and 650 for Avpr1a were used. DAPI was applied for 30 seconds prior to mounting using fluoromount.

2.6 Drugs

For hM4D activation, i.p. administration of clozapine-N-oxide dihydrochloride (CNO, HB6149 Hello Bio) dissolved in physiological saline (0.9% NaCl) at a dose of 3 mg kg−1 in a volume of 10 ml kg−1, was used 30 minutes before the behavioral experiments. I.p. injections of saline (0.9% naCl) were used 30 minutes before the behavioral experiments as a control condition. All animals (control and iD) received i.p. CNO injections and saline injections. Saline experiments were performed with 3 days of interval for the sociability test and 1 week of interval for the resident-intruder test to prevent heightened aggression resulting from close repetitive exposure to an intruder in the home-cage.

For the guide cannula experiments, C57BL/6 mice were infused in the dorsal region of middle of the septum with 1 µl of saline, 1 of the µl the antagonist of the vasopressin

receptor 1b (AVPR1b) (1 mM SSR149415 solution), or 1 µl of the antagonist of the vasopressin receptor 1a (AVPR1a) (SR49059 1 mM solution). *Shank3B*$^{+/-}$ mice were infused in the dorsal region of middle of the septum with 1 µl of saline, 1 µl of Desmopressin, the agonist of the vasopressin receptor 1b (AVPR1b) (100 µM DDAVP solution), or 1 µl of AVP together with the antagonist of AVPR1b SSR149415 (AVP 1 mM + SSR149415 2 µM solution) to selectively activate AVPR1a only.

All drugs came from Tocris. Drugs were infused at a rate of 0.2 µl per minute using a programmable syringe pump (Chemyix Inc.) mounted with a 2 µl syringe (Hamilton #88511). After infusion, animals were undisturbed for 5 minutes before the start of the experiment. Drugs were randomized per animal during the sessions and each session was performed with 3 days interval for the sociability test, and 1 week of interval for the resident-intruder test. For checking the guide cannula infusion localization in the brain, mini-Ruby (Invitrogen, D1868) was used. A total of 1 µl was infused at a rate of 0.2 µl per minute. 60 minutes after infusion, animals were perfused.

2.7 Behavioral tests

All animals were housed preferentially with littermates (maximum of 5 per cage) at a temperature of 24 C° in the Institute of Neuroscience animal facility with 12-hour daily illumination and food and water ad libitum.

Open arena test

Animals were placed in a white open arena (OA) (60cm x 60cm) and allowed to explore freely the space for 10 minutes. Automatic tracking software (Any-Maze 7, Stoelting) was used to quantify the time spent in the center and surroundings, as well as the total distance travelled by the animal.

Social interaction test

Animals were insolated in their home-cage and 2 minutes calcium recording sessions were conducted in the empty home-cage. Subsequently, a stimulus mouse (Balb/cByJ) was introduced for another 2 minutes. Animals were allowed to freely explore, and the frequency and amplitude of the calcium signal was quantified for both conditions.

Sociability test

Wire cup cages were placed diagonally in opposite corners of the OA. One of the cups was empty and the other had a male same-aged unfamiliar mouse under it. Test subjects were allowed to freely explore the OA for 5 minutes. The same automatic tracking software described above was used to generate regions of interest around the cups and to provide an output of the total time spent interacting with both cups. A discrimination index was used to calculate the interaction time with both cups: (time with social cup – time with empty cup) / total interaction time.

Social novelty preference test

For the learning trial, mice were placed in the OA containing two wire cups with one male same-age unfamiliar mouse under each cup. The cups were placed diagonally at opposite sides of the arena and the test mouse could freely explore for 5 minutes. The test mouse was then single housed in a chamber for 30 minutes. For the recall trial, one of the animals under the wire cup was replaced with a novel unfamiliar mouse. The test mouse was then placed again in the OA and could freely explore. The automated software for tracking was used for quantifying the interaction time with both animals under the cup. A discrimination index was used to calculate the interaction time with familiar and novel mouse for the recall condition: (time with novel – time with familiar) / total interaction time.

Resident-intruder test

Animals were single housed in a cage with food and water *ad libitum* for a week prior to the testing day. During this week, animals were undisturbed, and the bedding of their cage was not changed in order to preserve odors that can favor the development of territoriality. An intruder male mouse (Balb/cByJ) was placed inside the cage and the social interactions were recorded for 10 minutes. The software Any-Maze (Stoelting) was used for manual assignment of the social behaviors displayed through key pressing. The following social behaviors were quantified: **social exploration** (facial and ano-genital sniffing), **dominance** (resident mouse rising onto its hindlimbs to paw at the intruder's head, as well as excessive grooming, chasing or mounting), and **attack** (biting attack followed by fighting and tail rattling) (Fig. 6). For the c-Fos experiments, the same protocol was followed but following completion of the test,

animals were undisturbed for 60 minutes for the expression of the immediate-early gene and then perfused as previously described.

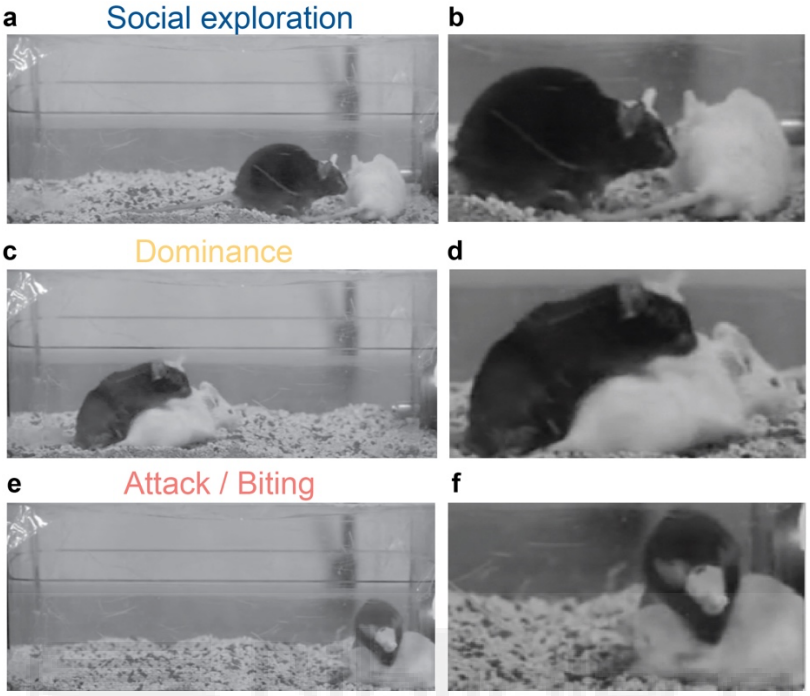

Figure 4. Example frames showing the quantified behaviors during the resident-intruder test. a. Social exploration. **b.** Zoom in of the social exploratory behavior. **c.** Dominance. **d.** Zoom in of the dominance behavior. **e.** Attack / biting. **f.** Zoom in of the biting moment. (Figure modified from Leroy et al., 2018).

2.8 Development of the $GRAB_{AVP0.3}$ sensor

The development, optimization, and characterization strategy of the $GRAB_{AVP0.3}$ followed the methodology of our previously developed GRAB sensors[79]. The $GRAB_{AVP0.3}$ was developed based on human AVPR2 and optimized by mutagenesis screening of fluorescent protein, linker region and GPCR. Then $GRAB_{AVP0.3}$ was cloned into a pAAV vector and packaged into AAV virus for *in vivo* expression.

2.9 Fiber-photometry calcium recording data acquisition

Animals were habituated to the optical fiber patch cord for 1 day before the test. The optical fiber patch cord was placed on top of the mouse's implant and the sociability test and resident-intruder test were performed as previously described while recording calcium activity from vasopressinergic BNST terminals in LS. Data acquisition was performed using the FP3002 system from Neurophotometrics controlled via Bonsai

(Open-Ephys). LEDs delivering two excitation wavelengths (470 nm for detection of GCaMP6f signal and 415 nm for a calcium-independent control) intercalated at 40 Hz throughout recording sessions. Fluorescence emission was focused onto a CMOS sensor for detection with a region of interest drawn around the end of the plug of the patch cord. A key press trigger was used in Bonsai to save the timestamps of precise social interactions aligned to the calcium signal (social exploration and biting).

2.10 Fiber-photometry vasopressin recording data acquisition

AVP biosensor data acquisition was conducted using a DORIC system (Basic FMC). Two LEDs (405 nm and 465 nm) were coupled to a fluorescence mini-cube (FMC) to deliver light into optical ferrules permanently implanted above the dLS. Light was delivered at a final intensity of 12 µW (465nm) and 249.5 µW (405 nm) at the tip of the patch-cord. Emitted light between 420 and 450 nm (with 405 nm excitation) and 500 and 540 nm (with 465 nm excitation) were collected through the FMC on separate fiber-coupled Newport 2151 photo-receiver modules. The fluorescent signals were collected in AC-low mode and converted to voltage via the formula $V = PRG$, where V is the collected voltage, P is the optical input power in watts, R is photodetector responsivity in amps/watts (0.2 – 0.4), and G is the trans-impedance gain of the amplifier. Raw signals and 405 nm excitation (isosbestic signal) were recorded using Doric Neuroscience Studio software.

2.11 Optogenetic silencing

Animals were habituated to the optical fiber patch cord for 1 day before the test. The optical fiber patch cord was placed on top of the mouse's implant and the sociability test and resident-intruder test were performed as previously described. In the experimental condition of silencing, light stimulation was supplied using the Cobolt-Jive 561nm adjusted at 5mW and applied during all the testing time. In control conditions, mice were subjected to the test with the patch cord connected but with no light stimulation. The experimental and control condition were randomized between batches of animals and performed with an interval of 3 days between the sociability test and 1 week between the resident-intruder test, to prevent heightened aggression resulting from close repetitive exposure to an intruder in the home-cage.

2. 12 Data analysis

Quantification of the density of cell bodies

In situ hybridization was used to label AVP and Avpr1a mRNA in the BNST and LS of *Shank3B*$^{+/-}$ and WT littermates, as previously described. Equivalent-sized images of the anterior and posterior LS and BNST were acquired with an inverted confocal microscope (SPEII, Leica) with identical settings. The pictures were loaded in the software Fiji (Schneider et al., 2012) and subjected to manual quantification using the cell counting function.

Quantification of the density of axonal fibers

Immunohistochemistry for labelling vasopressin was performed accordingly to the descriptions above. Equivalent-sized images of the anterior and posterior LS of *Shank3b*$^{+/-}$ and WT littermates were acquired with an epifluorescent microscope (Thunder, Leica). The settings for image acquisition was the same for all samples. The pictures were loaded in Fiji software and transformed in to an 8-bit image. A threshold was set to cover all the white pixels of the image, which corresponded to the GFP signal. A selection of the white pixels was then generated and the area corresponding to the GFP labelling was measured. Data was plotted as the total area of GFP pixels labelled.

Quantification of density of VGLUT1 clusters

Immunohistochemistry for labelling VGLUT1 was performed accordingly to the descriptions above. For both *Shank3b*$^{+/-}$ and WT controls, equivalent-sized images of the BNST were acquired (x63 magnification) with identical settings on a confocal microscope (SPEII, Leica). The images were then converted to 8-bit format using ImageJ. A threshold was uniformly applied to all images to enhance the detection and count the different VGLUT1 clusters present on the soma and fibers of AVP cells. Finally, the ROIs used to outline the AVP cells are associated with the number of clusters to generate the VGLUT1 synapse density for each quantified cell.

Quantification of c-fos$^+$ cells

The automated program SimpylCellCounter (Bal et al., 2020) was used for the quantification of c-fos$^+$ cells. Equivalent-sized images from anterior and posterior BNST and LS of *Shank3B$^{+/-}$* and WT littermates were acquired with identical settings in the Thunder microscope (Leica) were loaded in the program. The software utilized a binary thresholding and morphological functions from the open-source computer vision library OpenComputerVision (OpenCV) to identify and quantify the cells based on the shape and size. The size was defined as 5 and the circularity threshold as 0.8. An output of the images with the quantified cells was generated and the cells on the total area were plotted.

Fiber photometry and AVP biosensor data analysis

The Guppy software[77] was used for fiber photometry and AVP biosensor data analysis. The raw data and the behavioral timestamps were loaded, and the first seconds of recording were removed for artifact correction. A subtraction of the background fluorescence was calculated using a time-fitted running average of the 470 nm channel relative to the 415 nm control channel using a least squares polynomial fit of degree 1. The $\Delta F/F$ was calculated by subtracting the fitted control channel from the signal channel and dividing by the fitted control channel using the formula: (470 nm – 415 nm)/415 nm. A peak enveloping Fourier transform was applied to the $\Delta F/F$ signal across the entire trace to identify peaks in activity. The data was presented as the deviation of the $\Delta F/F$ from its mean (z-score) using the formula: ($\Delta F/F$ – mean of $\Delta F/F$/ Standard deviation of $\Delta F/F$). The z-score of each interaction of interest were analyzed during the sessions based on a time window of -3 to 3 seconds for the PSTH analysis. For the sociability test, the interaction with the object only (empty cup) was used as control condition. For the resident-intruder test, the pre-biting or pre-social interaction transients were used as control condition from -3 to -1 seconds. The area under the curve and the peak amplitude were plotted accordingly to these time windows.

Decoder analysis

Fiber photometry recordings of calcium or AVP biosensor signal were used to discriminate between non-social and social transients. In each session, we detected the transients and computed the peak amplitude and the area under curve of each

transient. To discriminate whether the recording came from a non-social or social condition, we trained linear support vector machine (SVM) decoders, using both peak amplitude and transient strength of all detected transients. We trained decoders by randomly selecting 70% data points as training set and evaluated the decoder performance using the rest 30% as testing set. To correct for class imbalance, as a standard procedure, we implemented a cost for misclassification that is inversely proportional to the number of samples in each class. This random sampling procedure was repeated 20 times to avoid sampling bias, and the results were averaged across repeats for each session. To generate a baseline distribution, we shuffled the labels (non-social vs social condition) of the data points, and trained decoders as above. This shuffling procedure was repeated 1000 times. Decoder performance was evaluated as the area under curve (AUC) of the receiver operating characteristic (ROC) curve. Statistical test (one-sided Wilcoxon signed-rank test) was performed to compare the AUC between the real data and the top 95% quantile of the shuffled distribution. For the biosensor data, we performed the decoder analysis to discriminate between social and non-social transients in WT and *Shank3B*$^{+/-}$ mice, using the same procedure as described above.

Supervised annotation in DeepOF analysis

Videos of WT or *Shank3B*$^{+/-}$ mice freely interacting in an open arena with a stimulus mouse were captured using a DMK 27BUR0135 (The IMAGING SOURCE) camera, positioned 130 cm above the arena for a top-down perspective. The recordings were acquired with Bonsai-RX software. Initially, the test mouse was allowed to explore the arena freely for 10 minutes. Following this, a stimulus mouse (BALB/c, males, 7-11 weeks old) was introduced into the arena, and a 2 min interaction period was recorded and saved for subsequent analysis. The interactions between the test and stimulus mice were analyzed using DeepOF software (version 0.7.2).[89,90] To facilitate this, the body parts of both mice were tracked with DeepLabCut (version 2.2.3)[91] using a custom-trained model. DeepOF analysis was then conducted based on the calculated trajectories for each body part.[89,90] Finally, each frame was classified into specific behaviors using DeepOF's pre-trained network.

2.13 Statistics and Reproducibility

Statistical analyses and figure plotting were performed using Prism version 9 (GraphPad). No statistical methods were used to predetermine sample sizes, but sample size was selected based on previous experience and on estimation from related studies. Unless specified otherwise, bar graphs represent mean ± s.e.m. Sample sizes and statistical tests are reported in the figure legends. * indicates $p < 0.05$, ** indicates $p < 0.01$, *** indicates $p < 0.001$ and **** indicates $p < 0.0001$. When multiple observations were done in the same mouse, nested statistical tests were used to take into account the lower degree of freedom.

Experiments using viral injections for anterograde and retrograde tracing were independently repeated a minimum of three times, producing similar outcomes. For experiments involving viral expression or fiber optic implant placement, only animals exhibiting proper viral expression and accurate fiber optic localization were included in the analysis.

3 | Discussion

Chapter 3 | Discussion

Vasopressin (AVP) release in the lateral septum (LS) supports social interactions in male mice

The involvement of vasopressin (AVP) in the regulation of social interactions has been extensively studied, with a particular emphasis on social memory, the ability to recognize and remember a conspecific[42–47]. These investigations have examined both peripheral and brain-specific mechanisms, consistently highlighting the relevance of brain regions such as the lateral septum (LS) in this context.

In the present study, we focused on the role of AVP neuromodulation in sociability, defined here as the preference to interact with a conspecific over an object, as well as in social exploration (following, tail investigation and ano-genital sniffing) within the home-cage setting. These behaviors, particularly within the framework of the resident-intruder test, can be considered part of a continuum of territorial investigation that precedes agonistic interactions. By examining AVP's involvement in both social preference and social exploration, our findings aim to broaden the understanding of how this neuropeptide modulates social behaviors beyond its well-established role in social memory.

We found that AVP release from the bed nucleus of the stria terminalis (BNST) to LS is involved in the facilitation of sociability. Using a circuit manipulation approach, we silenced AVP^{+} synaptic terminals in LS and demonstrated that these neurons are necessary for the expression of social preference. While this finding indicates the importance of AVP^{+} neurons, it does not confirm that AVP itself is the sole mediator, as these neurons may co-express other neurotransmitters. To address this limitation, we employed a short-hairpin RNA (shRNA) strategy to knock-down *Avp* expression in these cells, which resulted in impaired social preference.

Our results align with a recent study that used optogenetics to show that inhibiting $BNST^{AVP}$ cells reduces social investigation in males, but not in females[123]. Interestingly, stimulating the same population increased social investigation in both sexes[123]. They also found that optogenetic stimulation of $BNST^{AVP}$ projections to the LS promoted social investigation and induced some anxiety-like behavior in males, but not in females[123]. Contrary to their findings, we did not observe any changes in anxiety-

like behavior when manipulating $BNST^{AVP}$ cell activity. This discrepancy may be explained by methodological differences, as we used the open field test to assess anxiety, whereas they employed the elevated zero maze.

An important consideration in this context is the role of different AVP receptor subtypes expressed in the murine brain. Prior studies have shown that knockdown of the vasopressin receptor 1a (AVPR1a) impairs social interaction and disrupts social recognition in some mouse lines[34,35]. Additional work has demonstrated that AVPR1a knockout mice show profound deficits in social recognition, which can be rescued by re-expressing the AVPR1a specifically in the LS[44]. Building on these findings, we tested whether pharmacological blockade of AVP receptors could differentially affect sociability. Our results indicate that an antagonist of AVPR1a can decrease social preference, whereas blockade of vasopressin receptor 1b (AVPR1b) had no significant effect. These findings suggest a receptor-specific mechanism underlying AVP's modulation of social interactions. Together, our results emphasize the critical role of the BNST-LS AVP circuit and AVPR1a signaling in promoting sociability and social exploration, offering new insights into the neurobiological substrates of social interactions.

AVP release in the LS facilitates social aggression in male mice

Beyond its involvement in non-aversive social interactions, AVP has also been implicated in agonistic social behaviors, particularly social aggression. While findings from peripheral AVP manipulations and interspecies comparisons are often conflicting[60], experiments in laboratory rodents increasingly suggest a role for AVP release in LS in the promotion of aggression[62,65], but the source of AVP to LS, as well as a direct causal link to behavior, remained unclear. Some studies have reported a negative correlation between AVP-immunoreactive innervation in the LS and bed nucleus of the stria terminalis (BNST) and aggressive behavior in rodents[63,64]. However, it is important to note that these conclusions are primarily based on latency to attack, rather than more comprehensive measures such as the proportion of aggressive behavior or total number of attacks.

In our hands, experimental manipulation of AVP release during the resident-intruder test, a widely used assay for assessing territorial aggression in male mice, demonstrated that AVP release from the BNST to LS does promote social aggression. Through optogenetic and chemogenetic silencing, as well as targeted AVP knock-down, we observed significant reductions in both aggression duration and the proportion of aggressive behavior. Importantly, these effects were reversible under control conditions, supporting the specificity of this circuit's role in modulating aggression. Overall, our findings are consistent with these and other studies that implicate the BNST in the regulation of social aggression[124,125].

While we conceptualize the social exploratory behaviors observed in the resident-intruder test as part of a continuum of territorial behaviors, with social investigation often preceding dominance and attack, it is essential to distinguish between social exploration and social aggression. Despite involving the same neuropeptide and brain circuit, these behaviors are functionally distinct. This raises the question: how can AVP modulate different behavioral outputs through the same projections?

Our hypothesis posited that differential modulation might occur via distinct AVP receptor subtypes. Previous research has demonstrated that AVP facilitates social aggression through AVPR1b-mediated potentiation of the CA2-to-LS synapse, and that infusion of AVPR1b antagonists into the LS reduces aggressive behavior[39]. Furthermore, AVPR1b knockout mice consistently exhibit decreased aggression[70–72], while knockdown of AVPR1a appears to have no such effect[69]. Our own findings support this model: pharmacological activation of AVPR1b increases aggressive behavior, while blockade of this receptor diminishes it. In contrast, manipulation of AVPR1a had no observable impact on aggression.

Moreover, our fiber photometry recordings reveal an increase in AVP release during aggressive behavior compared to social interaction. This elevation in AVP signalling within the LS may reflect the need to engage distinct receptor populations, with AVPR1a broadly distributed in the lateral and ventral regions, and AVPR1b more localized to the dorsal LS. These findings also suggest that a higher threshold of AVP release may be required to initiate aggression, whereas lower levels may be sufficient to promote social interaction.

These results highlight a receptor-specific mechanism through which AVP within the BNST-LS circuit modulates social aggression, further distinguishing its role in agonistic versus affiliative social interactions.

Reduced septal AVP release in an ASD male mouse model

Our results have demonstrated that the *Shank3B*$^{+/-}$ mouse model of ASD presents not only the well-documented deficits in social interaction, but also decreased social aggression. Using automated behavioral analysis, we showed that *Shank3B*$^{+/-}$ mice do not display deficits in the most commonly measured form of social exploration in the literature, nose-to-nose interactions, but instead exhibit impairments in other socially exploratory behaviors that are often overlooked. Specifically, these mice showed reduced following behavior, which can indicate motivation to interact or explore the conspecific, and nose-to-tail investigation, a key feature of social exploration in animals.

One technical reason that nose-to-nose interactions were not significantly affected may be because the tracking software could not distinguish which animal initiates the contact (i.e., the test mouse or the stimulus mouse), whereas following behavior and nose-to-tail interactions can be clearly attributed to the behavior of the test mouse. While humans often rely on face-to-face interaction, animals engage in a broader set of exploratory behaviors, which should be seriously considered when studying social interaction in animal models.

When examining AVP expression in the BNST and LS of *Shank3B*$^{+/-}$ mice, we found a significant reduction in the number of AVP^{+} cells in the BNST, which was associated with decreased AVP^{+} fiber innervation in the anterior region of LS. Previous work using another ASD mouse model, *Magel2*, has similarly shown deficits in AVP^{+} fiber innervation in the LS that correlate with impaired social discrimination, the ability to differentiate between familiar and unfamiliar individuals[105]. However, that study did not investigate the role of the BNST in mediating this innervation deficit, nor did it assess other aspects of social behavior such as sociability.

We hypothesized that the observed reduction in AVP^{+} cells in the BNST may be linked to the *Shank3* mutation, given that the *Shank3* gene encodes essential proteins

involved in the formation of core signaling complexes and the scaffolding of postsynaptic densities at excitatory glutamatergic synapses[107]. To test this hypothesis, we quantified the number of glutamatergic synaptic puncta surrounding AVP$^+$ cells in the BNST of *Shank3B*$^{+/-}$ *x Avp*-Cre mice, compared to wild-type controls, and found a significant reduction in excitatory inputs. This reduction in excitatory drive could potentially contribute to the loss or dysfunction of AVP$^+$ neurons in this region. Further studies are required to confirm this mechanism.

To directly assess AVP activity in the LS during social exploration and aggression, we used a novel AVP biosensor and observed a significant reduction in AVP signaling in *Shank3B*$^{+/-}$ mice compared to wild-type controls. Although the biosensor was injected directly into the LS and could potentially detect AVP fibers from regions beyond the BNST, our tracing experiments did not identify AVP$^+$ projections from the paraventricular nucleus (PVN), a brain region known for its high density of vasopressinergic neurons. Additionally, we did not observe a reduction in AVP$^+$ cell counts in the PVN of mutant mice, supporting the idea that the BNST is the primary source of the affected AVP projections.

Altogether, these findings suggest that reduced excitatory input onto BNST AVP$^+$ neurons in *Shank3B*$^{+/-}$ mice may underlie a circuit-specific deficit in AVP signaling, contributing to both impaired social exploration and diminished social aggression in this ASD model.

New directions in vasopressin-based treatments

Previous studies in laboratory mice have demonstrated that AVP treatment can ameliorate social deficits in certain ASD mouse models, either through direct activation of AVP receptors or via cross-reactivity with oxytocin receptors (OXTR), which AVP is also capable of binding[97,104].

Building upon our hypothesis that selective modulation of distinct AVP receptors in the LS could differentially influence affiliative versus agonistic social behaviors, we investigated whether it would be possible to rescue social interaction in *Shank3B*$^{+/-}$ mice without simultaneously increasing aggression, a symptom frequently associated with ASD, especially in children[83–85]. We found that pharmacological infusion of an

AVPR1a agonist into the LS successfully rescued sociability in *Shank3B*$^{+/-}$ mice without enhancing social aggression. In contrast, infusion of an AVPR1b agonist had the opposite effect, increasing aggression without improving sociability.

These findings provide critical insight for future vasopressin-based therapeutic approaches. Most ongoing or previous clinical trials have focused on the use of AVP receptor antagonists, such as Balovaptan, to reduce AVP signaling. However, these trials have consistently failed to pass Phase 3[119–122], suggesting a need to reevaluate this strategy. Our findings shed some light on why this strategy has failed. On the other hand, studies using intranasal AVP administration have reported improvements in social functioning and responsiveness in children, particularly in individuals with elevated plasma AVP levels[116]. Based on our findings in mice, AVP administration might also increase aggression which would constitute a highly undesirable side effect for ASD patients. In conclusion, our results support a more targeted and receptor-specific approach to AVP-based treatment strategies, aiming to selectively enhance affiliative social behavior while minimizing the risk of promoting aggression in individuals with ASD.

Limitations of the study and future directions

One major limitation of our study is its exclusive focus on male mice. Because AVP expression in the BNST is sexually dimorphic and steroid-dependent, where males exhibit a higher density of AVP^{+} cells and greater AVP^{+} fibre innervation in the LS compared to females[13,14], we focused on males to better characterize this pathway under conditions of maximal AVP expression. However, this choice also limits the generalizability of our findings across sexes. This dimorphism must be taken into account when studying autism and developing pharmacological interventions in humans, as both the prevalence and symptomatology of ASD differ significantly between males and females[86–88].

Future research should aim to clarify the role of AVP and other neuropeptides in ASD-related behaviors in females. For instance, while we demonstrated that AVP modulates aggression in male mice, studies in female rats suggest a different

relationship, where septal AVP is inversely correlated with aggression and oxytocin may play a more dominant role[74]. While in female mice, optogenetic inhibition of AVP^+ fibers in LS did not affect social investigation, suggesting that septal AVP release in female mice do not facilitate social interactions to the same extent as in males[123]. Investigating these sex-dependent mechanisms is critical, as combining male and female data without accounting for biological differences may obscure meaningful findings and reduce statistical power.

Additionally, examining various ASD animal models can help address the heterogeneity of symptoms observed in human populations. Different mouse models often exhibit distinct profiles of social impairment, repetitive behaviors or cognitive deficits. Understanding how neuropeptides like AVP contribute to these variations could inform the development of more targeted treatments tailored to specific symptom clusters within the autism spectrum.

Altogether, future studies that incorporate sex differences and model diversity will be essential for advancing precision therapies that reflect the complexity of ASD.

4 | Conclusions

Chapter 4 | Conclusions

This thesis aimed to investigate how the neuropeptide vasopressin (AVP) modulates social behaviors and how dysregulation of the vasopressinergic system in specific brain circuits contributes to the social deficits observed in the *Shank3B*$^{+/-}$ male mouse model of Autism Spectrum Disorder (ASD). The key findings of this work are as follows:

1. *Shank3B*$^{+/-}$ male mice exhibits not only the already established deficit in sociability, but also a deficit in social aggression.
2. *Shank3B*$^{+/-}$ male mice show a reduced number of AVP^{+} cells in the bed nucleus of the stria terminalis (BNST), a decrease in AVP^{+} fibers of the lateral septum (LS), and a reduced AVPR1a expression in both the BNST and LS.
3. Chemogenetic silencing of AVP^{+} cells in the BNST of WT mice impairs both sociability and social aggression, without affecting locomotion, anxiety-like behavior or social memory.
4. AVP^{+} axon terminals from the BNST are active during episodes of sociability and social aggression, showing heightened activity during aggressive biting compared to social exploration.
5. Silencing the BNST-LS projections in WT mice results in deficits in sociability and social aggression.
6. Knockdown of AVP expression in the BNST of wild-type (WT) mice similarly leads to reduced sociability and social aggression.
7. *Shank3B*$^{+/-}$ male mice exhibit decreased AVP release in the LS during both social exploration and social aggression.
8. Specific activation of AVPR1a in the LS of *Shank3B*$^{+/-}$ males rescues sociability without increasing aggression, whereas activation of AVPR1b enhances aggression without rescuing sociability.

Overall, these findings highlight the critical role a vasopressinergic release from the BNST to LS in modulating both sociability and social aggression under normal and pathological conditions. The results demonstrate that dysfunction in this circuit contributes to the social impairments observed in the *Shank3B*$^{+/-}$ model of ASD. Moreover, this work reveals the potential for selective behavioral modulation via different AVP receptor subtypes within the same circuit, offering promising avenues for the development of targeted therapeutic strategies for ASD.

Chapter 4 | Conclusiones

Esta tesis tuvo como objetivo investigar cómo el neuropéptido vasopresina (AVP) modula los comportamientos sociales y cómo la desregulación del sistema vasopresinérgico en circuitos cerebrales específicos contribuye a los déficits sociales observados ratones macho del modelo murino *Shank3B*$^{+/-}$ del Trastorno del Espectro Autista (TEA). Los principales resultados de este trabajo son los siguientes:

1. Los ratones macho *Shank3B*$^{+/-}$ no solo presentan el déficit de sociabilidad previamente descrito, sino también un déficit en agresión social.
2. Los ratones macho *Shank3B*$^{+/-}$ muestran una reducción en el número de células AVP^{+} en el núcleo de la estría terminal (BNST), una disminución de fibras AVP^{+} en el septo lateral (LS) y una menor expresión de AVPR1a tanto en el BNST como en el LS.
3. El silenciamiento quimiogenético de las células AVP^{+} en el BNST de ratones WT afecta tanto la sociabilidad como la agresión social, sin alterar la locomoción, el comportamiento tipo ansioso ni la memoria social.
4. Las terminales axónicas AVP^{+} provenientes del BNST están activas durante episodios de sociabilidad y agresión social, mostrando una mayor actividad durante las mordidas agresivas en comparación con la exploración social.
5. El silenciamiento de las proyecciones BNST-LS en ratones WT provoca déficits en sociabilidad y agresión social.
6. La reducción de la expresión de AVP en el BNST de ratones WT también conduce a una disminución de la sociabilidad y la agresión social.
7. Los ratones macho *Shank3B*$^{+/-}$ presentan una menor liberación de AVP en el LS tanto durante la exploración social como durante la agresión social.
8. La activación específica de AVPR1a en el LS de ratones *Shank3B*$^{+/-}$ rescata la sociabilidad sin aumentar la agresión, mientras que la activación de AVPR1b incrementa la agresión sin rescatar la sociabilidad.

En conjunto, estos resultados destacan el papel fundamental de la liberación vasopresinérgica desde el BNST hacia el LS en la modulación de la sociabilidad y la

agresión social tanto en condiciones normales como patológicas. Los datos demuestran que la disfunción de este circuito contribuye a las alteraciones sociales observadas en el modelo *Shank3B*$^{+/-}$ de TEA. Además, este trabajo revela el potencial de una modulación conductual selectiva a través de diferentes subtipos de receptores de AVP dentro del mismo circuito, lo que abre nuevas vías prometedoras para el desarrollo de estrategias terapéuticas dirigidas para el TEA.

References

1. Sparapani, S. *et al.* The Biology of Vasopressin. *Biomedicines* **9**, 89 (2021).

2. Schmale, H., Heinsohn, S. & Richter, D. Structural organization of the rat gene for the arginine vasopressin-neurophysin precursor. *EMBO J.* **2**, 763–767 (1983).

3. Da Silva, M. P., Merino, R. M., Mecawi, A. S., Moraes, D. J. & Varanda, W. A. In vitro differentiation between oxytocin- and vasopressin-secreting magnocellular neurons requires more than one experimental criterion. *Mol. Cell. Endocrinol.* **400**, 102–111 (2015).

4. Anderson, T. R. & Slotkin, T. A. Maturation of the adrenal medulla--IV. Effects of morphine. *Biochem. Pharmacol.* **24**, 1469–1474 (1975).

5. Tiwari, S. & Ecelbarger, C. M. Molecular Biology and Gene Regulation. in *Textbook of Nephro-Endocrinology* 95–116 (Elsevier, 2018). doi:10.1016/B978-0-12-803247-3.00006-4.

6. Zhang, B. *et al.* Reconstruction of the Hypothalamo-Neurohypophysial System and Functional Dissection of Magnocellular Oxytocin Neurons in the Brain. *Neuron* **109**, 331-346.e7 (2021).

7. Wang, Y., Xu, H. & Zhang, X. Breakthrough in Structural and Functional Dissection of the Hypothalamo-Neurohypophysial System. *Neurosci. Bull.* **37**, 1087–1089 (2021).

8. Talpo, F. *et al.* Neuromodulatory functions exerted by oxytocin on different populations of hippocampal neurons in rodents. *Front. Cell. Neurosci.* **17**, 1082010 (2023).

9. Wacker, D. & Ludwig, M. The role of vasopressin in olfactory and visual processing. *Cell Tissue Res.* **375**, 201–215 (2019).

10. Crestani, C. *et al.* Mechanisms in the Bed Nucleus of the Stria Terminalis Involved in Control of Autonomic and Neuroendocrine Functions: A Review. *Curr. Neuropharmacol.* **11**, 141–159 (2013).

11. Herman, J. P. *et al.* Central mechanisms of stress integration: hierarchical circuitry controlling hypothalamo–pituitary–adrenocortical responsiveness. *Front. Neuroendocrinol.* **24**, 151–180 (2003).

12. Ulrich-Lai, Y. M. & Herman, J. P. Neural regulation of endocrine and autonomic stress responses. *Nat. Rev. Neurosci.* **10**, 397–409 (2009).

13. De Vries, G. J. & Buijs, R. M. The origin of the vasopressinergic and oxytocinergic innervation of the rat brain with special reference to the lateral septum. *Brain Res.* **273**, 307–317 (1983).

14. De Vries, G. J., Buijs, R. M. & Van Leeuwen, F. W. Sex Differences in Vasopressin and Other Neurotransmitter Systems in the Brain. in *Progress in Brain Research* vol. 61 185–203 (Elsevier, 1984).

15. De Vries, G. J. & Panzica, G. C. Sexual differentiation of central vasopressin and vasotocin systems in vertebrates: Different mechanisms, similar endpoints. *Neuroscience* **138**, 947–955 (2006).

16. Laflamme, N., Nappi, R. E., Drolet, G., Labrie, C. & Rivest, S. Expression and neuropeptidergic characterization of estrogen receptors (ER? and ER?) throughout the rat brain: Anatomical evidence of distinct roles of each subtype. *J. Neurobiol.* **36**, 357–378 (1998).

17. Campi, K. L., Jameson, C. E. & Trainor, B. C. Sexual Dimorphism in the Brain of the Monogamous California Mouse (Peromyscus californicus). *Brain. Behav. Evol.* **81**, 236–249 (2013).

18. Dong, H. & Swanson, L. W. Projections from bed nuclei of the stria terminalis, posterior division: Implications for cerebral hemisphere regulation of defensive and reproductive behaviors. *J. Comp. Neurol.* **471**, 396–433 (2004).

19. Shin, J., Geerling, J. C. & Loewy, A. D. Inputs to the ventrolateral bed nucleus of the stria terminalis. *J. Comp. Neurol.* **511**, 628–657 (2008).

20. Ni, R.-J., Luo, P.-H., Shu, Y.-M., Chen, J.-T. & Zhou, J.-N. Whole-brain mapping of afferent projections to the bed nucleus of the stria terminalis in tree shrews. *Neuroscience* **333**, 162–180 (2016).

21. Rigney, N., De Vries, G. J. & Petrulis, A. Sex differences in afferents and efferents of vasopressin neurons of the bed nucleus of the stria terminalis and medial amygdala in mice. *Horm. Behav.* **154**, 105407 (2023).

22. Bester-Meredith, J. K. & Marler, C. A. Vasopressin and Aggression in Cross-Fostered California Mice (Peromyscus californicus) and White-Footed Mice (Peromyscus leucopus). *Horm. Behav.* **40**, 51–64 (2001).

23. Rigney, N., De Vries, G. J., Petrulis, A. & Young, L. J. Oxytocin, Vasopressin, and Social Behavior: From Neural Circuits to Clinical Opportunities. *Endocrinology* **163**, bqac111 (2022).

24. Powers, J. B., Newman, S. W. & Bergondy, M. L. MPOA and BNST lesions in male Syrian hamsters. *Behav. Brain Res.* **23**, 181–195 (1987).

25. Claro, F., Segovia, S., Guilamón, A. & Del Abril', A. Lesions in the medial posterior region of the BST impair sexual behavior in sexually experienced and inexperienced male rats. *Brain Res. Bull.* **36**, 1–10 (1995).

26. Liu, Y.-C., Salamone, J. D. & Sachs, B. D. Lesions in Medial Preoptic Area and Bed Nucleus of Stria Terminalis: Differential Effects on Copulatory Behavior and Noncontact Erection in Male Rats. *J. Neurosci.* **17**, 5245–5253 (1997).

27. Rood, B. D. *et al.* Site of origin of and sex differences in the vasopressin innervation of the mouse (*Mus musculus*) brain. *J. Comp. Neurol.* **521**, 2321–2358 (2013).

28. Otero-Garcia, M. *et al.* Extending the socio-sexual brain: arginine-vasopressin immunoreactive circuits in the telencephalon of mice. *Brain Struct. Funct.* **219**, 1055–1081 (2014).

29. Besnard, A. & Leroy, F. Top-down regulation of motivated behaviors via lateral septum sub-circuits. *Mol. Psychiatry* **27**, 3119–3128 (2022).

30. Menon, R., Süß, T., Oliveira, V. E. D. M., Neumann, I. D. & Bludau, A. Neurobiology of the lateral septum: regulation of social behavior. *Trends Neurosci.* **45**, 27–40 (2022).

31. De Vries, G. J., Buds, R. M. & Swaab, D. F. Ontogeny of the vasopressinergic neurons of the suprachiasmatic nucleus and their extrahypothalamic projections in the rat brain—presence of a sex difference in the lateral septum. *Brain Res.* **218**, 67–78 (1981).

32. Otero-Garcia, M. *et al.* Extending the socio-sexual brain: arginine-vasopressin immunoreactive circuits in the telencephalon of mice. *Brain Struct. Funct.* **219**, 1055–1081 (2014).

33. Rae, M., Lemos Duarte, M., Gomes, I., Camarini, R. & Devi, L. A. Oxytocin and vasopressin: Signalling, behavioural modulation and potential therapeutic effects. *Br. J. Pharmacol.* **179**, 1544–1564 (2022).

34. Egashira, N. *et al.* Impaired social interaction and reduced anxiety-related behavior in vasopressin V1a receptor knockout mice. *Behav. Brain Res.* **178**, 123–127 (2007).

35. Bielsky, I. F., Hu, S.-B., Szegda, K. L., Westphal, H. & Young, L. J. Profound Impairment in Social Recognition and Reduction in Anxiety-Like Behavior in Vasopressin V1a Receptor Knockout Mice. *Neuropsychopharmacology* **29**, 483–493 (2004).

36. Stevenson, E. L. & Caldwell, H. K. The vasopressin 1b receptor and the neural regulation of social behavior. *Horm. Behav.* **61**, 277–282 (2012).

37. Young, W. S., Li, J., Wersinger, S. R. & Palkovits, M. The vasopressin 1b receptor is prominent in the hippocampal area CA2 where it is unaffected by restraint stress or adrenalectomy. *Neuroscience* **143**, 1031–1039 (2006).

38. Wersinger, S. R., Ginns, E. I., O'Carroll, A.-M., Lolait, S. J. & Young Iii, W. S. Vasopressin V1b receptor knockout reduces aggressive behavior in male mice. *Mol. Psychiatry* **7**, 975–984 (2002).

39. Leroy, F. *et al.* A circuit from hippocampal CA2 to lateral septum disinhibits social aggression. *Nature* **564**, 213–218 (2018).

40. Dantzer, R., Bluthe, R.-M., Koob, G. F. & Le Moal, M. Modulation of social memory in male rats by neurohypophyseal peptides. *Psychopharmacology (Berl.)* **91**, 363–368 (1987).

41. Le Moal, M., Dantzer, R., Michaud, B. & Koob, G. F. Centrally injected arginine vasopressin (AVP) facilitates social memory in rats. *Neurosci. Lett.* **77**, 353–359 (1987).

42. Bluthe, R.-M., Schoenen, J. & Dantzer, R. Androgen-dependent vasopressinergic neurons are involved in social recognition in rats. *Brain Res.* **519**, 150–157 (1990).

43. Van Wimersma Greidanus, Tj. B. & Maigret, C. The role of limbic vasopressin and oxytocin in social recognition. *Brain Res.* **713**, 153–159 (1996).

44. Bielsky, I. F., Hu, S.-B., Ren, X., Terwilliger, E. F. & Young, L. J. The V1a Vasopressin Receptor Is Necessary and Sufficient for Normal Social Recognition: A Gene Replacement Study. *Neuron* **47**, 503–513 (2005).

45. Gabor, C. S., Phan, A., Clipperton-Allen, A. E., Kavaliers, M. & Choleris, E. Interplay of oxytocin, vasopressin, and sex hormones in the regulation of social recognition. *Behav. Neurosci.* **126**, 97–109 (2012).

46. Lukas, M., Bredewold, R., Landgraf, R., Neumann, I. D. & Veenema, A. H. Early life stress impairs social recognition due to a blunted response of vasopressin release within the septum of adult male rats. *Psychoneuroendocrinology* **36**, 843–853 (2011).

47. Engelmann, M. & Landgraf, R. Microdialysis administration of vasopressin into the septum improves social recognition in Brattleboro rats. *Physiol. Behav.* **55**, 145–149 (1994).

48. Wang, Z., Ferris, C. F. & De Vries, G. J. Role of septal vasopressin innervation in paternal behavior in prairie voles (Microtus ochrogaster). *Proc. Natl. Acad. Sci.* **91**, 400–404 (1994).

49. Insel, T. R., Gelhard, R. & Shapiro, L. E. The comparative distribution of forebrain receptors for neurohypophyseal peptides in monogamous and polygamous mice. *Neuroscience* **43**, 623–630 (1991).

50. Rilling, J. K. *et al.* Arginine Vasopressin Effects on Subjective Judgments and Neural Responses to Same and Other-Sex Faces in Men and Women. *Front. Endocrinol.* **8**, (2017).

51. Zink, C. F., Stein, J. L., Kempf, L., Hakimi, S. & Meyer-Lindenberg, A. Vasopressin Modulates Medial Prefrontal Cortex–Amygdala Circuitry during Emotion Processing in Humans. *J. Neurosci.* **30**, 7017–7022 (2010).

52. Shou, X.-J. *et al.* A Volumetric and Functional Connectivity MRI Study of Brain Arginine-Vasopressin Pathways in Autistic Children. *Neurosci. Bull.* **33**, 130–142 (2017).

53. Sailer, L., Duclot, F., Wang, Z. & Kabbaj, M. Consequences of prenatal exposure to valproic acid in the socially monogamous prairie voles. *Sci. Rep.* **9**, (2019).

54. Zhou, B. *et al.* Effects of arginine vasopressin on the transcriptome of prefrontal cortex in autistic rat model. *J. Cell. Mol. Med.* **26**, 5493–5505 (2022).

55. Clauss, J. A., Avery, S. N., Benningfield, M. M. & Blackford, J. U. Social anxiety is associated with BNST response to unpredictability. *Depress. Anxiety* **36**, 666–675 (2019).

56. Paul, M. J. *et al.* Sexually dimorphic role for vasopressin in the development of social play. *Front. Behav. Neurosci.* **8**, (2014).

57. Rigney, N., Zbib, A., De Vries, G. J. & Petrulis, A. Knockdown of sexually differentiated vasopressin expression in the bed nucleus of the stria terminalis reduces social and sexual behaviour in male, but not female, mice. *J. Neuroendocrinol.* **34**, (2022).

58. Fetter-Pruneda, I. *et al.* An oxytocin/vasopressin-related neuropeptide modulates social foraging behavior in the clonal raider ant. *PLOS Biol.* **19**, e3001305 (2021).

59. Stribley, J. M. & Carter, C. S. Developmental exposure to vasopressin increases aggression in adult prairie voles. *Proc. Natl. Acad. Sci.* **96**, 12601–12604 (1999).

60. Freeman, A. R., Hare, J. F., Anderson, W. G. & Caldwell, H. K. Effects of arginine vasopressin on Richardson's ground squirrel social and vocal behavior. *Behav. Neurosci.* **132**, 34–50 (2018).

61. Ferris, C. F. & Delville, Y. Vasopressin and serotonin interactions in the control of agonistic behavior. *Psychoneuroendocrinology* **19**, 593–601 (1994).

62. Veenema, A. H., Beiderbeck, D. I., Lukas, M. & Neumann, I. D. Distinct correlations of vasopressin release within the lateral septum and the bed nucleus of the stria terminalis with the display of intermale aggression. *Horm. Behav.* **58**, 273–281 (2010).

63. Compaan, J. C., Buijs, R. M., Pool, C. W., De Ruiter, A. J. H. & Koolhaas, J. M. Differential lateral septal vasopressin innervation in aggressive and nonaggressive male mice. *Brain Res. Bull.* **30**, 1–6 (1993).

64. Everts, H. G. J., De Ruiter, A. J. H. & Koolhaas, J. M. Differential Lateral Septal Vasopressin in Wild-type Rats: Correlation with Aggression. *Horm. Behav.* **31**, 136–144 (1997).

65. Bester-Meredith, J. K. & Marler, C. A. Vasopressin and Aggression in Cross-Fostered California Mice (Peromyscus californicus) and White-Footed Mice (Peromyscus leucopus). *Horm. Behav.* **40**, 51–64 (2001).

66. Frazier, C. R. M., Trainor, B. C., Cravens, C. J., Whitney, T. K. & Marler, C. A. Paternal behavior influences development of aggression and vasopressin expression in male California mouse offspring. *Horm. Behav.* **50**, 699–707 (2006).

67. Pagani, J. H. *et al.* Role of the vasopressin 1b receptor in rodent aggressive behavior and synaptic plasticity in hippocampal area CA2. *Mol. Psychiatry* **20**, 490–499 (2015).

68. Tan, O. *et al.* Oxytocin and vasopressin inhibit hyper-aggressive behaviour in socially isolated mice. *Neuropharmacology* **156**, 107573 (2019).

69. Wersinger, S. R. *et al.* Vasopressin 1a receptor knockout mice have a subtle olfactory deficit but normal aggression. *Genes Brain Behav.* **6**, 540–551 (2007).

70. Wersinger, S. R., Ginns, E. I., O'Carroll, A.-M., Lolait, S. J. & Young Iii, W. S. Vasopressin V1b receptor knockout reduces aggressive behavior in male mice. *Mol. Psychiatry* **7**, 975–984 (2002).

71. Wersinger, S. R. *et al.* Social motivation is reduced in vasopressin 1b receptor null mice despite normal performance in an olfactory discrimination task. *Horm. Behav.* **46**, 638–645 (2004).

72. Wersinger, S. R., Caldwell, H. K., Christiansen, M. & Young, W. S. Disruption of the vasopressin 1b receptor gene impairs the attack component of aggressive behavior in mice. *Genes Brain Behav.* **6**, 653–660 (2007).

73. Blanchard, R. *et al.* AVP V selective antagonist SSR149415 blocks aggressive behaviors in hamsters. *Pharmacol. Biochem. Behav.* **80**, 189–194 (2005).

74. Oliveira, V. E. de M. *et al.* Oxytocin and vasopressin within the ventral and dorsal lateral septum modulate aggression in female rats. (2021) doi:10.5283/EPUB.51717.

75. Coccaro, E. F., Kavoussi, R. J., Hauger, R. L., Cooper, T. B. & Ferris, C. F. Cerebrospinal Fluid Vasopressin Levels: Correlates With Aggression and Serotonin Function in Personality-Disordered Subjects. *Arch. Gen. Psychiatry* **55**, 708 (1998).

76. Thompson, R., Gupta, S., Miller, K., Mills, S. & Orr, S. The effects of vasopressin on human facial responses related to social communication. *Psychoneuroendocrinology* **29**, 35–48 (2004).

77. Thompson, R. R., George, K., Walton, J. C., Orr, S. P. & Benson, J. Sex-specific influences of vasopressin on human social communication. *Proc. Natl. Acad. Sci.* **103**, 7889–7894 (2006).

78. Virkkunen, M. CSF Biochemistries, Glucose Metabolism, and Diurnal Activity Rhythms in Alcoholic, Violent Offenders, Fire Setters, and Healthy Volunteers. *Arch. Gen. Psychiatry* **51**, 20 (1994).

79. Harony, H. & Wagner, S. The Contribution of Oxytocin and Vasopressin to Mammalian Social Behavior: Potential Role in Autism Spectrum Disorder. *Neurosignals* **18**, 82–97 (2010).

80. Lukas, M. & Neumann, I. D. Oxytocin and vasopressin in rodent behaviors related to social dysfunctions in autism spectrum disorders. *Behav. Brain Res.* **251**, 85–94 (2013).

81. Zhang, R., Zhang, H.-F., Han, J.-S. & Han, S.-P. Genes Related to Oxytocin and Arginine-Vasopressin Pathways: Associations with Autism Spectrum Disorders. *Neurosci. Bull.* **33**, 238–246 (2017).

82. American Psychiatric Association. *Diagnostic and Statistical Manual of Mental Disorders*. (American Psychiatric Association, 2013). doi:10.1176/appi.books.9780890425596.

83. Quetsch, L. B. *et al.* Understanding aggression in autism across childhood: Comparisons with a non-autistic sample. *Autism Res.* **16**, 1185–1198 (2023).

84. Neuhaus, E. *et al.* Language and Aggressive Behaviors in Male and Female Youth with Autism Spectrum Disorder. *J. Autism Dev. Disord.* **52**, 454–462 (2022).

85. Woodman, A. C., Mailick, M. R. & Greenberg, J. S. Trajectories of internalizing and externalizing symptoms among adults with autism spectrum disorders. *Dev. Psychopathol.* **28**, 565–581 (2016).

86. Baio, J. *et al.* Prevalence of Autism Spectrum Disorder Among Children Aged 8 Years — Autism and Developmental Disabilities Monitoring Network, 11 Sites, United States, 2014. *MMWR Surveill. Summ.* **67**, 1–23 (2018).

87. Salari, N. *et al.* The global prevalence of autism spectrum disorder: a comprehensive systematic review and meta-analysis. *Ital. J. Pediatr.* **48**, 112 (2022).

88. Leblond, C. S. *et al.* Operative list of genes associated with autism and neurodevelopmental disorders based on database review. *Mol. Cell. Neurosci.* **113**, 103623 (2021).

89. Cataldo, I., Azhari, A. & Esposito, G. A Review of Oxytocin and Arginine-Vasopressin Receptors and Their Modulation of Autism Spectrum Disorder. *Front. Mol. Neurosci.* **11**, 27 (2018).

90. Tansey, K. E. *et al.* Functionality of promoter microsatellites of arginine vasopressin receptor 1A (AVPR1A): implications for autism. *Mol. Autism* **2**, 3 (2011).

91. Yang, S. Y. *et al.* Family-based association study of microsatellites in the 5′ flanking region of AVPR1A with autism spectrum disorder in the Korean population. *Psychiatry Res.* **178**, 199–201 (2010).

92. Oztan, O., Garner, J. P., Constantino, J. N. & Parker, K. J. Neonatal CSF vasopressin concentration predicts later medical record diagnoses of autism spectrum disorder. *Proc. Natl. Acad. Sci.* **117**, 10609–10613 (2020).

93. Carson, D. S. *et al.* Arginine Vasopressin Is a Blood-Based Biomarker of Social Functioning in Children with Autism. *PLOS ONE* **10**, e0132224 (2015).

94. Zhang, H.-F. *et al.* Plasma Oxytocin and Arginine-Vasopressin Levels in Children with Autism Spectrum Disorder in China: Associations with Symptoms. *Neurosci. Bull.* **32**, 423–432 (2016).

95. Voinsky, I. *et al.* Peripheral Blood Mononuclear Cell Oxytocin and Vasopressin Receptor Expression Positively Correlates with Social and Behavioral Function in Children with Autism. *Sci. Rep.* **9**, 13443 (2019).

96. Xu, X.-J. *et al.* Mothers of Autistic Children: Lower Plasma Levels of Oxytocin and Arg-Vasopressin and a Higher Level of Testosterone. *PLoS ONE* **8**, e74849 (2013).

97. Sala, M. *et al.* Pharmacologic Rescue of Impaired Cognitive Flexibility, Social Deficits, Increased Aggression, and Seizure Susceptibility in Oxytocin Receptor Null Mice: A Neurobehavioral Model of Autism. *Biol. Psychiatry* **69**, 875–882 (2011).

98. Willemsen, R. & Kooy, R. F. Mouse models of fragile X-related disorders. *Dis. Model. Mech.* **16**, dmm049485 (2023).

99. Ergaz, Z., Weinstein-Fudim, L. & Ornoy, A. Genetic and non-genetic animal models for autism spectrum disorders (ASD). *Reprod. Toxicol.* **64**, 116–140 (2016).

100. Bucknor, M. C., Gururajan, A., Dale, R. C. & Hofer, M. J. A comprehensive approach to modeling maternal immune activation in rodents. *Front. Neurosci.* **16**, 1071976 (2022).

101. Roubertoux, P. L. *et al.* Construct Validity and Cross Validity of a Test Battery Modeling Autism Spectrum Disorder (ASD) in Mice. *Behav. Genet.* **50**, 26–40 (2020).

102. Ueoka, I., Pham, H. T. N., Matsumoto, K. & Yamaguchi, M. Autism Spectrum Disorder-Related Syndromes: Modeling with Drosophila and Rodents. *Int. J. Mol. Sci.* **20**, 4071 (2019).

103. Tayanloo-Beik, A. *et al.* Zebrafish Modeling of Autism Spectrum Disorders, Current Status and Future Prospective. *Front. Psychiatry* **13**, 911770 (2022).

104. Peñagarikano, O. *et al.* Exogenous and evoked oxytocin restores social behavior in the *Cntnap2* mouse model of autism. *Sci. Transl. Med.* **7**, (2015).

105. Borie, A. M. *et al.* Correction of vasopressin deficit in the lateral septum ameliorates social deficits of mouse autism model. *J. Clin. Invest.* **131**, e144450 (2021).

106. Balaan, C. *et al.* Juvenile Shank3b deficient mice present with behavioral phenotype relevant to autism spectrum disorder. *Behav. Brain Res.* **356**, 137–147 (2019).

107. Peça, J. *et al.* Shank3 mutant mice display autistic-like behaviours and striatal dysfunction. *Nature* **472**, 437–442 (2011).

108. Boccuto, L. *et al.* Prevalence of SHANK3 variants in patients with different subtypes of autism spectrum disorders. *Eur. J. Hum. Genet.* **21**, 310–316 (2013).

109. Harony-Nicolas, H. *et al.* Oxytocin improves behavioral and electrophysiological deficits in a novel Shank3-deficient rat. *eLife* **6**, e18904 (2017).

110. Song, T.-J. *et al.* Altered Behaviors and Impaired Synaptic Function in a Novel Rat Model With a Complete Shank3 Deletion. *Front. Cell. Neurosci.* **13**, 111 (2019).

111. Lacivita, E., Perrone, R., Margari, L. & Leopoldo, M. Targets for Drug Therapy for Autism Spectrum Disorder: Challenges and Future Directions. *J. Med. Chem.* **60**, 9114–9141 (2017).

112. Landry, M. *et al.* Fluoxetine treatment of prepubescent rats produces a selective functional reduction in the 5-HT2A receptor-mediated stimulation of oxytocin. *Synapse* **58**, 102–109 (2005).

113. Appenrodt, E. Effects of Methylphenidate on Oxytocin and Vasopressin Levels in Pinealectomized Rats During Light–Dark Cycle. *Pharmacol. Biochem. Behav.* **58**, 415–419 (1997).

114. Appenrodt, E. & Schwarzberg, H. Methylphenidate-induced motor activity in rats: modulation by melatonin and vasopressin. *Pharmacol. Biochem. Behav.* **75**, 67–73 (2003).

115. Zhou, B. *et al.* The Changes of Amygdala Transcriptome in Autism Rat Model After Arginine Vasopressin Treatment. *Front. Neurosci.* **16**, 838942 (2022).

116. Parker, K. J. *et al.* A randomized placebo-controlled pilot trial shows that intranasal vasopressin improves social deficits in children with autism. *Sci. Transl. Med.* **11**, eaau7356 (2019).

117. Watanabe, T. *et al.* Mitigation of Sociocommunicational Deficits of Autism Through Oxytocin-Induced Recovery of Medial Prefrontal Activity: A Randomized Trial. *JAMA Psychiatry* **71**, 166 (2014).

118. Hu, L., Du, X., Jiang, Z., Song, C. & Liu, D. Oxytocin treatment for core symptoms in children with autism spectrum disorder: a systematic review and meta-analysis. *Eur. J. Clin. Pharmacol.* **79**, 1357–1363 (2023).

119. Umbricht, D. *et al.* A Single Dose, Randomized, Controlled Proof-Of-Mechanism Study of a Novel Vasopressin 1a Receptor Antagonist (RG7713) in High-Functioning Adults with Autism Spectrum Disorder. *Neuropsychopharmacology* **42**, 1914–1923 (2017).

120. Bolognani, F. *et al.* A phase 2 clinical trial of a vasopressin V1a receptor antagonist shows improved adaptive behaviors in men with autism spectrum disorder. *Sci. Transl. Med.* **11**, eaat7838 (2019).

121. Schnider, P. *et al.* Discovery of Balovaptan, a Vasopressin 1a Receptor Antagonist for the Treatment of Autism Spectrum Disorder. *J. Med. Chem.* **63**, 1511–1525 (2020).

122. Hollander, E. *et al.* Balovaptan vs Placebo for Social Communication in Childhood Autism Spectrum Disorder: A Randomized Clinical Trial. *JAMA Psychiatry* **79**, 760 (2022).

123. Rigney, N. *et al.* A vasopressin circuit that modulates mouse social investigation and anxiety-like behavior in a sex-specific manner. *Proc. Natl. Acad. Sci.* **121**, e2319641121 (2024).

124. Takahashi, A. & Miczek, K. A. Neurogenetics of Aggressive Behavior: Studies in Rodents. in *Neuroscience of Aggression* (eds. Miczek, K. A. & Meyer-Lindenberg, A.) vol. 17 3–44 (Springer Berlin Heidelberg, Berlin, Heidelberg, 2013).

125. Trainor, B. C. & Nelson, R. J. Neuroendocrinology of Aggression. in *Handbook of Neuroendocrinology* 509–520 (Elsevier, 2012). doi:10.1016/B978-0-12-375097-6.10022-8.

Appendix

nature communications

Article

https://doi.org/10.1038/s41467-025-61994-6

Impaired vasopressin neuromodulation of the lateral septum leads to social behavior deficits in *Shank3B*$^{+/-}$ male mice

Received: 29 August 2024

Accepted: 4 July 2025

Published online: 23 July 2025

Check for updates

Maria Helena Bortolozzo-Gleich[1], Guillaume Bouisset[1], Lan Geng[2,3], Antonia Ruiz Pino[1], Yuki Nomura[1], Shuting Han[4,5,6], Yulong Li[2,3] & Félix Leroy[1]

The neuropeptide arginine-vasopressin (AVP) has been repeatedly associated with the autism spectrum disorder (ASD) but the underlying mechanisms remain unclear. As *Shank3B*$^{+/-}$ male mice, a model of ASD, exhibit deficits in sociability and social aggression, we focused on the lateral septum (LS), a brain region involved in the regulation of motivated behaviors and observed reduced AVP inputs from the bed nucleus of the stria terminalis (BNST) to LS. Manipulating AVP release from the BNST to LS of wild-type male mice, we found that AVP promotes both sociability and social aggression. Blocking the vasopressin receptor 1a (AVPR1a) in LS impaired sociability, while blocking the receptor 1b (AVPR1b) disrupted social aggression. Consequently, selective activation of AVPR1a or AVPR1b rescued the respective behavioral deficits in *Shank3B*$^{+/-}$ male mice. These findings reveal that AVP release in LS modulates two distinct social behaviors via different receptors and highlight a possible strategy to rescue sociability during ASD.

Impairment in social interactions is a hallmark of the autism spectrum disorder (ASD). Typical social deficits include initiating interactions, responding to the initiations of others, maintaining eye contact, sharing enjoyment, reading the non-verbal cues of others, and taking another person's perspective. Social interactions are tightly regulated by several neuropeptides, including arginine-vasopressin (AVP), and studies have linked changes in vasopressinergic neuromodulation to ASD[1–4]. Thus, variants in the adjacent AVP gene regions have been associated with ASD diagnosis and endophenotypes[3,5,6]. In addition, magnetic resonant imaging (MRI) revealed changes in structure and functional connectivity in brain regions containing AVP[7]. Moreover, AVP levels in the plasma of children with ASD or their mothers has been associated with autistic symptoms[8–12]. AVP can bind to four distinct receptors: AVP receptor 1a (AVPR1A), AVP receptor 1b (AVPR1B), AVP receptor 2 (AVPR2), and the oxytocin receptor (OXTR). Among these, AVPR1A, AVPR1B, and OXTR are primarily located in the central nervous system and show a high degree of polymorphism in patients with autism spectrum disorder (ASD)[13–19]. In contrast, AVPR2 is predominantly expressed in the kidney[20].

In rodent, subcutaneous administration of AVP in male rats extended the duration of social memory[21]. Further investigations showed that ventricular injections of AVP in male rats immediately after initial encounters with stimulus animals enhanced social memory[22], similar to peripheral AVP administration. Stimulation of the supraoptic nucleus and paraventricular nucleus in male rats led to AVP release in the hypothalamus and facilitated social recognition[23], similar to direct infusion of AVP in LS[24,25]. Conversely, peripheral AVP antagonist injections impaired social recognition in intact male rats but had no effect on castrated ones[26], suggesting that sex hormones may indirectly influence social recognition through modulation of the AVP system. Central administration of anti-AVP serum also resulted in impaired social recognition in male rats[27]. Knocking out AVPR1a

[1]Instituto de Neurociencias CSIC-UMH, Avenida Santiago Ramon y Cajal, San Juan, de Alicante, Spain. [2]State Key Laboratory of Membrane Biology, Peking University School of Life Sciences, Beijing, China. [3]PKU-IDG/McGovern Institute for Brain Research, Beijing, China. [4]Brain Research Institute, University of Zurich, Zurich, Switzerland. [5]Neuroscience Center Zurich (ZNZ), University of Zurich, Zurich, Switzerland. [6]University Research Priority Program (URPP), Adaptive Brain Circuits in Development and Learning, University of Zurich, Zurich, Switzerland. e-mail: felxfel@aol.com

impaired social recognition in male[28] but not in female[29] mice, although this effect was not seen in all AVPR1a-KO lines[30]. Knocking out AVPR1b also leads to a deficit in social recognition and social memory (including the Bruce effect) as well as decreased social aggression and social motivation[31]. Finally, intracerebral administration of AVP in male oxytocin receptor knockout mice lowers aggression and fully reverts social and learning defects by acting on AVPR1a receptors[32]. Despite the extensive evidence that AVP facilitates social interactions, the mechanisms by which defects in vasopressinergic neuromodulation may lead to the social interaction deficits exhibited by ASD patients and mouse models remain elusive.

The lateral septum (LS) is a key region of the limbic system that supports many social and affiliative behaviors, including sociability, social discrimination, and social aggression[33]. Autopsy and MRI studies of ASD patients have identified developmental changes in the septum[3,34,35]. In rodents, LS is richly innervated by vasopressinergic fibers and expresses AVP receptors[33]. Consequently, male Brattleboro rats lacking AVP showed impaired social recognition, which can be restored by micro-dialysis of AVP into LS[36]. While the source of septal AVP remained unclear for a long time[37,38], recent evidence suggests AVP inputs to LS in mice originate from the bed nucleus of the stria terminals (BNST) and promote social interactions[39]. In addition, our previous results demonstrate that AVPR1b activation in LS facilitates social aggression in male mice[40].

Here, we hypothesize that impairment of AVP release from the BNST to LS leads to the social behavior deficits exhibited by *Shank3B*$^{+/-}$ male mice, a mouse model of ASD[41]. We first show that sociability and intermale social aggression are decreased in *Shank3B*$^{+/-}$ male mice. Then, we confirmed that AVP^{+} fibers to LS originate from the BNST before investigating vasopressinergic modulation of LS in *Shank3B*$^{+/-}$ mice. We found a decrease in AVP^{+} fiber density in LS and AVP^{+} cell bodies in BNST, as well as a decrease in *Avpr1a* mRNA expression in LS and BNST of mutant mice. This decrease correlated with fewer excitatory terminals impinging on BNST^{AVP} neurons. Using calcium recording of BNST^{AVP} neurons terminals in LS and a biosensor for AVP in male WT mice, we probed the function of septal AVP release and correlated the fibers activation and AVP release with sociability and social aggression. We then used chemogenetic, terminal-specific silencing and gene expression knockdown to demonstrate that release of AVP from BNST to LS promotes sociability and social aggression in male WT mice. Consistent with the lower density of BNST^{AVP} neurons observed previously, AVP biosensor recordings in male *Shank3B*$^{+/-}$ mice indicated a decrease in AVP release during sociability and aggression. We then infused AVP receptor-specific

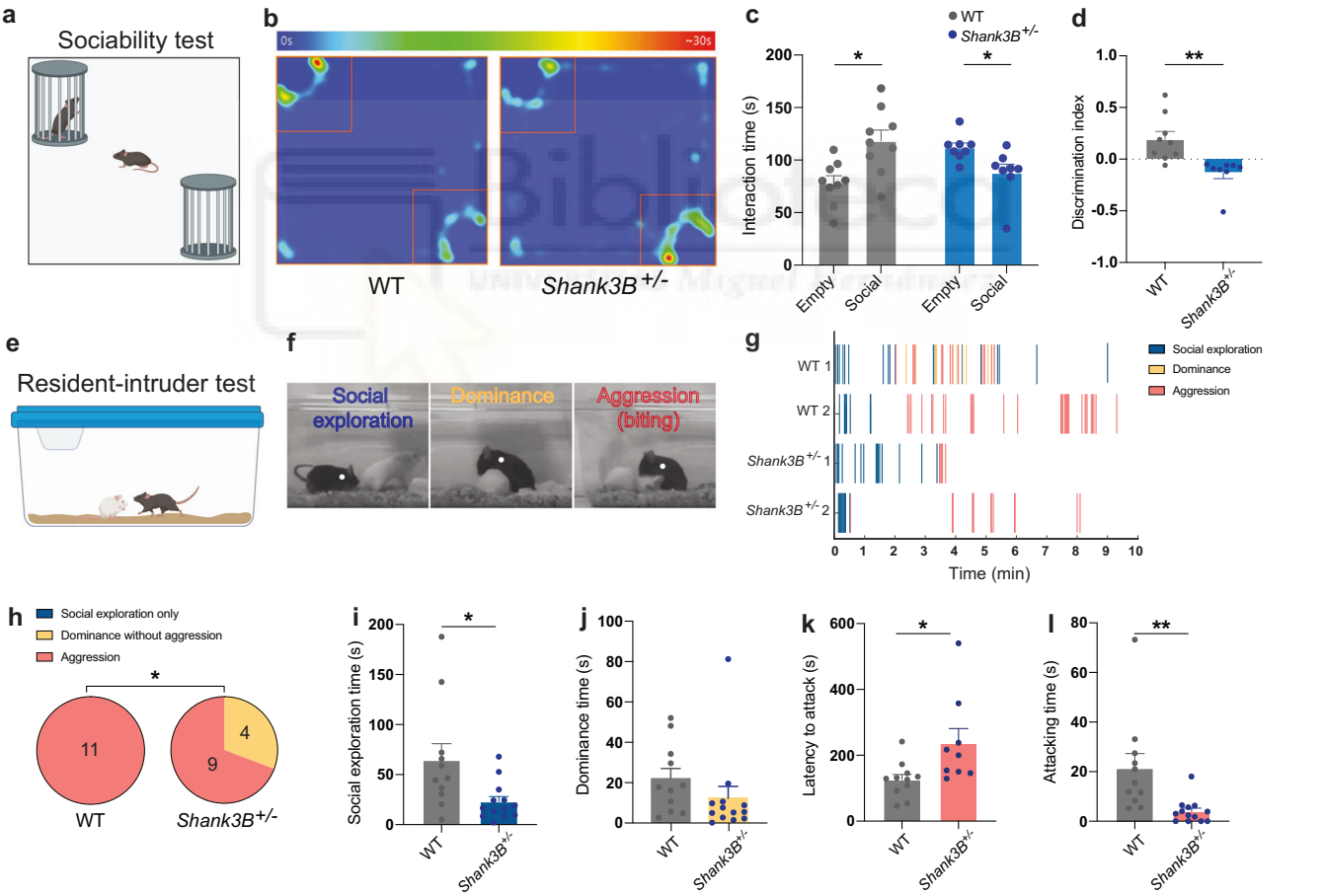

Fig. 1 | Sociability and social aggression are impaired in *Shank3B*$^{+/-}$ mice. **a** Schematic of the sociability test (Created in BioRender. Leroy, F. (2025) https://biorender.com/8v51vnv). **b** Heatmap of the accumulated time around the empty or social cup. **c** Time spent interacting with the empty or social cup (9/8 mice. Paired t test, WT: $p = 0.03$; Paired t test, *Shank3B*$^{+/-}$: $p = 0.01$). **d** Discrimination indexes for social preference (9/8 mice. Unpaired t test: $p = 0.003$). **e** Schematic of resident-intruder test (Created in BioRender. Leroy, F. (2025) https://BioRender.com/in0mntf). **f** Example frames showing social exploration, dominance, and aggression. **g** Raster plots showing social exploration, dominance, and aggression. **h** Proportions of mice exhibiting only social exploration, social dominance without aggression or aggression (at least one biting attack) (11/13 mice. Chi-squared test: $\chi^2(1) = 4.06$, $p = 0.04$). **i** Social interaction duration (11/13 mice. Unpaired t test: $p = 0.02$). **j** Social dominance duration (11/13 mice. Unpaired t test: $p = 0.2$). **k** Latencies to attack (11/9 mice. Unpaired t test: $p = 0.02$). **l** Attack durations (11/13 mice. Unpaired $t$test: $p = 0.005$). For the entire figure, bar graphs represent mean ± s.e.m. Each point is one mouse. * $p < 0.05$, ** $p < 0.01$, *** $p < 0.001$. Source data are provided as a Source Data file.

https://doi.org/10.1038/s41467-025-61994-6

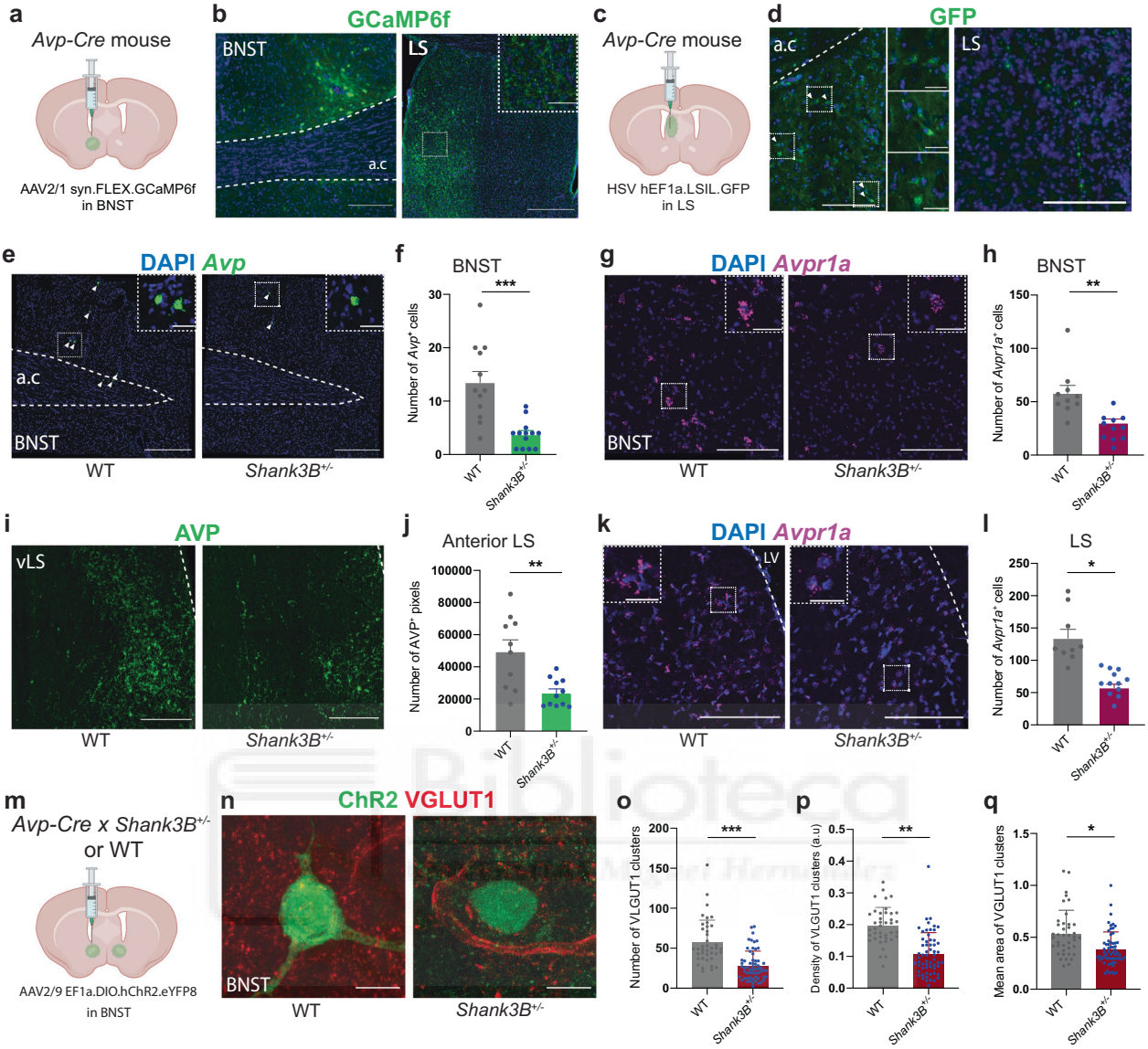

Fig. 2 | Vasopressinergic system from BNST (bed nucleus of stria terminalis) to LS (lateral septum) is decreased in *Shank3B*$^{+/-}$ mice. a *Avp*-Cre mice injected unilaterally with AAV2/1 syn.FLEX.GcaMP6f.WPRE.SV40 in BNST (Created in BioRender. Leroy, F. (2025) https://BioRender.com/zzherf1). **b** Virally labeled AVP^{+} neurons in the BNST (left, scale: 400 µm) and AVP^{+} fibers in LS (right, scale: 600 µm; zoom: 70 µm). **c** *Avp*-Cre mice injected in LS with hEF1a.LSIL.GFP (Created in BioRender. Leroy, F. (2025) https://BioRender.com/h1jqlsw). **d** Retrogradely labeled AVP^{+} neurons in BNST (scale: 200 µm; zoom: 50 µm) and AVP^{+} fibers in LS (scale: 50 µm). **e**, **f** In situ hybridization picture of *Avp* mRNA in BNST (scale: 300 µm; zoom: 30 µm) and cell number (3 mice/group, 3 observations/mouse. Nested *t* test: $p = 0.0001$). **g**, **h** In situ hybridization picture of *Avpr1a* (scale: 200 µm; zoom: 50 µm) and cell number *in* WT and *Shank3B*$^{+/-}$ mice (3 mice/group, 3 observations/mouse. Nested *t* test: $p = 0.002$). **i**, **j** Immunohistochemistry of AVP^{+} fibers in anterior LS (scale: 400 µm) and quantification (10/11 mice/group. Unpaired *t* test: $p = 0.002$). **k**, **l** In situ hybridization for *Avpr1a* in LS (scale: 200 µm; zoom: 25 µm) and cell number (3 mice/group, 3 observations/mouse. Nested *t* test: $p = 0.05$). **m** *Avp*-Cre x *Shank3B*$^{+/-}$ and WT mice injected in the BNST with AAV2/9EF1a.DIO.hChR2(E123T/T159C).eYFP (Created in BioRender. Leroy, F. (2025) https://BioRender.com/zzherf1). **n** BNST AVP^{+} cells labeled for YFP and VGLUT1 (scale: 10 µm). **o** VGLUT1 clusters per ROI (4/6 mice, 7 observations/mouse. Nested t test: $p = 0.0003$). **p** VGLUT1 clusters per ROI surface unit (4/6 mice, 7 observations/mouse. Nested t test: $p = 0.003$). **q** Mean area of VGLUT1 clusters (4/6 mice, 7 observations/mouse. Nested *t* test: $p = 0.02$). For the entire figure, bar graphs show mean ± s.e.m.; each point is one observation. $^{*}p < 0.05$, $^{**}p < 0.01$, $^{***}p < 0.001$. Source data are provided as a Source Data file.

antagonists in LS of WT mice and demonstrated that activation of AVPR1a in LS promotes sociability, while activation of AVPR1b is known to support social aggression[40]. Finally, we leveraged this functional segregation and activated one or the other septal AVP receptor in *Shank3B*$^{+/-}$ mice in order to rescue sociability or social aggression.

Results

Sociability and social aggression are impaired in *Shank3B*$^{+/-}$ mice

Prior studies have established that *Shank3B*$^{+/-}$ mice exhibit both genetic and behavioral parallels to symptoms observed in autism spectrum disorder (ASD), where sociability/social investigation deficits are predominant[41,42]. However, the exploration of other potential social behavior deficits was never particularly investigated, prompting us to investigate whether *Shank3B*$^{+/-}$ mice also exhibit changes in antagonistic behaviors, such as intermale social aggression. First, we confirmed the sociability deficits in *Shank3B*$^{+/-}$ mice. Male *Shank3B*$^{+/-}$ mice and WT littermates were introduced for 5 min in an open arena with two pencil cups in opposite corners. One pencil cup was empty while the other one had a C57Bl6/J mouse of the same age and sex (Fig. 1a). We measured the time the test mouse spent exploring each

https://doi.org/10.1038/s41467-025-61994-6

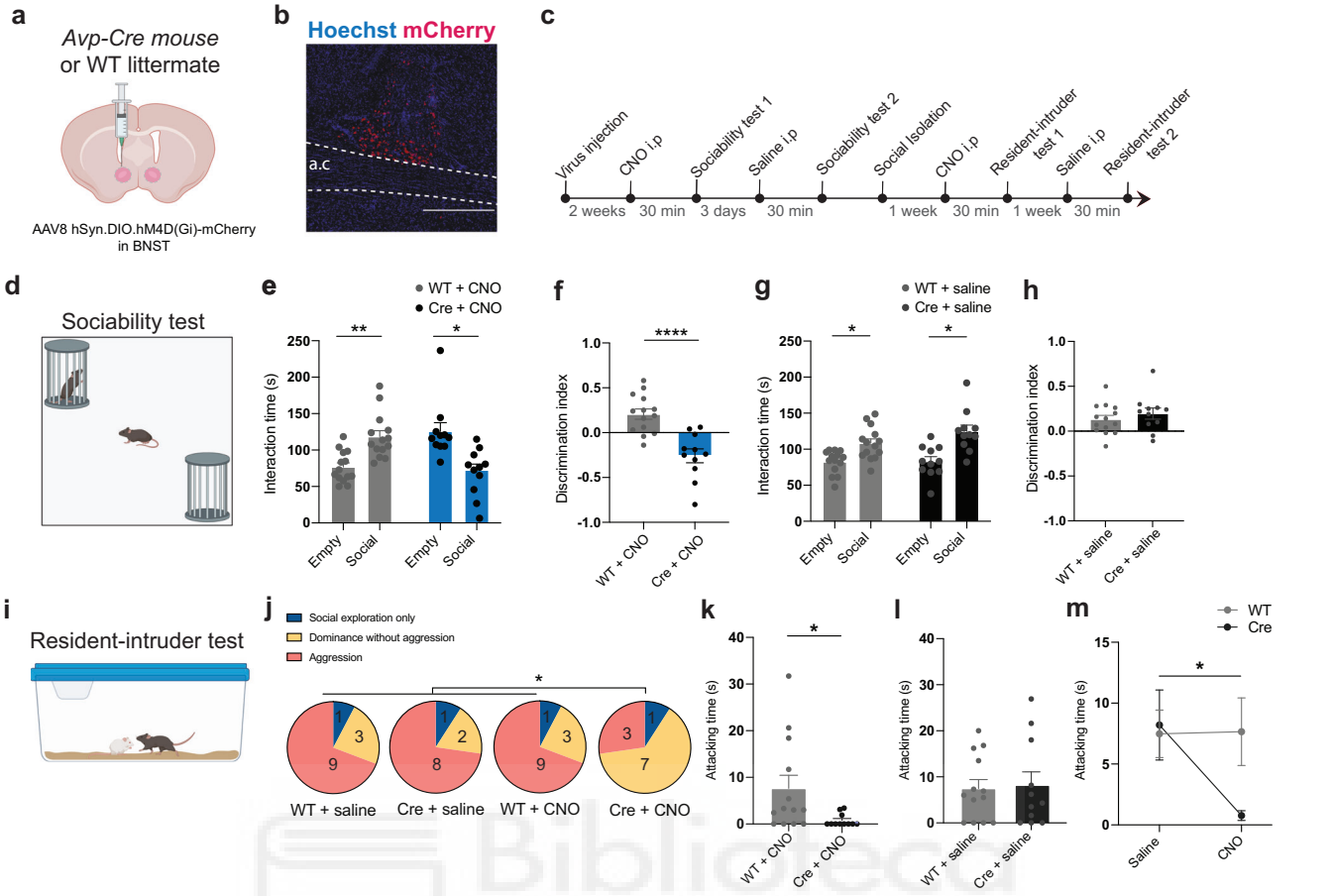

Fig. 3 | Silencing AVP+ neurons from the bed nucleus of the stria terminalis (BNST) impairs sociability and social aggression. a *Avp-Cre* mice and WT littermates injected bilaterally with AAV2/8 hSyn.DIO.hM4D(Gi)-mCherry in the BNST (bed nucleus of stria terminalis) (Created in BioRender. Leroy, F. (2025) https://BioRender.com/zzherf1). **b** Viral expression in the BNST of *Avp-Cre* mouse (scale bar: 300 µm). **c** Experimental timeline. **d** Schematic of the sociability test (Created in BioRender. Leroy, F. (2025) https://biorender.com/8v51vnv). **e** Interaction times with empty or social cup in CNO condition (14/11 mice. Paired t test WT + CNO group: $p = 0.005$; Paired *t* test Cre + CNO group: $p = 0.02$). **f** Discrimination indexes for social preference in CNO condition (14/11 mice. Unpaired *t* test: $p < 0.0001$). **g** Interaction times with social and empty cups in saline condition (14/11 mice. Paired *t* test, WT + saline: $p = 0.01$; Paired *t* test, Cre + saline: $p = 0.01$). **h** Discrimination indexes for social preference in saline condition (14/11 mice. Unpaired *t* test: $p = 0.4$). **i** Schematic of the resident-intruder test (Created in BioRender. Leroy, F. (2025) https://BioRender.com/in0mntf). **j** Proportions of mice exhibiting only social exploration, social dominance without aggression, or aggression in CNO and saline conditions (13/11 mice. Chi-square test: $\chi^2(2) = 7.39$, $p = 0.02$). **k** Attack durations in CNO condition (13/11 mice. Unpaired *t* test: $p = 0.03$). **l** Attack durations in saline condition (13/11 mice. Unpaired *t* test: $p = 0.83$). **m** Attack durations between saline and CNO conditions (13/11 mice. Paired t test WT group: $p = 0.91$; Paired *t* test Cre: $p = 0.02$). For the entire figure, bar graphs represent mean ± s.e.m. Each point is one mouse. * $p < 0.05$, ** $p < 0.01$, *** $p < 0.001$, **** $p < 0.0001$. Source data are provided as a Source Data file.

pencil cup and found that while WT littermates exhibited a preference for the social cup, *Shank3B*$^{+/-}$ male mice displayed sociability deficits (Fig. 1b–d) as previously reported[42].

Then, we tested the mutant mice for social aggression using the resident-intruder test, a behavioral assay designed to assess territorial intermale aggression[43]. Contrary to the sociability test, where the test mouse exhibits a preference but cannot fight, this test allows for direct interaction between two mice, where a wider range of social behaviors can be displayed (exploration, dominance, and aggression). Male *Shank3B*$^{+/-}$ mice and WT littermates were single-housed for a week before a male Balb/cBy mouse of the same age was introduced into their home-cage. We chose to use Balb/cBy mouse intruders for their low aggressivity[44] in order to minimize the likelihood of attacks being initiated by the intruder (Fig. 1e). Typically, introducing an unfamiliar mouse into the home cage of a singly-housed resident prompted social exploration from the resident mouse, usually followed by social dominance behavior (see "Methods"). In some cases, social dominance eventually escalated to social aggression, defined as one or several biting bouts (Fig. 1f). These male-to-male interactions can be viewed as territorial interactions. *Shank3B*$^{+/-}$ mice showed a decrease in social exploration (similar to the result of the sociability test) and a tendency for a decrease in social dominance (Fig. 1I, j). Regarding the aggressive behavior, while all WT littermates escalated from social interaction to aggression within the 10 min duration of the test, only two-third of the *Shank3B*$^{+/-}$ mice displayed social aggression (Fig. 1g–j). This difference led to an increase latency to attack and decreased attack duration (Fig. 1k, I). Overall, these results indicate that *Shank3B*$^{+/-}$ mice display deficits in intermale social aggression in addition to sociability deficits.

To further analyze the differences in social exploratory behavior between WT littermates and mutant mice, we applied a supervised annotation method on movies acquired during a 2 min period in an open arena containing a male Balb/cBy mouse of the same age (Supplementary Fig. 1a). We measured the time mice spent in nose-to-nose and nose-to-tail interactions, as well as following a same-sex adult conspecific (Supplementary Fig. S1b, c). The results indicated no significant differences in nose-to-nose interactions, which can also be initiated by the stimulus mouse. However, they revealed a significant reduction in exploratory social behavior initiated by the test mouse in

https://doi.org/10.1038/s41467-025-61994-6

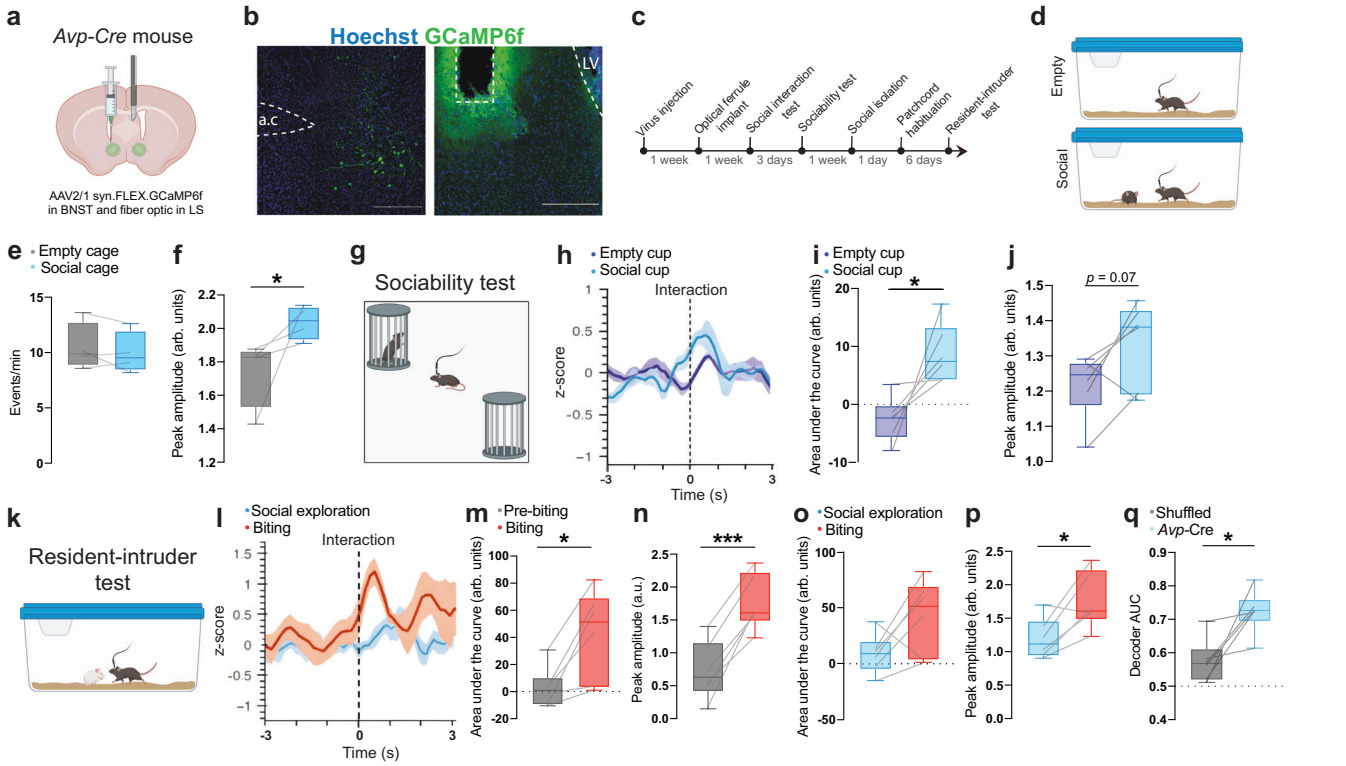

Fig. 4 | AVP$^+$ axons from the bed nucleus of stria terminalis (BNST) to the lateral septum (LS) are activated during sociability and social aggression. **a** *Avp*-Cre mice injected bilaterally with AAV2/syn.FLEX.GcaMP6f.WPRE.SV40 in BNST with an optical ferrule in LS (created in BioRender. Leroy, F. (2025) https://BioRender.com/rj3w3d6). **b** Image of BNST and LS showing virally-labeled AVP$^+$ cells (scale: 600 µm) and optical ferrule tip (scale bars: 400 µm). **c** Experimental timeline. **d** Schematic of the social interaction test (Created in BioRender. Leroy, F. (2025) https://BioRender.com/twqehea). **e** Frequencies of calcium transients before and during social interaction (4 mice. Paired *t* test: $p = 0.4$). **f** Amplitudes of the transients before and during social interaction (4 mice. Paired *t* test: $p = 0.04$). **g** Schematic of sociability test. **h** Peri-stimulus time histograms (PSTH) during interaction with each cup (6 mice) (Created in BioRender. Leroy, F. (2025) https://BioRender.com/yy20hso). **i** Areas under the curve of the PSTH during interaction with each cup (6 mice. Paired t test: $p = 0.02$). **j** Peak amplitudes of the PSTH during interaction with each cup (6 mice. Paired t test: $p = 0.07$). **k** Schematic of the resident-intruder test (Created in BioRender. Leroy, F. (2025) https://BioRender.com/vyq5lxl). **l** PSTH during social exploration and biting (6 mice). **m** Areas under the curve of the PSTH before and during biting (6 mice. Paired *t* test: $p = 0.01$). **n** Peak amplitudes of the PSTH before and during biting (6 mice. Paired *t* test: $p = 0.0003$). **o** Areas under the curve of the PSTH during social exploration and biting (6 mice. Paired *t* test: $p = 0.08$). **p** Peak amplitudes of the PSTH during social exploration and biting (6 mice. Paired *t* test: $p = 0.02$). **q** Performance of linear SVM decoders classifying social vs. non-social transients (6 mice. One-sided Wilcoxon signed-rank test: $p = 0.02$). For the entire figure, box plots show the median (central line) and the full range (minimum to maximum) across animals. PSTH plotted as mean ± s.e.m. Each point represents one mouse. * $p < 0.05$, ** $p < 0.01$, *** $p < 0.001$. Source data are provided as a Source Data file.

the mutant mice group (Supplementary Fig. 1d–f). There were no differences in the distance traveled during the test that could explain these findings (Supplementary Fig. 1g).

Vasopressinergic neuromodulation from the BNST to LS is dysregulated in *Shank3B*$^{+/-}$ mice

We decided to investigate AVP inputs to the septum and injected the BNST of *Avp-Cre* mice with a Cre-dependent adeno-associated virus (AVV) expressing GCaMP6f (Fig. 2a). Three weeks later, we perfused the mice and observed GCaMP6f$^+$ cells at the injection site and GCaMP6f$^+$ fibers in LS (Fig. 2b). As the injection site was unilateral, we observed mostly ipsilateral projections. To confirm this BNST-LS AVP projection, we injected a Cre-dependent monosynaptic retrograde herpes simplex virus (HSV) expressing GFP in LS of *Avp-Cre* mice (Fig. 2c) and observed retrogradely labeled GFP$^+$ cell bodies in posterior BNST as well as GFP$^+$ axon fibers in LS (Fig. 2d). Since AVP is also expressed in the hypothalamus and central amygdala[38], we carefully looked for GFP$^+$ cell bodies in these regions but could not find any. Overall, these results indicate that the BNST provides the major source of vasopressin to LS.

In order to investigate AVP release in LS in *Shank3B*$^{+/-}$ mice, and since antibodies against AVP are known to poorly label AVP$^+$ cell bodies in the BNST[37,38], we relied on in situ hybridizations to label *Avp* and *Avpr1a* mRNAs in the BNST of *Shank3B*$^{+/-}$ mice and WT littermates. We found a decrease in the number of *Avp*$^+$ and *Avpr1a*$^+$ cell bodies in the BNST of the mutant mice (Fig. 2e–h). Then, we used anti-AVP antibodies to label fibers and found a reduction in AVP$^+$ pixels in anterior but not posterior LS (Fig. 2l, j and Supplementary Fig. 2a, b). Since AVP$^+$ fibers in LS originate from the BNST, we can assume that the decrease in AVP$^+$ in LS is due to a lower number of AVP$^+$ cells in the BNST. Finally, we also observed a decrease in the number of *Avpr1a*$^+$ cell bodies in LS (Fig. 2k, l). All together, these results indicate that the vasopressinergic neuromodulation from BNST to LS is impaired in *Shank3B*$^{+/-}$ mice. Importantly, we did not find any difference in AVP$^+$ cell number in the paraventricular nucleus of the hypothalamus, the region containing the highest density of AVP$^+$ cells[38], suggesting that the dysregulation of AVP release is not generalized (Supplementary Fig. 2c, d).

SHANK proteins are multidomain scaffold proteins of the postsynaptic density of glutamatergic synapses and promote normal synaptic functioning[45]. As mutation of SHANK has been shown to lead to a decrease in excitatory synapses in the anterior cingulate cortex[46] and the hippocampal region CA1[47], we hypothesized that fewer glutamatergic synapses impinging onto BNST^{AVP} cells in *Shank3B*$^{+/-}$ mice may lead to a decrease in their density. We injected the BNST of

https://doi.org/10.1038/s41467-025-61994-6

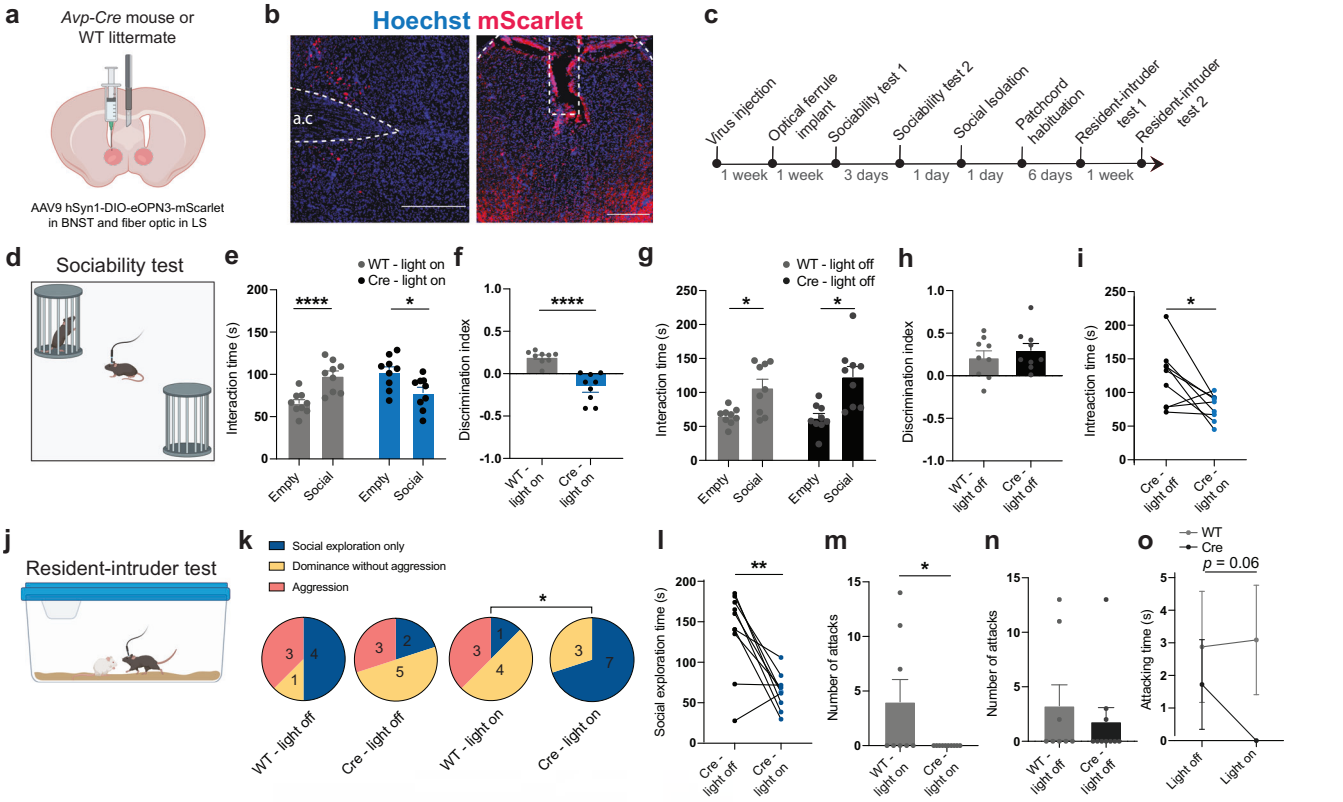

Fig. 5 | Silencing AVP$^+$ terminals from the bed nucleus of the stria terminalis (BNST) to the lateral septum (LS) impairs sociability and social aggression. **a** *Avp*-Cre mice and WT littermates injected bilaterally with AAV2/1hSyn1-DIO-eOPN3-mScarlet-WPRE in BNST with a fiber optic placed in LS (Created in BioRender. Leroy, F. (2025) https://BioRender.com/oa87ggm). **b** Images of BNST and LS showing AVP$^+$ cells labeled with the virus (scale bar: 300 µm) and the trace of the optical ferrule tip (scale bar: 200 µm). **c** Experimental timeline. **d** Schematic of the sociability test (Created in BioRender. Leroy, F. (2025) https://BioRender.com/yy20hso). **e** Interaction times with empty and social cups in light-on condition (9 mice/group. Paired *t* test, WT: $p < 0.0001$; Cre: $p = 0.02$). **f** Discrimination indexes for social preference in light-on condition (9 mice/group. Unpaired t test: $p < 0.0001$). **g** Interaction times with social or empty cup in light-off condition (9 mice/group. Paired t test, WT: $p = 0.02$; Cre: $p = 0.01$). **h** Discrimination indexes for social preference in the light-off condition (9 mice/group. Unpaired *t* test: $p = 0.5$). **i** Social interaction time in light-off vs. light-on condition for *Avp*-Cre mice (9 mice. Paired *t* test: $p = 0.02$). **j** Schematic of the resident-intruder test (Created in BioRender. Leroy, F. (2025) https://BioRender.com/vyq5lxl). **k** Proportions of mice showing only social exploration, social exploration and dominance without aggression, or aggression (8/10 mice. Chi-square test: $\chi^2(2) = 7.51$, $p = 0.02$). **l** Social exploration times in light-off and light-on conditions for *Avp*-Cre mice (9 mice. Paired *t* test: $p = 0.002$). **m** Number of attacks in light-on condition (8/10 mice. Paired *t* test: $p = 0.04$). **n** Number of attacks in light-off condition (8/10 mice. Unpaired *t* test: $p = 0.5$). **o** Attack durations between light-off and light-on (8/10 mice. Unpaired t test, light-off: $p = 0.6$; light-on: $p = 0.06$). For the entire figure, bar graphs show mean ± s.e.m. Each point is one mouse. * $p < 0.05$, ** $p < 0.01$, *** $p < 0.001$, **** $p < 0.0001$. Source data are provided as a Source Data file.

Avp-Cre x *Shank3B*$^{+/-}$ mice and WT controls with a Cre-dependent virus expressing channelrhodopsin coupled to YFP to label AVP$^+$ cells in this region (Fig. 2m). After two weeks of viral expression, animals were perfused, and slices containing the BNST were labeled for the presynaptic vesicular glutamatergic transport VGLUT1 to quantify glutamatergic inputs (Fig. 2n).

We observed a strong reduction in the number, density, and size of VGLUT1$^+$ clusters apposed to the BNST^{AVP} cells of *Shank3B*$^{+/-}$ mice (Fig. 2o–q), suggesting a reduced excitatory input for these cells. We made sure that although the ratio of VGLUT1$^+$ pixels differed (Supplementary Fig. 3a), the mean area of the surface used to count VGLUT1$^+$ clusters was unchanged (Supplementary Fig. S3). In addition, VLGUT1 cluster density in the entire BNST was not different between *Shank3B*$^{+/-}$ and WT littermates, indicating that the decrease in glutamatergic inputs is not global (Supplementary Fig. 3c, d).

To address whether the BSNT is involved in the social behavioral deficits observed in *Shank3B*$^{+/-}$ mice, we looked for differences in the expression of the immediate early gene c-fos following the resident-intruder test. We performed the resident-intruder test in *Shank3B*$^{+/-}$ mice and WT littermates. One hour later, we perfused the mice that displayed at least one aggressive episode and labeled the LS and BNST for c-fos (Supplementary Fig. 4a, b). We found a decrease in c-fos$^+$ cells in the posterior but not in the anterior BNST nor in anterior or posterior LS (Supplementary Fig. 4c–f). In addition, in situ hybridization showed that the posterior BNST contains a higher density of *Avp*$^+$ cells (22.9 ± 3.4 cells per mm^2) compared to the anterior BNST (8.8 ± 1.0 cells per mm^2, Supplementary Fig. 5a, b).

Silencing BNST^{AVP} neurons impairs sociability and social aggression

What are the behavioral functions supported by BNST^{AVP} cells, and could a defect in AVP release from the BNST to LS induce the social behavioral deficits observed in *Shank3B*$^{+/-}$ mice? To address these questions, we used chemogenetic to silence BNST^{AVP} cells. *Avp-Cre* mice and WT littermates were injected in the BNST with a Cre-dependent AAV expressing an inhibitory DREADD tagged with mCherry. After 2 weeks, mice were injected intra-peritoneally with the DREADD agonist CNO 30 min prior to the sociability test (Fig. 3a–d). Unlike control littermates, *Avp-Cre* mice expressing iDREADD failed to prefer the social cup (Fig. 3e, f). A week later, we injected the same mice with saline and performed the same test. Here, both groups exhibited a preference for the social cup (Fig. 3g, h). Overall, silencing BNST^{AVP} cells impaired sociability/social exploration between male

https://doi.org/10.1038/s41467-025-61994-6

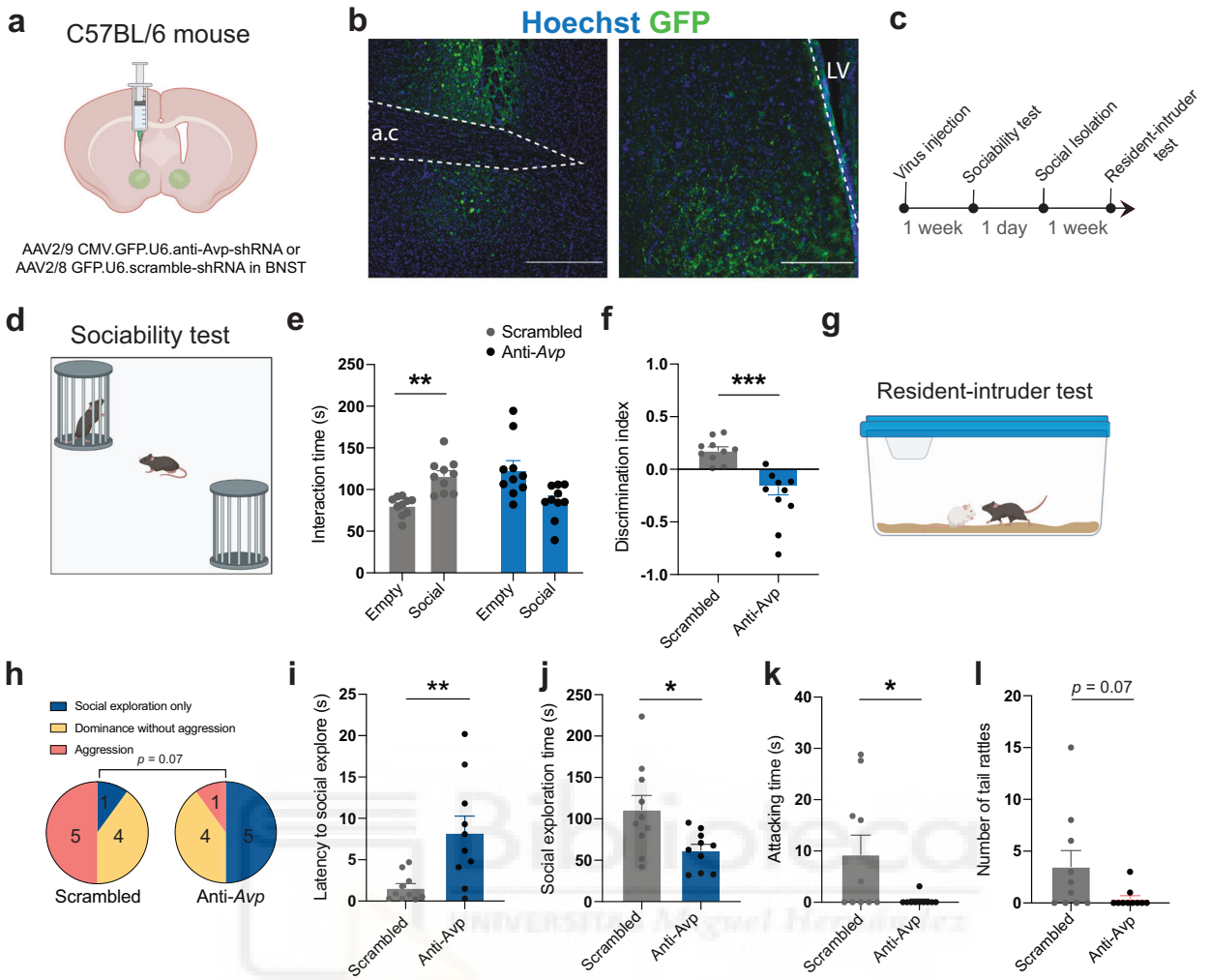

Fig. 6 | Knocking-down *Avp* expression in the bed nucleus of the stria terminalis (BNST) impairs sociability and social aggression. a WT mice bilaterally injected in the BNST with AAV2/9 CMV.GFP.U6.anti-*Avp*-shRNA or AAV2/8 GFP.U6.-scramble-shRNA (Created in BioRender. Leroy, F. (2025) https://BioRender.com/zzherf1). **b** Image of the BNST showing cells labeled with the virus (scale bar: 400 µm). Image of LS (lateral septum) with fibers anterogradely labeled with the virus (scale bar: 200 µm). **c** Experimental timeline. **d** Schematic of the sociability test (Created in BioRender. Leroy, F. (2025) https://biorender.com/8v51vnv). **e** Interaction times with empty and social cups (10 mice/group. Paired *t* test, scramble: $p = 0.001$; Paired *t* test, anti-*Avp*: $p = 0.06$). **f** Discrimination indexes for social preference (10 mice/group. Unpaired *t* test: $p = 0.0005$). **g** Schematic of the resident-intruder test (Created in BioRender. Leroy, F. (2025) https://BioRender.com/in0mntf). **h** Proportions of mice exhibiting only social exploration, social dominance without aggression, or aggression (at least one biting attack, 10 mice/group. Chi-squared test: $\chi^2(2) = 5.33$, $p = 0.07$). **i** Latencies to social explore during the resident-intruder test (10 mice/group. Unpaired *t* test: $p = 0.005$). **j** Social interaction duration (10 mice/group. Unpaired *t* test: $p = 0.02$). **k** Attack durations (10 mice/group. Unpaired *t* test: $p = 0.03$). **l** Number of tail rattles (10 mice/group. Unpaired *t* test: $p = 0.07$). For the entire figure, bar graphs represent mean ± s.e.m. Each point is one mouse. $^*p < 0.05$, $^{**}p < 0.01$ and $^{***}p < 0.001$. Source data are provided as a Source Data file.

mice. Mice were then singled housed for a week and subjected to the resident-intruder test following CNO injection (Fig. 3i). Only a small proportion of *Avp-Cre* mice demonstrated aggression as opposed to the majority of WT littermates (Fig. 3j). In addition, the time they spent attacking was decreased (Fig. 3k). A week later, the same mice were injected with saline and subjected to the same test. Both groups exhibited social aggression levels comparable to the WT littermates injected with CNO (Fig. 3l–m).

To better delineate the role of $BNST^{AVP}$ cells, we also silenced these cells during additional tests on similar cohorts of mice. First, mice explored an open arena for 10 min in order to assess locomotor activity and anxiety (Supplementary Fig. 6a). *Avp-Cre* mice and WT littermates traveled the same distance and spent a similar amount of time in the center vs. surrounds (Supplementary Fig. 6b–d), suggesting that $BNST^{AVP}$ cells do not regulate locomotion or anxiety. Then, we tested the mice for social novelty preference. Mice were introduced to an open arena containing 2 wire cups positioned diagonally, each of which housed an unfamiliar, same-age mouse. Animals could freely explore for 5 min and were removed from the open arena and individually placed in a cage for 30 min. We then replaced one of the now familiar animals under the wire cup with an unfamiliar mouse. The test animals were reintroduced in the arena and had the possibility to socially interact freely for 5 min with the familiar or novel stimulus mouse (Supplementary Fig. 6e)[48]. Both groups exhibited social novelty preference, and total interaction times during learning or recall were similar (Supplementary Fig. 6e–i). Overall, $BNST^{AVP}$ cells promote exploration and aggression of other males but do not support locomotion, anxiety, or social novelty preference.

$BNST^{AVP}$ cell axonal projections to LS are activated during sociability and social aggression

We then used fiber photometry to image the AVP^+ terminals in LS. We bilaterally injected the BNST of *Avp-Cre* mice with a Cre-dependent

https://doi.org/10.1038/s41467-025-61994-6

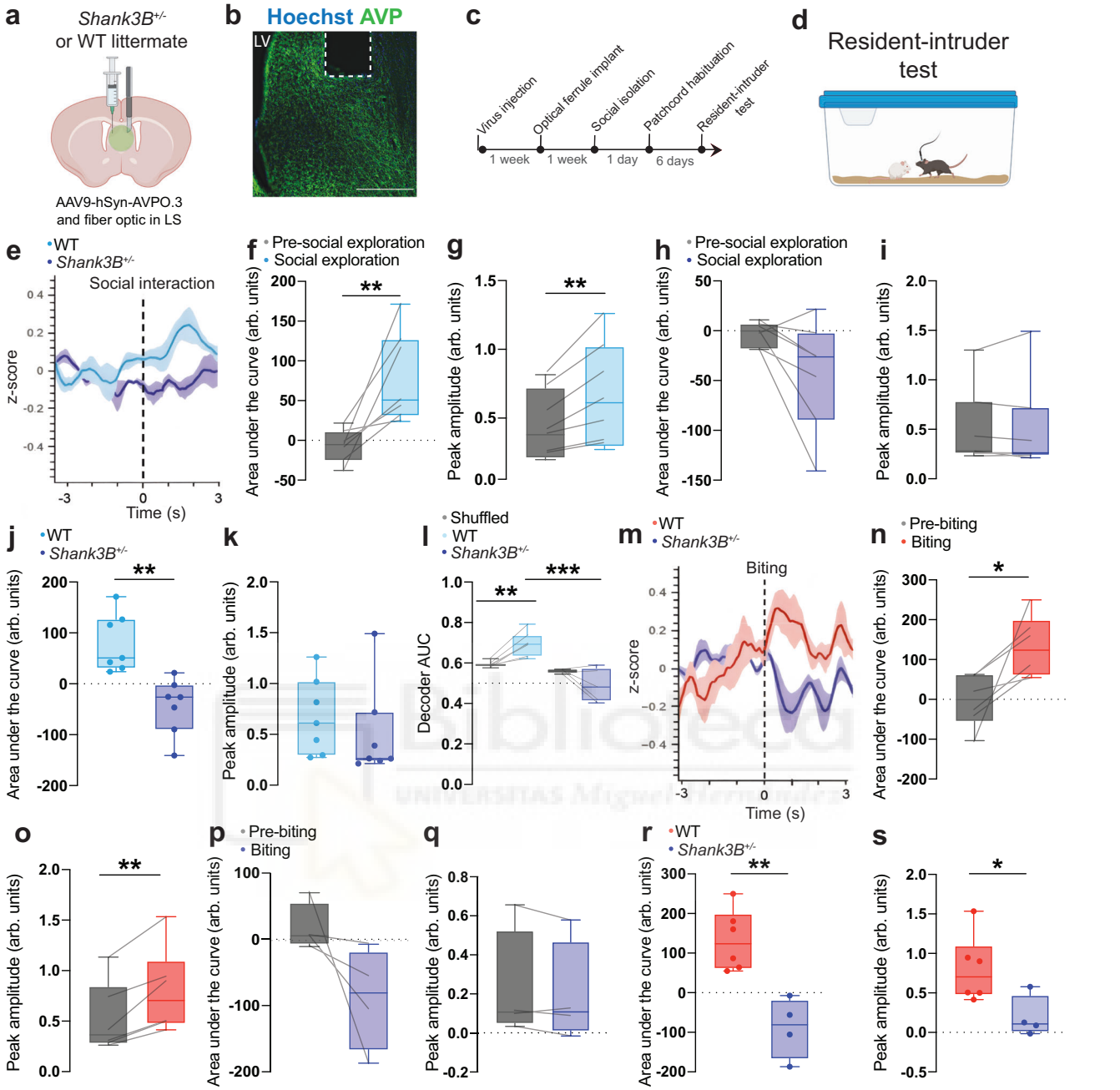

Fig. 7 | Septal AVP release is reduced in *Shank3B*$^{+/-}$ mice during social exploration and aggression. a WT and *Shank3B*$^{+/-}$ mice bilaterally injected with AAV9hSyn.AVP0.3 and implanted with an optical ferrule in the lateral septum (LS) (Created in BioRender. Leroy, F. (2025) https://BioRender.com/j3posib). **b** Image of trace of the optical ferrule tip in LS (scale bar: 400 µm). **c** Experimental timeline. **d** Schematic of the resident-intruder test (Created in BioRender. Leroy, F. (2025) https://BioRender.com/vyq5lxl). **e** Peri-stimulus time histogram (PSTH) during social exploration for WT and *Shank3B*$^{+/-}$ mice (7 mice/group). **f** Areas under the curve of the PSTH before and during social exploration for WT mice (7 mice. Paired *t* test: $p = 0.009$). **g** Peak amplitudes of the PSTH before and during social exploration for WT mice (7 mice. Paired *t*test: $p = 0.006$). **h** Areas under curve for *Shank3B*$^{+/-}$ mice (7 mice. Paired t test: $p = 0.07$). **i** Peak amplitudes for *Shank3B*$^{+/-}$ mice (7 mice. Paired *t* test: $p = 0.9$). **j** Areas under the curve during social exploration WT vs. *Shank3B*$^{+/-}$ mice (7 mice/group. Unpaired *t* test: $p = 0.001$). **k** Peak amplitudes during social exploration for WT vs. *Shank3B*$^{+/-}$ mice (7 mice/group. Unpaired *t* test: $p = 0.4$). **l** Linear SVM decoder performance (7/5 mice. Wilcoxon signed-rank test WT: $p = 0.01$; *Shank3B*$^{+/-}$: $p = 0.91$; WT vs. *Shank3B*$^{+/-}$: $p = 0.00$). **m** PSTH during biting for WT vs. *Shank3B*$^{+/-}$ mice (6/4 mice/group). **n** Areas under cthe urve before and during biting for WT mice (6 mice. Paired *t* test: $p = 0.03$). **o** Peak amplitudes during pre-biting vs biting for WT mice (6 mice. Paired *t* test: $p = 0.004$). **p** Areas under curve for *Shank3B*$^{+/-}$ mice (4 mice. Paired *t* test: $p = 0.14$). **q** Peak amplitudes for *Shank3B*$^{+/-}$ mice (4 mice. Paired t test: $p = 0.26$). **r** Areas under cthe urve during biting for WT vs. *Shank3B*$^{+/-}$ mice (6/4 mice. Unpaired *t* test: $p = 0.002$). **s** Peak amplitudes during biting (6/4 mice. Unpaired *t* test: $p = 0.04$). For the entire figure, box plots show the median (central line) and the full range (minimum to maximum) across animals. Each point is one mouse. PSTH plotted as mean ± s.e.m. *$p < 0.05$, **$p < 0.01$, ***$p < 0.001$. Source data are provided as a Source Data file.

AAV expressing the calcium sensor GCaMP6f before implanting an optical ferrule above the LS. (Fig. 4a–c). Two weeks after viral injection, animals were subjected to a direct social interaction test, which consisted in 2 min of baseline recording in the home-cage followed by 2 min of presentation of a novel mouse (Fig. 4d). We calculated the frequency and amplitude of the GCaMP6f fluorescent signal during baseline and social presentation. No significant difference was observed in the frequency of the signal, but the amplitude of the signal

was higher in the social condition, indicating that BNST^{AVP} fibers to LS are activated during social encounters (Fig. 4e, f).

Three days after, we performed the sociability test while recording terminal activity (Fig. 4g). We calculated the peri-stimulus time histogram using the start of interaction either with the social or the empty cup to synchronize traces and found that the area under the curve of the calcium peak was larger when interacting with the social cup (Fig. 4h–i). Similarly, the peak amplitude showed a tendency to be larger when approaching the social cup (Fig. 4j). These results confirmed the previous results of the direct social interaction test.

After the sociability test, animals were isolated for a week before recording the calcium activity during the resident-intruder test (Fig. 4k). Here, we calculated the peri-stimulus time histogram using the start of interaction or biting to synchronize traces (Fig. 4l). First, we compared the peak amplitude and area under the curve during biting to 3 s baseline before the biting. Both measures were significantly higher during biting, indicating that the vasopressinergic fibers originating from the BNST in the LS are also active during an aggressive encounter (Fig. 4m, n). We then asked if there was a difference between the magnitude of AVP^{+} fiber responses to social interactions or social aggression. As mice usually explore the intruder during the initial phase of the resident-intruder test, we calculated the peri-stimulus time histogram aligned to the start of social interaction and compared both responses. Peak amplitude of the response was higher during biting than social interaction, but not the area under the curve (Fig. 4o, p). We then employed a linear support vector machine (SVM) decoder to classify social from non-social transients (see "Methods"). Decoder performance was compared to a shuffled baseline where transient labels were randomly permuted. The decoder performed better on actual recordings compared to the shuffled distribution, indicating that social and non-social transients contain distinct activity patterns (Fig. 4q). Overall, BNST^{AVP} fibers projecting to LS are active during social interactions and aggression, with social aggression recruiting the fibers more efficiently.

Silencing BNST^{AVP} cell projection to LS impairs sociability and social aggression

To prove that this vasopressinergic projection from BNST to LS is necessary to promote sociability and social aggression, we used an optogenetic silencing approach. We injected the BNST of *Avp-Cre* mice and WT littermates with a Cre-dependent AAV expressing an enhanced mosquito homolog of the vertebrate encephalopsin (eOPN3) that can suppress synaptic output through a brief illumination of the pre-synaptic terminals[49]. We then implanted an optical ferrule above LS (Fig. 5a, b). After 2 weeks of viral expression, we performed the sociability test twice. Each test was performed 3 days apart with the light on and off conditions counterbalanced for each mouse (Fig. 5c, d). With the light on, WT littermates displayed a preference for the social cup while *Avp-Cre* mice did not (Fig. 5e, f). Without light, however, both groups exhibited social preference (Fig. 5g, h). When comparing light conditions for the same mice, *Avp-Cre* mice displayed reduced interaction with the social cup when the terminals were inhibited (Fig. 5i). Animals were then single-housed for a week and habituated to the patch cord in their home-cage before performing the resident-intruder test with counterbalanced light conditions (Fig. 5c, j). In line with results from the sociability test, turning on the light decreased social exploration for A*vp-Cre* mice (Fig. 5k, l). We then analyzed the social aggression exhibited by each group. *Avp-Cre* mice displayed a decrease in the number of attack bout only when with the light on (Fig. 5m, n). Finally, when comparing the same mice across light conditions, *Avp-Cre* mice but not WT littermates displayed a tendency toward a decrease in total attack time (Fig. 5o). Overall, these results indicate that silencing BNST^{AVP} pre-synaptic terminals to LS impairs male to male sociability and intermale social aggression, therefore recapitulating the chemogenetic silencing of BNST^{AVP} cells and demonstrating the importance of this projection in regulating these social behaviors.

Genetic silencing of *Avp* expression in the BNST impairs sociability and social aggression

We have demonstrated that BNST^{AVP} neurons projecting to LS promote sociability and social aggression, but it is unclear whether this is mediated by AVP release. To address this question, we used a short-hairpin RNA approach to silence *Avp* mRNA expression. We injected AAVs expressing a shRNA against *Avp* or a scrambled shRNA as well as GFP in the BNST of C57BL6/J WT mice and observed cell bodies labeled in the BNST and fibers in LS (Fig. 6a–c). Confirming the efficacity of our approach, AVP labeling in LS following anti-*Avp* shRNA expression in the BNST was decreased compared to control shRNA expression (Supplementary Fig. 7), similar to previous results[50]. After 1 week of viral expression (shRNAs under U6 promoter readily express within 1-2 days), mice performed the sociability test (Fig. 6d). While mice that expressed the scrambled shRNA demonstrated normal social preference, mice expressing the shRNA against *Avp* failed to prefer the social cup, suggesting that AVP release from BNST^{AVP} cells is necessary to support sociability (Fig. 6e, f). We subsequently single-housed animals for a week and subjected them to the resident-intruder test (Fig. 6g). In line with the results of the sociability test, mice expressing the shRNA against *Avp* exhibited a higher latency to interact and less interaction time during the resident-intruder test (Fig. 6h–j). Regarding aggressive behaviors, 5/10 control mice bit the intruder at least once during the test while only 1/10 mice expressing the shRNA against *Avp* did so (Fig. 6h). The attack duration was also decreased and there was a tendency for the number of tail rattles to decrease as well (Fig. 6k, l). Together, these results indicate that the release of AVP from BNST^{AVP} cells promotes social aggression in addition to sociability.

Septal AVP release is reduced in *Shank3B*$^{+/-}$ mice during social exploration and aggression

Given the behavioral deficits exhibited by *Shank3B*$^{+/-}$ mice and reduced density AVP^{+} fibers in their anterior LS, we sought to directly test whether septal AVP release during social interaction and social aggression was decreased in mutants compared to WTs. To achieve this, we leveraged a novel AVP biosensor called AVP0.3. *Shank3B*$^{+/-}$ and WT littermate mice were injected with AAV9.hSyn.AVP0.3 into vLS (ventral lateral septum) to turn every neuron near the injection site into an AVP detector. Then, we implanted an optical ferrule above the injection site (Fig. 7a–c). After recovery, mice were subjected to the resident-intruder test while monitoring vasopressinergic events using fiber-photometry (Fig. 7d). Aligning the fluorescent signals from WT mice to the onset of social interactions revealed an increase in both the area under the curve and peak amplitude compared to baseline (Fig. 7f, g). Mutant mice, in contrast, failed to exhibit increased activity during social interactions (Fig. 7h, i). Then, we directly compared the area under the curve or peak amplitude between WT and *Shank3B*$^{+/-}$ mice and observed that vasopressinergic events were significantly larger in WT mice (Fig. 7j, k). We then applied the same linear SVM decoder method as described previously to classify between social and non-social transients in WT and mutant mice. In WT, decoder performance on our recordings was significantly higher than the shuffled distribution, indicating distinct activity patterns between social and non-social transients, consistent with the calcium recordings results (Fig. 4q). In contrast, the decoder's performance was similar between the biosensor recordings from mutant mice and the shuffled distribution. Furthermore, decoder performance was lower in mutants compared to WT (Fig. 7l).

We also aligned the fluorescent signals to the biting onset and found that WT mice exhibited an increase in peak amplitude and a

higher area under the curve during biting compared to baseline (Fig. 7m–o). In contrast, no significant changes were observed in *Shank3B*$^{+/-}$ mice (Fig. 7p, q). As for social exploration, direct comparisons of the area under the curve or peak amplitude during biting revealed that WT exhibited higher activity compared to mutants (Fig. 7r, s). Overall, these findings indicate that AVP release is reduced in *Shank3B*$^{+/-}$ mice during social exploration or aggression of another male mouse.

Activation of AVPR1a and 1b rescues sociability and social aggression respectively in *Shank3B*$^{+/-}$ mice

Since the release of AVP and subsequent activation of AVPR1a in LS are decreased in *Shank3B*$^{+/-}$ mice, we sought to compensate for it by infusing receptor-specific agonizts in LS in order to rescue the social behavioral deficits exhibited by the mouse model of ASD. Prior studies have shown that septal AVPR1a and AVPR1b supports different social behaviors[51]. Indeed, knocking out AVPR1a impairs social discrimination, which can be rescued by in-trans expression of AVPR1a in LS[52]. On the other hand, AVPR1b is expressed at the presynaptic terminals of CA2 pyramidal neurons, where its activation facilitates the flow of information from CA2 to LS to promote social aggression[40]. In addition, infusion of the AVPR1b antagonist SSR149415 in dorsal LS abolishes social aggression[40]. First, to further characterize the effect of blocking AVPR1a or 1b on sociability, we implanted C57BL6/J WT mice with a cannula guide in LS and infused them with saline, SSR149415 (AVPR1b antagonist) or SR49059 (AVPR1a antagonist, Supplementary Fig. 8a, b). Each mouse was infused with one of the drugs in randomized order and subjected to 3 sessions of the sociability test (Supplementary Fig. 8c). Blocking of AVPR1a abolished sociability while blocking AVPR1b had no effect on it (Supplementary Fig. 8d, e). In addition, drug infusion had no effect on total interaction time with both cups and total distance traveled (Supplementary Fig. 8f, g). Overall, these results suggest a complete dichotomy of action of AVP in LS whereby activation of AVRP1a promotes sociability with no effect on social aggression, while activation of AVPR1b promotes social aggression with no effect on sociability. This is likely due to the organization of LS in parallel pathways, allowing separate regulation of different motivated behaviors[53].

Then, we implanted *Shank3B*$^{+/-}$ mice with a cannula guide in LS and infused them with saline, the AVPR1b agonist DDAVP, or a combination of AVP and SSR149415 in order to activate AVPR1a while blocking AVPR1b since there is no valid AVPR1a agonist (Fig. 8a, b). First, each mouse was infused with one of the drugs in randomized order and subjected to 3 sessions of the sociability test (Fig. 8c). Activating AVPR1a in *Shank3B*$^{+/-}$ mice rescued sociability, unlike activation of AVPR1b (Fig. 8d–f). In addition, drug infusion had no effect on total interaction time with both cups and total distance traveled (Supplementary Fig. 8a–c). Then, we isolated the mice for 1 week, and each mouse was infused with one of the drugs in randomized order and subjected to 3 sessions of the resident-intruder test (Fig. 8c, g). Here, activating AVPR1b in *Shank3B*$^{+/-}$ mice increased social aggression unlike activation of AVPR1a as indicated by the number of mice showing attack (Fig. 8h) and the number of attack bouts (Fig. 8i). Activation of AVPR1b also induced a tendency toward an increase in tail rattling duration (Supplementary Fig. 9e), while activation of either receptor induced a tendency toward an increase in dominance behavior (Supplementary Fig. 9f). Overall, these results show that activation of AVRP1a in *Shank3B*$^{+/-}$ mice rescues sociability with no effect on social aggression while activation of AVRP1b rescues social aggression with no effect on sociability.

Discussion

First, our results demonstrate the importance of AVP release in LS to facilitate social exploration between male mice and therefore promote sociability. The increase in social exploration led to an increase in sociability when mice had the choice to explore an empty cup versus a cup containing another male mouse. Our results are similar to a recent study which utilized optogenetics to show that inhibiting BNST^{AVP} cells reduces social investigation in male, but not in female mice, whereas stimulating the same cells increased social investigation in both sexes[39]. Further, they found that optogenetic stimulation of BNST^{AVP} cell inputs to LS increased social investigation and some anxiety-like behavior in males but not in females[39]. Contrary to this study, we did not observe a change in anxiety when manipulating the activity of BNST^{AVP} cells. This difference may stem from experimental reasons since we used the open arena test while they favored the elevated zero maze.

In addition to promoting social exploration, our results also demonstrate a function for AVP in promoting intermale social aggression. Indeed, male to male social exploration usually precedes social aggression, and both social interactions can be viewed as part of a continuum of territorial interaction behaviors facilitated by AVP release from the BSNT. Correlation between septal AVP release and social aggression was previously documented in male rats[54–56], but the source of AVP release in LS, as well as a direct causal link, remained missing. Despite a lack of evidence suggesting that vasopressin may originate from other sources that the BNST, we acknowledge that the AVP biosensor approach would respond to the release of AVP from any source, not just the BNST. In addition, we used virgin male mice with limited aggressive experience throughout this study since these two factors are known to increase aggression[57,58]. Overall, our findings are consistent with these and other studies involving the BNST in social aggression[59,60]. In addition, our previous study highlighted the role of presynaptic AVPR1b at the CA2 to LS synapse to facilitate social aggression without further investigating the source of AVP[40]. Now, we show that AVP is released from the BNST to LS to facilitate social aggression through AVPR1b-mediated potentiation of the CA2 to LS synapse. Interestingly, examination of the intruder-evoked immediate early gene activation in *Avpr1b*-KO male mice revealed a decrease in EGR-1 expression in the BNST, suggesting a lesser recruitment of the BNST in these mice during aggression[61]. This observation remained puzzling since AVPR1b is absent from the BNST[62]. Here, we propose that, because the BNST receives inputs from LS[63], hypo-activation of the BNST in *Avpr1b*-KO male mice likely stems from the decreased transmission of CA2 inputs to LS in the absence of pre-synaptic AVPR1b. A decrease in BNST activation may, in turn, decrease AVP release to LS. Disruption of this AVPR1b-dependent positive feedback loop between LS and the BNST would contribute to *Avpr1b*-KO male mice exhibiting less aggression[64]. In normal conditions, this loop might be responsible for the facilitation of aggression during repetitive intruder presentation[43], similar to the LS-ventral tegmental area loop involving dopamine release in LS[58,65].

In this study, we focused on male mice given the sexual dimorphism of the vasopressinergic projection from the BNST to LS[66,67] and the numerous factors regulating the differentiation of these cells. Thus, testosterone levels around P7 in rats determine the sexual differentiation of AVP projections to LS, and without testosterone, females and castrated males exhibit few BNST^{AVP} inputs to LS[66]. Consequently, peripheral AVP antagonist injection impairs social recognition in intact male rats but has no effect on castrated ones[68]. The fact that females and castrated males are able to perform social discrimination suggests that other mechanisms can also support this behavior. In addition, AVP^{+} cells in the BNST and medial amygdala also express progesterone receptors, acting to suppress AVP expression in these regions[69]. As a result, progesterone injection in male rats impairs social recognition[70], which can be rescued by direct AVP infusion into LS[25]. Finally, ablation of the pineal gland[71] or depletion of norepinephrine from the olfactory bulb[72] also blocks AVP-mediated social recognition. Overall, these results suggest that AVP expression in the

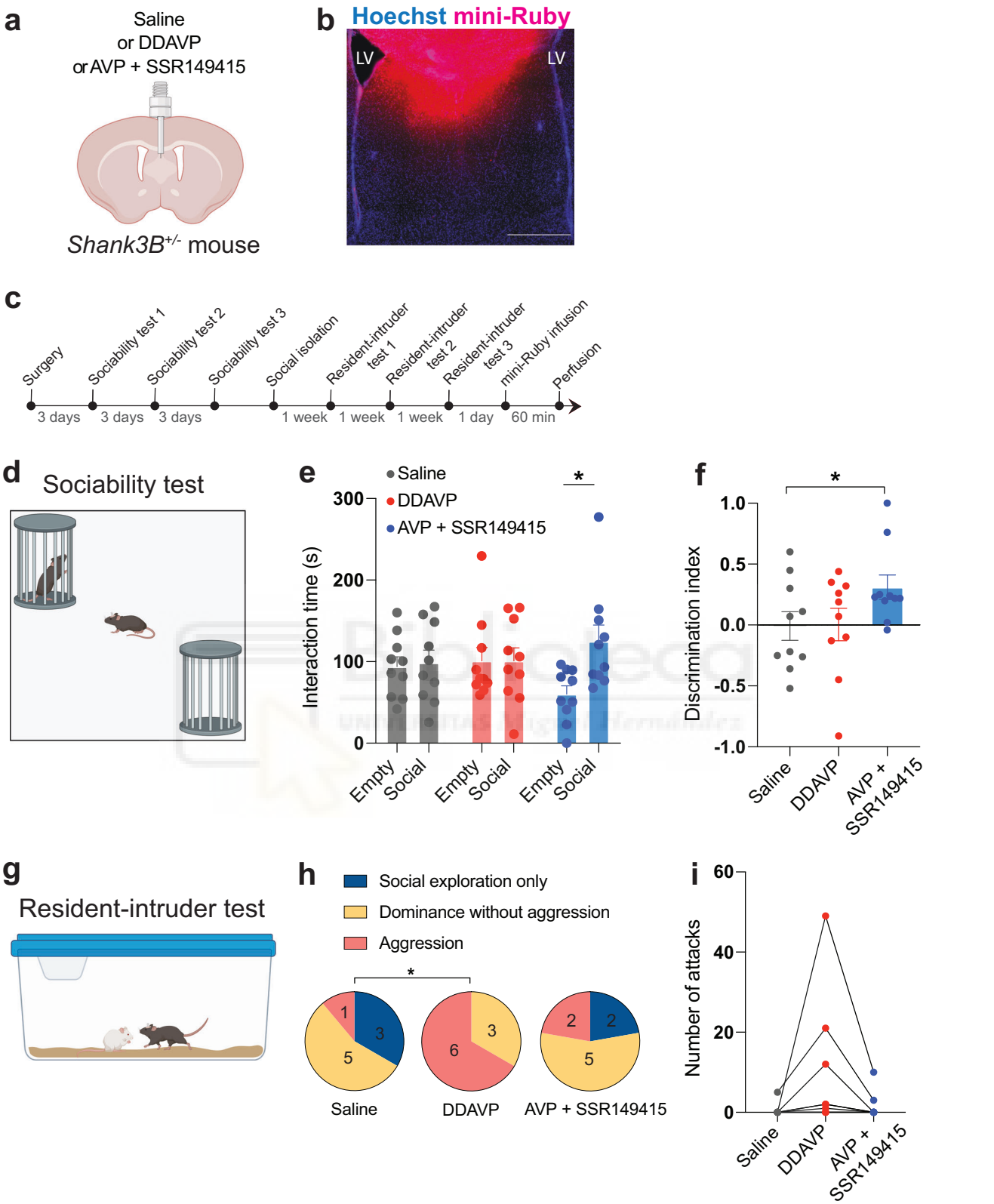

BNST is highly regulated in male rodents, particularly by reproductive hormones.

Female mice exhibit about half AVP$^+$ in BNST and less AVP$^+$ fibers in LS compared to males[67]. In addition, optogenetic inhibition in female mice did not affect social investigation, and optogenetic stimulation increased female investigation of males but not of females[39], suggesting that septal AVP release in female mice does not facilitate social interactions to the same extent, confirming similar results in female rats[26,32]. Septal AVP release might even have an opposite role in female rodents since enhanced oxytocin release within the ventral LS, combined with reduced AVP release within the dorsal LS, is required for aggression in virgin female rats[73]. Similarly, blocking AVPR1a in LS increased social play behavior in males but decreased it in females[74,75], demonstrating opposite regulation of the same behavior in the same

Fig. 8 | Activation of AVPR1a or AVPR1b in LS of *Shank3B*$^{+/-}$ mice rescues sociability or social aggression respectively. a *Shank3B*$^{+/-}$ mice implanted in the dorsal middle of the septum with a guide cannula guide for drug delivery (Created in BioRender. Leroy, F. (2025) https://BioRender.com/ouq4aao). **b** Image showing the mini-Ruby localization in LS (scale bar: 600 µm). **c** Experimental timeline. After cannula guide implantation, *Shank3B*$^{+/-}$ mice were infused with either saline, DDAVP, or AVP + SSR149415 before undergoing the sociability test. All animals were tested 3 times for sociability, with the infusion given in randomized order. Following social isolation, animals underwent 3 resident-intruder tests following the same infusions. **d** Schematic of the sociability test (Created in BioRender. Leroy, F. (2025) https://BioRender.com/irfm1dl). **e** Interaction times with empty and social cups (10 mice. Paired *t* test, saline condition: $p = 0.8$; Paired *t* test, DDAVP condition: $p = 1$; Paired *t* test, AVP + SSR149415 condition: $p = 0.04$). **f** Discrimination indexes for social preference (10 mice). Repeated measures one-way ANOVA followed with Tukey's multiple comparisons test: $F = 4.35$, $p = 0.04$. Tukey's multiple comparisons test: Saline vs. DDAVP $p = 1$; Saline vs. AVP + SSR149415 $p = 0.02$; DDAVP vs. AVP + SSR149415 $p = 0.09$). **g** Schematic of the resident-intruder test (Created in BioRender. Leroy, F. (2025) https://BioRender.com/mjn7ex8). **h** Proportions of mice exhibiting only social exploration, social dominance without aggression or aggression (9 mice. Chi-squared tests: Saline vs. DDAVP $\chi^2(2) = 7.07$, $p = 0.03$; Saline vs. AVP + SSR149415 $\chi^2(2) = 0.53$, $p = 0.8$; DDAVP vs. AVP + SSR149415 $\chi^2(2) = 4.5$, $p = 0.1$). **i** Number of attacks (9 mice. Repeated measures one-way ANOVA: F (2, 8) = 3.07, $p = 0.1$). For the entire figure, bar graphs represent mean ± s.e.m. Each point is one mouse. $^*p < 0.05$, $^{**}p < 0.01$ and $^{***}p < 0.001$. Source data are provided as a Source Data file.

study. Further studies on the mechanisms of AVP release in female rodents are warranted to fully understand its function. Finally, AVPR1a antagonist infusion in the amygdala of rats impair impairs maternal memory but not the memory of other adults[76], which suggests that AVP release in different regions supports distinct types of social memory/preferences. Overall, whether AVP expression in the BNST of female rodents is subject to the same control remains to be explored.

Extending our findings to a pathological context, our results in *Shank3B*$^{+/-}$ mice point to an impairment of AVP neuromodulation in LS due to a decrease in *Avp*$^+$ cells in the BNST and *Avpr1a*$^+$ cells in LS. This correlates with a decrease of VGLUT1$^+$ excitatory terminals impinging on BNST^{AVP} neurons. As SHANK3b is a presynaptic protein located on excitatory terminals, we propose that the mutation carried by the mutant mice led to a decrease in excitatory inputs received by BNST^{AVP} neurons and consequently to their death. Interestingly, the decrease was specific to BNST^{AVP} neurons and not general to the entire BNST, suggesting that the SHANK3b mutation does not affect every excitatory terminal to the same extent. We also found a decrease in *Avpr1a*$^+$ cells in the BNST of the mutant mice. Given the 50 % overlap between *Avp*$^+$ and *Avpr1a*$^+$ cells in the BNST (Supplementary Fig. 10a, b), we suppose that autocrine activation of these cells provides a negative feedback loop for AVP release. This may explain the negative correlation between AVP release and social aggression observed in the BNST[56]. AVP release from PVN to BNST might also dampen BNST^{AVP} cell activity[77]. A previous study of *Magel2*-knockout male mice modeling the Prader-Willi and Schaaf-Yang neurodevelopmental syndromes associated to ASD also showed a decrease in AVP$^+$ fibers in LS[78]. *Magel2*-KO mice exhibit impaired social novelty preference[79], which can be rescued using AVP infusion in LS or optogenetic stimulation[78]. In our study, however, social novelty preference was not affected by chemogenetic silencing of BNST^{AVP} cells (Supplementary Fig. S6e–i). Whether dysregulation of AVP inputs to LS is a common feature of ASD models and whether social deficits exhibited by other ASD models can be rescued by manipulating AVP signaling in LS remains to be explored.

Building on these findings, the discovery that AVPR1a promotes sociability while AVPR1b facilitates social aggression demonstrates how a single peptide release can facilitate separate behaviors via specific receptor activation. This segregation of action enabled us to selectivity rescue sociability in our ASD model without affecting social aggression. Previous studies in humans have demonstrated the potential for using AVP agonizts or AVPR1a antagonists to improve social deficits in children[80] or rescue social communications in adults[81–83] respectively, but without mechanism, these studies have generated limited interest. Our results open the way to novel AVP-based therapeutic approaches[84], aiming at rescuing sociability deficits in ASD patients without facilitating other undesirable behaviors such as social aggression.

Methods

Further information and requests for reagents may be directed to Felix Leroy (felxfel@aol.com).

Ethical approval

All the experimental procedures were in conformity with the directive 2010/63/EU of the European Parliament and of the Council, and the RD 53/2013 Spanish regulation on the protection of animals use for scientific purposes, approved by the government of the Autonomous Community of Valencia, under the supervision of the Consejo Superior de Investigaciones Científicas Committee for Animal use in Laboratory.

Animals

8- to 16-week-old male C57BL6/J (Jackson Laboratories, #000664), *Avp-Cre*$^{+/-}$ mice (Jackson Laboratories, #023530) and *Shank3B*$^{+/-}$ mice (Jackson Laboratories, #017688) were used as experimental subjects. For experiments with mutant mice, the same age wild-type (WT) littermates were used as the control group. Male Balb/cBy mice (Jackson Laboratories, #001026) were used as intruders during the resident intruder test, and C57BL6/J male mice (Jackson Laboratories, #000664) as stimulus mice during the social interaction tests.

Stereotaxic surgeries

Surgical procedure. Animals were anesthetized with isoflurane and placed in the stereotaxic apparatus. An intramuscular injection of Carprofen was used as an anti-inflammatory drug. Eyes were covered with ophthalmic gel (Viscotears 2 mg/g) to prevent corneal desiccation. The hair of the head was removed, and the tissue was sterilized. Following the opening of the head's tissue, a small craniotomy was performed above the target region, and a thin glass pipette was placed on the desired depth to deliver the viral content. Injections were performed using the nano-inject II (Drummond Scientific) with a rate of 23 nl every 11 s with a 10 s delay between each. The skin was then closed with surgical glue, and animals rested in a recovery chamber until restoration of normal locomotor activity.

Viral vectors. For anterograde tracing, 100 nL of AAV2/1 syn.-FLEX.GCaMP6f.WPRE.SV40 (Addgene, #100833-AAV1) was injected unilaterally in the posterior BNST of *Avp-Cre* mice (injection coordinates accordingly to the Allen Brain Atlas: AP: +0.02 mm, ML: ±0.75, DV: −4.75 from the cranium). These coordinates were used for all subsequent BNST injections.

- For retrograde tracing, 100 nl of the herpes simplex virus hEF1a.LSIL.GFP (Rachael Neve, Massachusetts General Hospital, #RN406) was injected into the LS of *Avp-Cre* mice (coordinates: AP: +0.24 mm, ML: ±0.50, DV: −3.30 from the cranium). These coordinates were used for all subsequent LS injections.
- For AVP$^+$ cell labeling in VGLUT1 experiments, AAV2/9EF1a.-DIO.hChR2 (E123T/T159C).eYFP8 (Addgene, #35509) was injected in the posterior BNST of *Avp-Cre* x *Shank3B*$^{+/-}$ and WT controls mice.
- For chemogenetic experiment, 200 nl of AAV2/8 hSyn.-DIO.hM4D(Gi)-mCherry (Addgene, #44362-AAV8) was bilaterally

injected in the posterior BNST of *Avp-Cre* mice and WT littermates.
- For fiber-photometry calcium recording, 100 nl of AAV2/1 syn.-FLEX.GCaMP6f.WPRE.SV40 (Addgene, #100833-AAV1) was bilaterally injected in the posterior BNST of *Avp-Cre* mice.
- For AVP biosensor recordings, 200 nl of AAV9-hSyn-AVP0.3 was unilaterally injected in LS of C57BL6/J.
- For optogenetic silencing experiments, 200 nl of AAV2/1 hSyn1-DIO-eOPN3-mScarlet-WPRE (Addgene, #125713-AAV1) was injected bilaterally in the posterior BNST of *Avp-Cre* and WT littermates.
- For the *Avp* knock-down experiment, 200 nl of AAV2/9 GFP.U6.anti-*Avp*-shRNA or AAV2/9 GFP.U6.scramble-shRNA (Vector Biolabs, #253437-shAAV) were injected bilaterally in the BNST of C57BL6/J mice as experimental or control condition respectively. All viruses expressed for a minimum of 2 weeks before the beginning of experiments, except for the shRNA-expressing AAVs, that expressed for 1 week only.

Fiber optic implants. Animals were anesthetized with isoflurane and placed in the stereotaxic apparatus. An intramuscular injection of Carprofen was used as an anti-inflammatory drug. The scalp was sterilized and completely removed. VetbondTM (3 M™ #7000002814) was applied on the peripheries of the cut to hold the tissue. Two screws were placed on the back of the cranium to provide a sturdy foundation for the implant. A craniotomy was performed above the target region, and an optical ferrule (200 μm core, black ceramic ferrule, Neurophotometrics) was lowered until the desired depth. Superglue was applied to hold the lens in position, and dental cement (GC FujiCEM 2) was applied to cover the exposed skull and to maintain the optical ferrule in place. For fiber-photometry calcium and vasopressin recordings, the optical ferrule implant was placed in LS at the following coordinates AP: + 0.24, ML: 0.5, DV: − 2.80 (from the cranium). For optogenetics silencing of BNST terminals, the optical ferrule implant was placed in LS at the following coordinates AP: + 0.24, ML: 0, DV: − 2.80 (from the cranium). Animals remained undisturbed for a week after the procedure.

Guide cannula implants. The mouse scalp was removed and scored before a hole was drilled (AP: + 0.24, ML: ± 0.00). A cannula guide extending 2.4 mm below the pedestal (Plastics One, #C315G 2-G11-SPC) was lowered slowly and kept in place using superglue. The skull was then covered with dental cement (GC FujiCEM 2), and dummy cannulas (Plastics One, #C315DC-SPC) were inserted into the guides. The mice were returned to their home cages and left to recover for at least 3 days. Mice were immobilized by the experimenter, and the dummy cannula was removed. A cannula (Plastics One, #C315I-SPC) projecting 1.7 mm from the tip of the cannula guide was mounted.

Histology and immunohistochemistry

Animals were anesthetized with isoflurane and intracardially perfused with 10 mL of saline. The brains were quickly extracted and incubated in 4% PFA overnight. The brains were washed for 1 h in PBS, and 50 μm slices of the regions of interest were sliced using a Leica VT1000S vibratome (Leica Biosystems).

Immunohistochemistry. The slices were permeabilized for 2 h in PBS with 0.5% Triton-X100 (T9284, Sigma-Aldrich) before being incubated overnight at 4 °C with primary antibodies diluted in PBS with 0.5% Triton-X in PBS. The slices were washed in PBS for 1 h, then incubated for 2 h or overnight at 4 °C with secondary antibodies from ThermoFisher Scientific at a concentration of 1:500 diluted in PBS with 0.1% Triton-X. Hoechst counterstain was applied (Hoechst 33342 at 1:1000 for 30 min in PBS at RT) prior to mounting the slice using fluoromount (Sigma-Aldrich).

c-fos labeling. For c-fos labeling, primary incubation was performed overnight at 4 °C with anti-c-fos antibody (1:1000, Abcam, #ab190289). Secondary incubation was performed with an anti-rabbit antibody conjugated to Alexa 488 (#A11039) at a concentration of 1:500 for 2 h at room temperature.

Anti-vasopressin labeling. For vasopressin labeling, primary incubation was performed overnight at 4 °C with anti-vasopressin antibody (1:1000, Merck, #PC234L). Secondary incubation was performed with an anti-rabbit antibody conjugated to Alexa 488 (#A11039) (1:500) overnight.

Anti-VGLUT1 labeling. For anti-VGLUT1 labeling, primary incubation was performed overnight at 4 °C with anti-VGLUT1 antibody (1:2000, Millipore, #ab5905). Secondary incubation was performed with an anti-guinea pig antibody conjugated to Alexa 594 (#A11076) (1:500) for 2 h at room temperature.

RFP labeling. For RFP labeling intensification of the signal, primary incubation was performed overnight at 4 °C with rabbit anti-RFP (1:500, Rockland Antibody, #600-401-379), and secondary incubation was performed with anti-rabbit antibody conjugated to Alexa 568 (#A11011) (1:500) for 2 h at room temperature.

GFP labeling. For intensification of the GFP labeling, primary incubation was performed overnight at 4 °C with and chicken anti-GFP (1:1000, Aves, #GFP-1020) antibodies. Secondary incubation was performed with anti-chicken antibody conjugated to 488 (#A11039) (1:500) overnight.

In situ hybridization

Animals were anesthetized using isoflurane and decapitated. The brains were quickly extracted and immersed in cooled 2-methylbutane for 6 s before being stored at 80 °C. 20 μm slices of the region of interest were prepared using a Leica cryostat (CM3050 S, Leica Biosystems) and mounted on Superfrost Plus microscope slides (12-550-15, FisherBrand). The slices were then processed following the RNAscope® Multiplex Fluorescent Detection Reagents v2 (CN:232110, ACD Bio) with the probes for *Avp* in C1 (#401391) and *Avpr1a* in C3 (#418061-C3). Protease IV was applied for 2 min, and TSA Vivid Dyes 520 was used to visualize *Avp* and 650 for *Avpr1a* DAPI was applied for 30 s prior to mounting using fluoromount.

Drugs

For hM4D activation, i.p. administration of clozapine-N-oxide dihydrochloride (CNO, Hello Bio, HB6149) dissolved in physiological saline (0.9% NaCl) at a dose of 3 mg kg−1 in a volume of 10 ml kg−1, was used 30 min before the behavioral experiments. I.p. injections of saline (0.9% NaCl) were used 30 min before the behavioral experiments as a control condition. All animals (control and ID) received i.p. CNO injections and saline injections. Saline experiments were performed with 3 days of interval for the sociability test and 1 week of interval for the resident-intruder test to prevent heightened aggression resulting from close repetitive exposure to an intruder in the home-cage.

For the guide cannula experiments on WT mice, C57BL/6 mice were infused in LS with 1 µl of saline, 1 µl of the AVPR1b antagonist SSR149415 at 2 µM, or 1 µl of the AVPR1a antagonist SR49059. For the guide cannula experiments on mutant mice, *Shank3B*$^{+/-}$ mice were infused in LS with 1 µl of saline, 1 µl of the AVPR1b agonist DDAVP at 100 µM solution, or 1 µl of AVP at 1 mM combined with together with the antagonist of AVPR1b, SSR149415 at 2 µM to selectively activate AVPR1a only. All drugs came from Tocris (Table 1). Drugs were infused at a rate of 0.2 µl per minute using a programmable syringe pump (Chemyix Inc.) mounted with a 2 µl syringe (Hamilton #88511). After infusion, animals were undisturbed for 5 min before the start of the

Table 1 | Reagents and resources information

REAGENT or RESOURCE	SOURCE	IDENTIFIER
Antibodies		
Anti-c-fos antibody produced in rabbit	Abcam	#ab190289 RRID:AB_2737414
Anti-GFP antibody produced in chicken	AVES Labs	#GFP-1020 RRID:AB_10000240
Anti-vasopressin antibody produced in a rabbit	Merck	#PC234L RRID:AB_565256
Anti-RFP antibody produced in a rabbit	Rockland Antibody	#600-401-379 RRID:AB_2209751
Anti-VGLUT1 antibody produced in a guinea pig	Merck	#ab5905 RRID:AB_2301751
Goat anti-rabbit IgG (H + L) secondary antibody, Alexa Fluor 488 conjugate	Thermo-Fisher Scientific	#A11039 RRID:AB_142924
Goat anti-rabbit IgG (H + L) secondary antibody, Alexa Fluor 568 conjugate	Thermo-Fisher Scientific	#A11011 RRID:AB_143157
Goat anti-guinea-pig IgG (H + L) secondary antibody, Alexa Fluor 594 conjugate	Thermo-Fisher Scientific	#A11076 RRID:AB 2534120
Goat Anti-chicken IgG (H + L) secondary antibody, Alexa Fluor 488 Conjugate	Thermo-Fisher Scientific	#A11039 RRID:AB_142924
In situ hybridization probes		
Avp in C1	ACD Bio	#401391
Avpr1a in C3	ACD Bio	#418061-C3
Chemicals, Peptides, and Recombinant Proteins		
CNO	Cayman Chemical	#16882
SR49059	Tocris	#2310
Desmopressin	Tocris	#3396
[Arg^{8}]-Vasopressin	Tocris	#2935
SSR149415	Tocris	#6195
Experimental Models: Organisms/Strains		
C57BL/6 J Mus musculus	Jackson Laboratories	RRID:IMSR_JAX:000664
Avp-Cre$^{+/-}$	Jackson Laboratories	RRID:IMSR_JAX:023530
Shank3B$^{+/-}$	Jackson Laboratories	RRID:IMSR_JAX:017688
Balb/cByJ	Jackson Laboratories	RRID:IMSR_JAX:001026
Recombinant DNA		
HSV hEF1a.LSIL.GFP (HT)	Massachusetts General Hospital	#RN406
AAV2/1 syn.FLEX.GCaMP6f.WPRE.SV40	Addgene	#100833-AAV1
AAV2/9EF1a.DIO.hChR2 (E123T/T159C).eYFP8	Addgene	#35509-AAV9
AAV2/8 hSyn.DIO.hM4D(Gi)-mCherry	Addgene	#44362-AAV8
AAV2/1 hSyn1-DIO-eOPN3-mScarlet-WPRE	Addgene	#125713-AAV1
AAV2/9 GFP.U6.anti-*Avp*-shRNA	Vector Biolabs	#253437-shAAV[50]
AAV2/9 GFP.U6.scramble-shRNA	Vector Biolabs	[50]
AAV9-hSyn-AVP0.3	Yulong Li	
Software		
PRISM 8	Graphpad	8.4.1 (455)
Microsoft Office Word	Microsoft	2019 16.56
Microsoft Office Excel	Microsoft	2019
Adobe Illustrator	Adobe	2023
Fiji	GPL v2	2.3.0/1.53 f
Python		3.10.2
MATLAB	Mathworks	2024b
Guppy	Lerner Lab[88]	1.1.4
SimpylCellCounter	https://github.com/aneeshbal/SimpylCellCounter[87]	2.0
Leica Application Suite X	Leica	v3.7.4
ANY-maze	Stoelting Co.	4.99
Bonsai	Open Ephys	2.8.2
Doric Neuroscience Studio	Doric	5.4.1.23

experiment. Drugs were randomized per animal during the sessions, and each session was performed with 3 days interval for the sociability test, and 1 week of interval for the resident-intruder test. For checking the guide cannula infusion localization in the brain, mini-Ruby (Invitrogen, D1868) was used. A total of 1 µl was infused at a rate of 0.2 µl per minute. 60 min after infusion, animals were perfused.

Behavioral tests

All animals were housed with littermates (maximum of 5 per cage) at a temperature of 24 °C with 12 h daily illumination and food and water ad libitum. The light cycle was not inverted, and experiments were conducted under dim light conditions.

Open arena test. Animals were placed in a white open arena (OA) (60 cm x 60 cm) and allowed to explore freely the space for 10 min. Automatic tracking software (Any-Maze 7, Stoelting) was used to quantify the time spent in the center and surroundings, as well as the total distance traveled by the animal.

Social interaction test. Animals were insolated in their home-cage, and 2 min calcium recording sessions were conducted in the empty home-cage. Subsequently, a stimulus mouse (Balb/cByJ) was introduced for another 2 min. Animals were allowed to freely explore, and the frequency and amplitude of the calcium signal was quantified for both conditions.

Sociability test. Wire cup cages were placed diagonally in opposite corners of the open arena. One of the cups was empty, and the other had a male, same-aged, unfamiliar mouse under it. Test subjects were allowed to freely explore the arena for 5 min. The same automatic tracking software described above was used to generate regions of interest around the cups and to provide an output of the total time spent interacting with both cups. A discrimination index was used to calculate the interaction time with both cups: (time with social cup − time with empty cup) / total interaction time.

Social novelty preference test. For the learning trial, mice were placed in the open arena containing two wire cups with one male same-age unfamiliar mouse under each cup. The cups were placed diagonally at opposite sides of the arena, and the test mouse could freely explore for 5 min. The test mouse was then single-housed in a chamber for 30 min. For the recall trial, one of the animals under the wire cup was replaced with a novel, unfamiliar mouse. The test mouse was then placed again in the open arena and could freely explore. The automated software for tracking was used for quantifying the interaction time with both animals under the cup. A discrimination index was used to calculate the interaction time with familiar and novel mouse for the recall condition: (time with novel − time with familiar) / total interaction time.

Resident-intruder test. Animals were single-housed in a cage with food and water ad libitum for a week prior to the testing day. During this week, animals were undisturbed, and the bedding of their cage was not changed in order to preserve odors that can favor the development of territoriality. Test mice were virgin and did not receive any sexual or aggressive experience during isolation. An intruder male mouse (Balb/cBy) was placed inside the cage, and the social interactions were recorded for 10 min. The software Any-Maze (Stoelting) was used for manual scoring of the social behaviors displayed. Similar to our previous study[40], the following social behaviors were quantified: **social exploration** (facial and ano-genital sniffing initiated by the resident mouse), **social dominance** (resident mouse rising onto its hindlimbs to scruff the intruder's head, as well as excessive allogrooming, chasing or mounting) and **attack** (biting attack followed by fighting and tail rattling). We show example pictures (Fig. 1f), and example videos can be found in our previous publication[40]. For the c-fos experiments, the same protocol was followed, but following completion of the test, animals were undisturbed for 60 min for the expression of the immediate-early gene and then perfused as previously described.

Development of the $GRAB_{AVP0.3}$ sensor

The development, optimization, and characterization strategy of the $GRAB_{AVP0.3}$ followed the methodology of our previously developed GRAB sensors[85]. The $GRAB_{AVP0.3}$ was developed based on human AVPR2 and optimized by mutagenesis screening of fluorescent protein, linker region, and GPCR. Then $GRAB_{AVP0.3}$ was cloned into a pAAV vector and packaged into an AAV virus for in vivo expression.

Fiber-photometry calcium recording data acquisition

Animals were habituated to the optical fiber patch cord for 1 day before the test. The optical fiber patch cord was placed on top of the mouse's implant, and the sociability test and resident-intruder test were performed as previously described while recording calcium activity from vasopressinergic BNST terminals in LS. Data acquisition was performed using the FP3002 system from Neurophotometrics controlled via Bonsai (Open-Ephys). LEDs delivering two excitation wavelengths (470 nm for detection of GCaMP6f signal and 415 nm for a calcium-independent control) intercalated at 40 Hz throughout recording sessions. Fluorescence emission was focused onto a CMOS sensor for detection, with a region of interest drawn around the end of the plug of the patch cord. A key press trigger was used in Bonsai to save the timestamps of precise social interactions aligned to the calcium signal (social exploration and biting).

Fiber-photometry vasopressin recording data acquisition

AVP biosensor data acquisition was conducted using a DORIC system (Basic FMC). Two LEDs (405 nm and 465 nm) were coupled to a fluorescence mini-cube (FMC) to deliver light into optical ferrules permanently implanted above the dLS. Light was delivered at a final intensity of 12 µW (465 nm) and 249.5 µW (405 nm) at the tip of the patch-cord. Emitted light between 420 and 450 nm (with 405 nm excitation) and 500 and 540 nm (with 465 nm excitation) were collected through the FMC on separate fiber-coupled Newport 2151 photo-receiver modules. The fluorescent signals were collected in AC-low mode and converted to voltage via the formula $V = PRG$, where V is the collected voltage, P is the optical input power in watts, R is the photodetector responsivity in amps/watts (0.2 − 0.4), and G is the trans-impedance gain of the amplifier. Raw signals and 405 nm excitation (isosbestic signal) were recorded using Doric Neuroscience Studio software.

Optogenetic silencing

Animals were habituated to the optical fiber patch cord for 1 day before the test. The optical fiber patch cord was placed on top of the mouse's implant, and the sociability test and resident-intruder test were performed as previously described. In the experimental condition of silencing, light stimulation was supplied using the Cobolt-Jive 561 nm, adjusted at 5 mW, and applied during all the testing time. In control conditions, mice were subjected to the test with the patch cord connected but with no light stimulation. The experimental and control conditions were randomized between batches of animals and performed with an interval of 3 days between the sociability test and 1 week between the resident-intruder test, to prevent heightened aggression resulting from close repetitive exposure to an intruder in the home-cage.

Data analysis

Quantification of the density of cell bodies. In situ hybridization was used to label AVP and Avpr1a mRNA in the BNST and LS of *Shank3B*$^{+/-}$

and WT littermates, as previously described. Equivalent-sized images of the anterior and posterior LS and BNST were acquired with an inverted confocal microscope (SPEII, Leica) with identical settings. The pictures were loaded in the software Fiji (Schneider et al., 2012) and subjected to manual quantification using the cell counting function.

Quantification of the density of axonal fibers. Immunohistochemistry for labeling vasopressin was performed accordingly to the descriptions above. Equivalent-sized images of the anterior and posterior LS of *Shank3b*$^{+/-}$ and WT littermates were acquired with an epifluorescent microscope (Thunder, Leica). The settings for image acquisition was the same for all samples. The pictures were loaded in Fiji software and transformed in to an 8-bit image. A threshold was set to cover all the white pixels of the image, which corresponded to the GFP signal. A selection of the white pixels was then generated, and the area corresponding to the GFP labeling was measured. Data was plotted as the total area of GFP pixels labeled[86].

Quantification of density of VGLUT1 clusters. Immunohistochemistry for labeling VGLUT1 was performed accordingly to the descriptions above. For both *Shank3b*$^{+/-}$ and WT controls, equivalent-sized images of the BNST were acquired (x63 magnification) with identical settings on a confocal microscope (SPEII, Leica). The images were then converted to 8-bit format using ImageJ. A threshold was uniformly applied to all images to enhance the detection and count the different VGLUT1 clusters present on the soma and fibers of AVP cells. Finally, the ROIs used to outline the AVP cells are associated with the number of clusters to generate the VGLUT1 synapse density for each quantified cell.

Quantification of c-fos+ cells. The automated program SimpylCellCounter[87] was used for the quantification of c-fos^{+} cells. Equivalent-sized images from anterior and posterior BNST and LS of *Shank3B*$^{+/-}$ and WT littermates were acquired with identical settings in the Thunder microscope (Leica) were loaded in the program. The software utilized binary thresholding and morphological functions from the open-source computer vision library OpenComputerVision (OpenCV) to identify and quantify the cells based on shape and size. The size was defined as 5, and the circularity threshold as 0.8. An output of the images with the quantified cells was generated, and the cells on the total area were plotted.

Fiber photometry and AVP biosensor data analysis. The Guppy software[88] was used for fiber photometry and AVP biosensor data analysis. The raw data and the behavioral timestamps were loaded, and the first seconds of recording were removed for artifact correction. A subtraction of the background fluorescence was calculated using a time-fitted running average of the 470 nm channel relative to the 415 nm control channel using a least squares polynomial fit of degree 1. The ΔF/F was calculated by subtracting the fitted control channel from the signal channel and dividing by the fitted control channel using the formula: (470–415 nm)/415 nm. A peak enveloping Fourier transform was applied to the ΔF/F signal across the entire trace to identify peaks in activity. The data was presented as the deviation of the ΔF/F from its mean (z-score) using the formula: (ΔF/F − mean of ΔF/F/ Standard deviation of ΔF/F). The z-score of each interaction of interest were analyzed during the sessions based on a time window of − 3 to 3 s for the PSTH analysis. For the sociability test, the interaction with the object only (empty cup) was used as a control condition. For the resident-intruder test, the pre-biting or pre-social interaction transients were used as a control condition from − 3 to −1 seconds. The area under the curve and the peak amplitude were plotted accordingly to these time windows.

Decoder analysis. Fiber photometry recordings of calcium or AVP biosensor signal were used to discriminate between non-social and social transients. In each session, we detected the transients and computed the peak amplitude and the area under the curve of each transient. To discriminate whether the recording came from a non-social or social condition, we trained linear support vector machine (SVM) decoders, using both peak amplitude and transient strength of all detected transients. We trained decoders by randomly selecting 70% data points as a training set and evaluated the decoder performance using the rest 30% as a testing set. To correct for class imbalance, as a standard procedure, we implemented a cost for misclassification that is inversely proportional to the number of samples in each class. This random sampling procedure was repeated 20 times to avoid sampling bias, and the results were averaged across repeats for each session. To generate a baseline distribution, we shuffled the labels (non-social vs social condition) of the data points and trained decoders as above. This shuffling procedure was repeated 1000 times. Decoder performance was evaluated as the area under the curve (AUC) of the receiver operating characteristic (ROC) curve. A statistical test (one-sided Wilcoxon signed-rank test) was performed to compare the AUC between the real data and the top 95% quantile of the shuffled distribution. For the biosensor data, we performed the decoder analysis to discriminate between social and non-social transients in WT and *Shank3B*$^{+/-}$ mice, using the same procedure as described above.

Supervised annotation in DeepOF analysis. Videos of WT or *Shank3B*$^{+/-}$ mice freely interacting in an open arena with a stimulus mouse were captured using a DMK 27BUR0135 (The IMAGING SOURCE) camera, positioned 130 cm above the arena for a top-down perspective. The recordings were acquired with Bonsai-RX software. Initially, the test mouse was allowed to explore the arena freely for 10 min. Following this, a stimulus mouse (BALB/c, males, 7–11 weeks old) was introduced into the arena, and a 2 min interaction period was recorded and saved for subsequent analysis. The interactions between the test and stimulus mice were analyzed using DeepOF software (version 0.7.2)[89,90]. To facilitate this, the body parts of both mice were tracked with DeepLabCut (version 2.2.3)[91] using a custom-trained model. DeepOF analysis was then conducted based on the calculated trajectories for each body part[89,90]. Finally, each frame was classified into specific behaviors using DeepOF's pre-trained network.

Statistics and reproducibility

Statistical analyses and figure plotting were performed using Prism version 9 (GraphPad). No statistical methods were used to predetermine sample sizes, but sample size was selected based on previous experience and on estimation from related studies. Unless specified otherwise, bar graphs represent mean ± s.e.m. Sample sizes and statistical tests are reported in the figure legends. * indicates $p < 0.05$, ** indicates $p < 0.01$, *** indicates $p < 0.001$ and **** indicates $p < 0.0001$. When multiple observations were done in the same mouse, nested statistical tests were used to take into account the lower degree of freedom. Experiments using viral injections for anterograde and retrograde tracing were independently repeated a minimum of three times, producing similar outcomes. For experiments involving viral expression or optical ferrule implant, only animals exhibiting proper viral expression and accurate optical ferrule localization were included in the analysis.

Reporting summary

Further information on research design is available in the Nature Portfolio Reporting Summary linked to this article.

Data availability

The data generated in this study are provided in the Source Data file. Request for raw data files should be directed to Felix Leroy (felxfel@aol.com). Source data are provided in this paper.

Code availability

The code used to create the classifiers analysis of the fiber-photometry data is available at https://github.com/hanshuting/AVP_decoder_manuscript. Any additional information required to reanalyze the data reported in this paper is available from the lead contact upon request.

References

1. Harony, H. & Wagner, S. The contribution of oxytocin and vasopressin to mammalian social behavior: Potential role in Autism Spectrum Disorder. *Neurosignals* **18**, 82–97 (2010).
2. Lukas, M. & Neumann, I. D. Oxytocin and vasopressin in rodent behaviors related to social dysfunctions in autism spectrum disorders. *Behav. Brain Res.* **251**, 85–94 (2013).
3. Zhang, R., Zhang, H. F., Han, J. S. & Han, S. P. Genes related to oxytocin and arginine-vasopressin pathways: Associations with Autism Spectrum Disorders. *Neurosci. Bull.* **33**, 238–246 (2017).
4. Cataldo, I., Azhari, A. & Esposito, G. A review of oxytocin and arginine-vasopressin receptors and their modulation of Autism Spectrum Disorder. *Front. Mol. Neurosci.* **11**, https://doi.org/10.3389/fnmol.2018.00027 (2018).
5. Francis, S. M. et al. Variants in adjacent oxytocin/vasopressin gene region and associations with ASD diagnosis and other Autism autism-related endophenotypes. *Front. Neurosci.* **10**, https://doi.org/10.3389/fnins.2016.00195 (2016).
6. Dempster, E. L. et al. Further genetic evidence implicates the vasopressin system in childhood-onset mood disorders. *Eur. J. Neurosci.* **30**, 1615–1619 (2009).
7. Shou, X. J. et al. A volumetric and functional connectivity MRI study of brain arginine-vasopressin pathways in autistic children. *Neurosci. Bull.* **33**, 130–142 (2017).
8. Xu, X. J. et al. Mothers of autistic children: Lower plasma levels of oxytocin and arg-vasopressin and a higher level of testosterone. *PLoS ONE* **8**, https://doi.org/10.1371/journal.pone.0074849 (2013).
9. Zhang, H. F. et al. Plasma oxytocin and arginine-vasopressin levels in children with Autism Spectrum Disorder in China: associations with symptoms. *Neurosci. Bull.* **32**, 423–432 (2016).
10. Oztan, O. et al. Cerebrospinal fluid vasopressin and symptom severity in children with autism. *Ann. Neurol.* **84**, 611–615 (2018).
11. Oztan, O., Garner, J. P., Constantino, J. N. & Parker, K. J. Neonatal CSF vasopressin concentration predicts later medical record diagnoses of autism spectrum disorder. *Proc. Natl. Acad. Sci. USA* **117**, 10609–10613 (2020).
12. Carson, D. S. et al. Arginine Vasopressin Is a Blood-Based Biomarker of Social Functioning in Children with Autism. *PLoS ONE* **10**, e0132224 (2015).
13. Yirmiya, N. et al. Association between the arginine vasopressin 1a receptor (AVPR1a) gene and autism in a family-based study: mediation by socialization skills. *Mol. Psychiatry* **11**, 488–94 (2006).
14. Kim, S. J. et al. Transmission disequilibrium testing of arginine vasopressin receptor 1A (AVPR1A) polymorphisms in autism. *Mol. Psychiatry* **7**, 503–507 (2002).
15. Wassink, T. H. et al. Examination of AVPR1a as an autism susceptibility gene. *Mol. Psychiatry* **9**, 968–72 (2004).
16. Francis, S. M. et al. ASD and Genetic associations with receptors for oxytocin and vasopressin—AVPR1A, AVPR1B, and OXTR. *Front. Neurosci.* **10**, 516 (2016).
17. Dempster, E. L. et al. Evidence of an association between the vasopressin V1b receptor gene (AVPR1B) and childhood-onset mood disorders. *Arch. Gen. Psychiatry* **64**, 1189–1195 (2007).
18. Tansey, K. E. et al. Functionality of promoter microsatellites of arginine vasopressin receptor 1A (AVPR1A): implications for autism. *Mol. Autism* **2**, 3 (2011).
19. Yang, S. Y. et al. Family-based association study of microsatellites in the 5′ flanking region of AVPR1A with autism spectrum disorder in the Korean population. *Psychiatry Res.* **178**, 199–201 (2010).
20. van den-Ouweland, A. M. W. et al. Mutations in the vasopressin type 2 receptor gene (AVPR2) associated with nephrogenic diabetes insipidus. *Nat. Genet.* **2**, 99–102 (1992).
21. Dantzer, R., Bluthe, R. M., Koob, G. F. & Le Moal, M. Modulation of social memory in male rats by neurohypophyseal peptides. *Psychopharmacology* **91**, 363–368 (1987).
22. Le Moal, M., Dantzer, R., Michaud, B. & Koob, G. F. Centrally injected arginine vasopressin (AVP) facilitates social memory in rats. *Neurosci. Lett.* **77**, 353–359 (1987).
23. Engelmann, M., Ludwig, M. & Landgraf, R. Simultaneous monitoring of intracerebral release and behavior: endogenous vasopressin improves social recognition. *J. Neuroendocrinol.* **6**, 391–395 (1994).
24. Dantzer, R., Koob, G. F., Bluthé, R. M. & Le Moal, M. Septal vasopressin modulates social memory in male rats. *Brain Res.* **457**, 143–147 (1988).
25. Bychowski, M. E., Mena, J. D. & Auger, C. J. Vasopressin infusion into the lateral septum of adult male rats rescues progesterone-induced impairment in social recognition. *Neuroscience* **246**, 52–58 (2013).
26. Bluthe, R.-M. & Dantzer, R. Social recognition does not involve vasopressinergic neurotransmission in female rats. *Brain Res.* **535**, 301–304 (1990).
27. van Wimersma Greidanus, T.jB. & Maigret, C. The role of limbic vasopressin and oxytocin in social recognition. *Brain Res.* **713**, 153–159 (1996).
28. Bielsky, I. F., Hu, S. B., Szegda, K. L., Westphal, H. & Young, L. J. Profound impairment in social recognition and reduction in anxiety-like behavior in vasopressin V1a receptor knockout mice. *Neuropsychopharmacology* **29**, 483–493 (2004).
29. Bielsky, I. F., Hu, S. B. & Young, L. J. Sexual dimorphism in the vasopressin system: lack of an altered behavioral phenotype in female V1a receptor knockout mice. *Behav. Brain Res.* **164**, 132–136 (2005).
30. Wersinger, S. R. et al. Vasopressin 1a receptor knockout mice have a subtle olfactory deficit but normal aggression. *Genes Brain Behav.* **6**, 540–551 (2007).
31. Caldwell, H., Wersinger, S. & Young, W. in *Advances in Vasopressin and Oxytocin; From Genes to Behaviour to Disease*. (Elsevier, 2008).
32. Sala, M. et al. Pharmacologic rescue of impaired cognitive flexibility, social deficits, increased aggression, and seizure susceptibility in oxytocin receptor null mice: A neurobehavioral model of Autism. *Biol. Psychiatry* **69**, 875–882 (2011).
33. Menon, R. et al. Neurobiology of the lateral septum: Regulation of social behavior. *Trends Neurosci.* **45**, 27–40 (2022).
34. Courchesne, E. Brainstem, cerebellar and limbic neuroanatomical abnormalities in autism. *Curr. Opin. Neurobiol.* **7**, 269–278 (1997).
35. Kotagiri, P., Chance, S. A., Szele, F. G. & Esiri, M. M. Subventricular zone cytoarchitecture changes in Autism. *Dev. Neurobiol.* **74**, 25–41 (2014).
36. Engelmann, M. & Landgraf, R. Microdialysis administration of vasopressin into the septum improves social recognition in Brattleboro rats. *Physiol. Behav.* **55**, 145–149 (1994).
37. De Vries, G. J., Buijs, R. M. & Van Leeuwen, F. W. Sex differences in vasopressin and other neurotransmitter systems in the brain. *Prog. Brain Res.* **61**, 185–203 (1984).
38. Rood, B. D. & De Vries, G. J. Vasopressin innervation of the mouse (Mus musculus) brain and spinal cord. *J. Comp. Neurol.* **519**, 2434–2474 (2011).
39. Rigney, N. et al. A vasopressin circuit that modulates mouse social investigation and anxiety-like behavior in a sex-specific manner.

Proc. Natl. Acad. Sci. USA **121**, https://doi.org/10.1073/pnas.2319641121 (2024).
40. Leroy, F. et al. A circuit from hippocampal CA2 to lateral septum disinhibits social aggression. *Nature* **564**, 213–218 (2018).
41. Peça, J. et al. Shank3 mutant mice display autistic-like behaviours and striatal dysfunction. *Nature* **472**, 437–442 (2011).
42. Sgritta, M. et al. Mechanisms underlying microbial-mediated changes in social behavior in mouse models of Autism Spectrum Disorder. *Neuron* **101**, 246–259 (2019).
43. Koolhaas, J. M. et al. The Resident-Intruder Paradigm: A standardized test for aggression, violence and social stress. *J. Vis. Exp.***77**, e4367 (2013).
44. Velez, L., Sokoloff, G., Miczek, K. A., Palmer, A. A. & Dulawa, S. C. Differences in aggressive behavior and DNA copy number variants between BALB/cJ and BALB/cByJ substrains. *Behav. Genet.* **40**, 201 (2010).
45. Sheng, M. & Kim, E. The Shank family of scaffold proteins. *J. Cell Sci.* **113**, 1851–1856 (2000).
46. Wang, M. et al. Decrease of GSK-3β activity in the anterior cingulate cortex of Shank3b−/− mice contributes to synaptic and social deficiency. *Front. Cell Neurosci.* **13**, https://doi.org/10.3389/fncel.2019.00447 (2019).
47. Bozdagi, O. et al. Haploinsufficiency of the autism-associated Shank3 gene leads to deficits in synaptic function, social interaction, and social communication. *Mol. Autism* **1**, (2010).
48. Leroy, F. et al. Enkephalin release from VIP interneurons in the hippocampal CA2/3a region mediates heterosynaptic plasticity and social memory. *Mol. Psychiatry* **27**, 2879 (2022).
49. Mahn, M. et al. Efficient optogenetic silencing of neurotransmitter release with a mosquito rhodopsin. *Neuron* **109**, 1621–1635 (2021).
50. Rigney, N., Zbib, A., de Vries, G. J. & Petrulis, A. Knockdown of sexually differentiated vasopressin expression in the bed nucleus of the stria terminalis reduces social and sexual behaviour in male, but not female, mice. *J. Neuroendocrinol.* **34**, https://doi.org/10.1111/jne.13083 (2022).
51. Zai, C. C. et al. Possible genetic association between vasopressin receptor 1B and child aggression. *Psychiatry Res.* **200**, 784–788 (2012).
52. Bielsky, I. F., Hu, S.-B., Ren, X., Terwilliger, E. F. & Young, L. J. The V1a vasopressin receptor is necessary and sufficient for normal social recognition: A gene replacement study. *Neuron* **47**, 503–513 (2005).
53. Besnard, A. & Leroy, F. Top-down regulation of motivated behaviors via lateral septum sub-circuits. *Mol Psychiatry* **8**, 3119–3128 (2022).
54. Trainor, B. C., Greiwe, K. M. & Nelson, R. J. Individual differences in estrogen receptor alpha in select brain nuclei are associated with individual differences in aggression. *Horm. Behav.* **50**, 338–345 (2006).
55. Beiderbeck, D. I., Neumann, I. D. & Veenema, A. H. Differences in intermale aggression are accompanied by opposite vasopressin release patterns within the septum in rats bred for low and high anxiety. *Eur. J. Neurosci.* **26**, 3597–3605 (2007).
56. Veenema, A. H., Beiderbeck, D. I., Lukas, M. & Neumann, I. D. Distinct correlations of vasopressin release within the lateral septum and the bed nucleus of the stria terminalis with the display of intermale aggression. *Horm. Behav.* **58**, 273–81 (2010).
57. Oliveira, V. E. de M. in *Handbook of Anger, Aggression, and Violence*. (2023).
58. Dai, B. et al. Experience-dependent dopamine modulation of male aggression. *Nature* **639**, 430–437 (2025).
59. Takahashi, A. & Miczek, K. A. Neurogenetics of aggressive behavior: Studies in rodents. *Curr. Top. Behav. Neurosci.* **17**, 3–44 (2013).
60. Trainor, B. C. & Nelson, R. J. in *Handbook of Neuroendocrinology*. (2012).
61. Witchey, S. K., Stevenson, E. L. & Caldwell, H. K. Genotypic differences in intruder-evoked immediate early gene activation in male, but not female, vasopressin 1b receptor knockout mice. *BMC Neurosci.* **17**, https://doi.org/10.1186/s12868-016-0310-7 (2016).
62. Young, W. S., Li, J., Wersinger, S. R. & Palkovits, M. The vasopressin 1b receptor is prominent in the hippocampal area CA2 where it is unaffected by restraint stress or adrenalectomy. *Neuroscience* **143**, 1031–1039 (2006).
63. Sun, Y., Zweifel, L. S., Holmes, T. C. & Xu, X. Whole-brain input mapping of the lateral versus medial anterodorsal bed nucleus of the stria terminalis in the mouse. *Neurobiol. Stress* **23**, https://doi.org/10.1016/j.ynstr.2023.100527 (2023).
64. Wersinger, S. R., Ginns, E. I., O'Carroll, A.-M., Lolait, S. J. & Young, W. S. III Vasopressin V1b receptor knockout reduces aggressive behavior in male mice. *Mol. Psychiatry* **7**, 975–984 (2002).
65. Luo, A. H., Tahsili-Fahadan, P., Wise, R. A., Lupica, C. R. & Aston-Jones, G. Linking Context with reward: A functional circuit from hippocampal CA3 to ventral tegmental area. *Science* **333**, 353–357 (2011).
66. Wang, Z., Bullock, N. A. & De Vries, G. J. Sexual differentiation of vasopressin projections of the bed nucleus of the stria terminals and medial amygdaloid nucleus in rats. *Endocrinology* **132**, 2299–2306 (1993).
67. Rigney, N., Whylings, J., Mieda, M., De Vries, G. J. & Petrulis, A. Sexually dimorphic vasopressin cells modulate social investigation and communication in sex-specific ways. *eNeuro* **6**, https://doi.org/10.1523/eneuro.0415-18.2019 (2019).
68. Bluthe, R. M., Schoenen, J. & Dantzer, R. Androgen-dependent vasopressinergic neurons are involved in social recognition in rats. *Brain Res.* **519**, 150–157 (1990).
69. Auger, C. J. & Vanzo, R. J. Progesterone treatment of adult male rats suppresses arginine vasopressin expression in the bed nucleus of the stria terminalis and the centromedial amygdala. *J. Neuroendocrinol.* **18**, 187–194 (2006).
70. Bychowski, M. E. & Auger, C. J. Progesterone impairs social recognition in male rats. *Horm. Behav.* **61**, 598–604 (2012).
71. Appenrodt, E., Juszczak, M. & Schwarzberg, H. Septal vasopressin induced preservation of social recognition in rats was abolished by pinealectomy. *Behav. Brain Res.* **134**, 67–73 (2002).
72. Dluzen, D. E., Muraoka, S. & Landgraf, R. Olfactory bulb norepinephrine depletion abolishes vasopressin and oxytocin preservation of social recognition responses in rats. *Neurosci. Lett.* **254**, 161–164 (1998).
73. Oliveira, V. E. de M. et al. Oxytocin and vasopressin within the ventral and dorsal lateral septum modulate aggression in female rats. *Nat. Commun.* **12**, 2900 (2021).
74. Veenema, A. H., Bredewold, R. & De Vries, G. J. Sex-specific modulation of juvenile social play by vasopressin. *Psychoneuroendocrinology* **38**, 2554–2561 (2013).
75. Bredewold, R., Smith, C. J. W., Dumais, K. M. & Veenema, A. H. Sex-specific modulation of juvenile social play behavior by vasopressin and oxytocin depends on social context. *Front. Behav. Neurosci.* **8**, https://doi.org/10.3389/fnbeh.2014.00216 (2014).
76. Nephew, B. C. & Bridges, R. S. Arginine vasopressin V1a receptor antagonist impairs maternal memory in rats. *Physiol. Behav.* **95**, 182–186 (2008).
77. Rigney, N., de Vries, G. J. & Petrulis, A. Modulation of social behavior by distinct vasopressin sources. *Front. Endocrinol.* **14**, https://doi.org/10.3389/fendo.2023.1127792 (2023).
78. Borie, A. M. et al. Correction of vasopressin deficit in the lateral septum ameliorates social deficits of the mouse autism model. *J. Clin. Invest.* **131**, https://doi.org/10.1172/jci144450 (2021).
79. Fountain, M. D., Tao, H., Chen, C. A., Yin, J. & Schaaf, C. P. Magel2 knockout mice manifest altered social phenotypes and a deficit in preference for social novelty. *Genes Brain Behav.* **16**, 592–600 (2017).

80. Parker, K. J. et al. A randomized placebo-controlled pilot trial shows that intranasal vasopressin improves social deficits in children with autism. *Sci. Transl. Med* **11**, https://doi.org/10.1126/scitranslmed.aau7356 (2019).
81. Hollander, E. et al. Balovaptan vs placebo for social communication in childhood Autism spectrum disorder: A randomized clinical trial. *JAMA Psychiatry* **79**, 760–769 (2022).
82. Schnider, P. et al. Discovery of balovaptan, a vasopressin 1a receptor antagonist for the treatment of Autism Spectrum Disorder. *J. Med. Chem*. **63**, 1511–1525 (2020).
83. Bolognani, F. et al. A phase 2 clinical trial of a vasopressin V1a receptor antagonist shows improved adaptive behaviors in men with autism spectrum disorder. *Sci. Transl. Med.* **11**, https://doi.org/10.1126/scitranslmed.aat7838 (2019).
84. László, K. et al. Vasopressin as possible treatment option in Autism Spectrum Disorder. *Biomedicines* **11**, https://doi.org/10.3390/biomedicines11102603 (2023).
85. Wang, H. et al. A tool kit of highly selective and sensitive genetically encoded neuropeptide sensors. *Science* **382**, https://doi.org/10.1126/science.abq8173 (2023).
86. Montanari, R. et al. Callosal inputs generate side-invariant receptive fields in the barrel cortex. *Sci. Adv.* **9**, https://doi.org/10.1126/sciadv.adi3728 (2023).
87. Bal, A., Maureira, F. & Arguello, A. A. SimpylCellCounter: an automated solution for quantifying cells in brain tissue. *Sci. Rep*. **10**, 12570 (2020).
88. Sherathiya, V. N., Schaid, M. D., Seiler, J. L., Lopez, G. C. & Lerner, T. N. GuPPy, a Python toolbox for the analysis of fiber photometry data. *Sci. Rep.* **11**, 1–9 (2021).
89. Miranda, L., Bordes, J., Pütz, B., Schmidt, M. V. & Müller-Myhsok, B. DeepOF: a Python package for supervised and unsupervised pattern recognition in mice motion tracking data. *J. Open Source Softw.* **8**, 5394 (2023).
90. Bordes, J. et al. Automatically annotated motion tracking identifies a distinct social behavioral profile following chronic social defeat stress. *Nat. Commun.* **14**, 4319 (2023).
91. Mathis, A. et al. DeepLabCut: markerless pose estimation of user-defined body parts with deep learning. *Nat. Neurosci.* **21**, 1281–1289 (2018).

Acknowledgements

We thank Antoine Besnard for comments on the manuscript. This project has received funding from the European Research Council (ERC) under the European Union's Horizon 2020 research, innovation program (grant agreement No 949652 to F.L.), NIH grant (U01NS120824 to Y.L.), National Natural Science Foundation of China (323B2033 to L.G.), and an Ambizione Grant from the Swiss National Science Foundation (PZ00P3_216312 to S.H.). S.H. also received funding from the University Research Priority Program (URPP) "Adaptive Brain Circuits in Development and Learning" (AdaBD). F.L. also acknowledges support from the CIDEGENT grant from the Valencian Community, the Proyecto de Generación de Conocimiento (PID2022-141262NA-I00) from the Agencia Estatal de Investigacion and the Severo Ochoa Foundation. The project that gave rise to these results received the support of a fellowship from "la Caixa" Foundation (ID 100010434) to M.H.B-G. The fellowship code is LCF/BQ/DI20/11780018.

Author contributions

Conceptualization: M.H.B-G. and F.L. Investigation: M.H.B-G., G.B., L.G., A.R.P. Y.N., and S.H. Writing – original draft: M.H.B-G. Writing – review & editing: M.H.B-G. and F.L. Visualization: M.H.B-G. Supervision: F.L. Funding acquisition: M.H.B-G., Y.L., F.L.

Competing interests

The authors declare no competing interests.

Additional information

Supplementary information The online version contains supplementary material available at https://doi.org/10.1038/s41467-025-61994-6.

Correspondence and requests for materials should be addressed to Félix Leroy.

Peer review information *Nature Communications* thanks Nicole Rigney, Toru Takumi, and the other anonymous reviewer(s) for their contribution to the peer review of this work. A peer review file is available.